FUNDAMENTAL STUDIES ON ULTRAFAST SEPARATIONS AND DEVELOPMENT OF GEOPOLYMER BASED BASE-STABLE STATIONARY PHASE MEDIA

by

RASANGI MADHUMALI WIMALASINGHE K.K.D.G.

Presented to the Faculty of the Graduate School of

The University of Texas at Arlington in Partial Fulfillment

of the Requirements

for the Degree of

DOCTOR OF PHILOSOPHY

THE UNIVERSITY OF TEXAS AT ARLINGTON

December 2018

Acknowledgments

My first and foremost sincere acknowledgment goes to my Ph.D. supervisor, Prof. D.W. Armstrong who always guided me to achieve the best of the best. He deserves this special gratitude for understanding my strengths and giving me not only knowledge but also wisdom. I am not who I am today without his incredible guidance. I want to express a special acknowledgment to my ever loving mother and father. This would remain as a dream if they were not behind me until this moment. I am proud that I am the reason behind their smile. I want to thank my only sister for her efforts to encourage me every possible moment. My husband, Udayanga deserves an exceptional appreciation for his patience, support and for being the strength of my life. I am nobody without your love and support. I am thankful to little Anya for making me happy all the time and being a good kid. Spending the weekends in the laboratory may be too much for you, but we made it together.

I want to thank my graduate committee, Prof. P. Dasgupta, Prof. K.A. Schug, and Prof. A. Bugarin and Prof. S. Mandal for their valuable guidance and support. I would like to appreciate and acknowledge Dr. M.F. Wahab and Dr. Z.S. Breitbach their valuable guidance and unconditional support. I want to thank Darshan, Chandan, Lily, Rahul, Mohsen, Yadi, Siqi, Garrett, Nimisha, Beth, Roy, and Abuid. We made a good team. Also, AZYP LLC, Dr. J.T Lee, and Mrs. Barbara Smith are kindly acknowledged for their kind support. I am thankful to all my teachers since kindergarten to graduate school, you all deserve a very sincere acknowledgment for the support and encouragement. Finally, I would like to thank every kind person who was around me for their support and kind heart throughout this journey.

November 20, 2018

Abstract

FUNDAMENTAL STUDIES ON ULTRAFAST SEPARATIONS AND

DEVELOPMENT OF GEOPOLYMER BASED

BASE-STABLE STATIONARY

PHASE MEDIA

Rasangi M. Wimalasinghe K.K.D.G., PhD

The University of Texas at Arlington, 2018

Supervising Professor: Daniel W. Armstrong

This thesis consists of two sections. In the first section fundamentals of ultrafast separations is discussed. Ultrafast chromatography is an emerging area of separation science due to its applicability in high-throughput separations and purifications. State of the art superficially porous particles packed short and ultrashort columns are utilized to obtain the amenable speed and chromatographic efficiency required in ultrafast chromatography. Modifications to state of the art HPLC and UHPLC instrumentation required in cases where ultrafast separations are needed. Sub-second liquid chromatographic separations and ultrafast separations of biomolecules and complex mixtures are demonstrated. Fundamentals behind the analytical chromatographic column

packing are discussed as efficiently packed columns are necessary in ultrafast chromatography.

Secondly, first reported utilization of geopolymers in liquid chromatography is discussed. A simple synthesis route has been proposed, and complete characterization of porous geopolymer particles has been performed using various characterization techniques. Geopolymer stationary phases have been successfully utilized in normal phase chromatography and hydrophilic interaction liquid chromatography (HILIC). Further, its HILIC characteristics are compared with other existing HILIC phases. This dissertation will be a resource to understand the fundamentals of ultrafast separations and utilization of geopolymers in the field of separation sciences.

Table of Contents

List of Illustrations

List of Tables

Chapter 1

INTRODUCTION

1.1 Fundamental Studies on Ultrafast Separations

1.1.1 General Introduction to Ultrafast Chromatography

Improving analysis speed has been recognized as one of the major challenges for separation scientists for past few decades. As needs for complex sample analysis and the number of samples increase, chromatographic speed and efficiency are among the features in demand to increase the peak capacity and throughput.[1] Utilizing conventional high pressure liquid chromatography (HPLC) columns (250 mm x 4.6 mm i.d.) with 5 µm fully porous particles (FPPs), achiral and chiral separations can be obtained within a time window of several minutes to hours with adequate efficiency. Significant developments in particle technology have taken place in the last decade. The introduction of sub 2 µm FPP and superficially porous particle (SPP) technologies allowed tremendous advances in field of liquid chromatography in terms of speed and an increase in the number of theoretical plates in short columns.[2]

The definition of ultrafast chromatography changed over time. The limit always decreases with advances in column technology and instrumentation. Contemporary standards of ultrafast chromatography are separations under 60 seconds. Regardless, most achiral and chiral ultrafast separations are now under 30 seconds.[2-4] Ultrafast separations, even in the milliseconds time domain have been attempted using classical techniques such as capillary zone electrophoresis, specialized electrophoretic microchips and wide bore hydrodynamic separations utilizing unique detection techniques such as on-column detection along with digital image processing. [5-10] Sub-minute or sub-second HPLC

separations are more challenging due to instrument hardware and computational limitations such as: difficulties in minimization of extra column dispersion, flow rate limitations, and inadequate sampling frequencies.[11] Systematic approaches to overcome these limitations will be discussed in the following sections.

1.1.2 Requirements for Ultrafast Chromatography

Maintaining the chromatographic resolution of a particular critical pairs of analytes will be challenging when using very short columns compared to traditional long columns. Resolution can be improved by improving efficiency, retention of the analytes and increasing selectivity of the stationary phase. When short columns are chosen, improvements in efficiency will significantly influence the resolution. Efficiency can be improved by the utilization of small particles (e.g., 1.7 µm superficially porous particles (SPP)), optimization of column packing, and controlling extra column band broadening. Selectivity and retention factors can be optimized by choosing the appropriate stationary phase. Another crucial consideration in the ultrafast domain is the detector performance of the chromatography system. This includes the sampling frequency and response time of the detector.

1.1.2.1 Utilization of Small Particle Packed Short Columns and Packing Optimization

A straightforward approach to improve chromatographic efficiency is to decrease the particle size. The particle diameter is inversely proportional to chromatographic efficiency. Sub 2 micron fully porous particles (FPP) results in improved chromatographic efficiencies at the cost of very high back pressure (usually more than the upper pressure limits of ordinary HPLC: 400 bar). SPP technology is increasing in popularity as it provides similar chromatographic performances to sub 2 µm FPPs with a more permeable chromatographic bed resulting a reduced operating back pressure. Note that back pressure

is inversely proportional to the square of particle diameter.[12] Higher surface roughness of SPP results in a packed bed with more axial heterogeneity minimizing the contribution of eddy dispersions in band broadening. [12] Also, SPP based columns can be operated at high flow rates with a less significant loss of efficiency. The morphology of a superficially porous particle is shown in Figure 1.1.

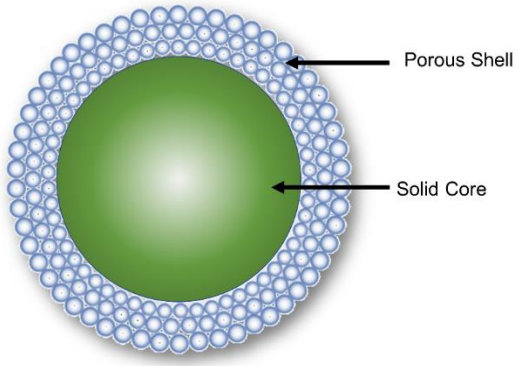

Figure 1.1 Morphology of a superficially porous particle

The improved efficiencies of SPP columns for small molecules are due to the packed bed uniformity and lower eddy dispersion compared to FPP packed columns. [13-15] Contribution of mass transfer effects on band broadening is reduced for larger molecules such as proteins, oligonucleotides, etc. with small diffusion coefficients and small molecules exhibiting sluggish adsorption-desorption kinetics even at higher flow rates when SPP packed columns are utilized. [16-18] The solid core of these particles results in reduced trans particle length, therefore, the accessibility for longitudinal diffusion is limited and reduced. [9-21] As a result, a smaller van-Deemter B term is expected. [19-21]

Column packing is a vital process in producing high efficiency column. Traditionally HPLC column packing is considered as an art more than a science. The quality of the packed bed is determined mainly by,

- Suspension rheology and microscopic properties – Shear thickening *vs.* shear thinning, dispersed slurry *vs.* agglomerated slurry
- Slurry concentration
- Packing pressure – packing pressure >> operating pressure.

In slurry packing, the empty analytical column is connected to the slurry chamber with a pre-column. The slurry is pushed downward using a pneumatic pump under high pressure usually with a push solvent. Usually, columns packed with disperse slurries produce higher efficiencies (approximately two fold increment) and resolutions compared to columns packed with agglomerated slurries.[2,22] Non-optimal slurry concentrations can give arise to fronting peaks.[22] In packing optimization, all these factors must be addressed.

1.1.2.2 Controlling Extracolumn Band Broadening

To accomplish ultrafast separations, it is crucial to select correct column dimensions since retention time, and resolution is compromised with very short columns are used. Extracolumn band broadening has a significant effect on efficiency in ultrafast chromatography since columns as short as 0.5 cm are utilized. In general, early eluting peaks are impacted by extra column band broadening more than the late eluting peaks. Consequently, in ultra-fast separations, special attention must be paid to minimize extra column band broadening as much as possible. Therefore, UHPLC is the instrument of choice for ultra-fast separations rather than ordinary HPLC. The primary sources of extra column dispersion are the detector cell and connection tubings. Furthermore, the injection needle and needle seat volume also have a considerable contribution to extracolumn band broadening. Narrow diameter connection tubing such as Thermo NanoViper (75 µm ID), and Agilent A-Line (75 µm ID) can be utilized at the cost of elevated back pressure to

minimize connection tubing volume. Further required instrument modifications will be discussed in Chapter 5.

1.1.2.3 Detector Settings

A chromatogram is a concentration profile over time. The detector should be able to exactly track the analyte concentration as it is coming off from the column. In modern state of the art HPLC/UHPLC systems, the user has a certain degree of freedom to choose detector parameters such as sampling frequency (number of data points collected per second) and response time (time for the signal to increase from 10% to 90%). Recently it has been reported that sampling frequency and rise time has an effect on peak shapes and these parameters play an important role in ultrafast separations.[11]

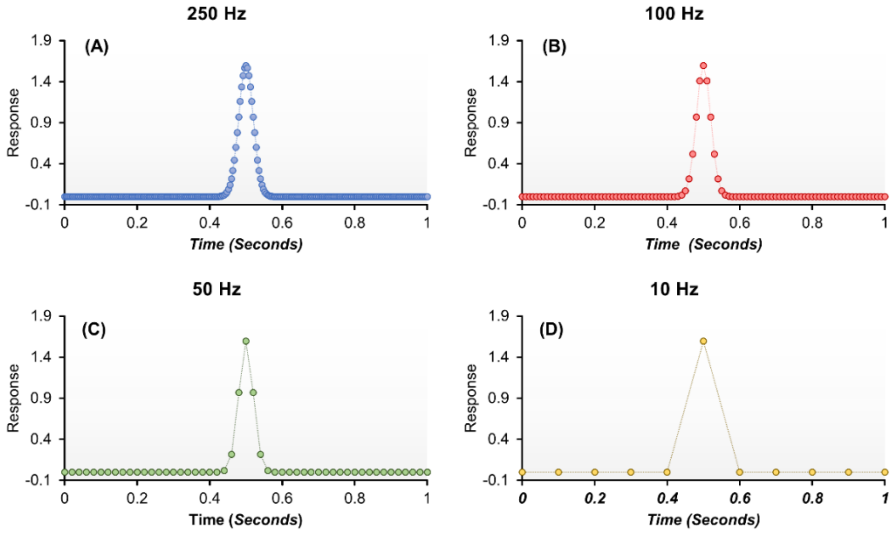

Figure 1.2 Effect of sampling frequency on the output signal in sub-second chromatography. Chromatograms are simulated with appropriate sampling frequency on Microsoft Excel 2016. Standard deviation at the time domain is set to be 0.02 s.

Figure 1.2 shows chromatographic peak profiles detected at different sampling frequencies. At 50 Hz and 10 Hz (Figure 1.2c and d) distorted peak shapes are observed (Compare with 250 Hz and 100 Hz (Figure 1.2a and b)). Therefore, permanent data loss occurs. The required sampling frequency is determined as described by the sampling theorem. [23] According to the sampling theorem, a continuous time signal is represented and recovered when the sampling frequency is greater than or equal to the twice the highest frequency component of the parent signal. [23] When the sampling frequency is above the required sampling frequency, noisy baselines are expected. In general, higher sampling frequencies are advantageous in ultrafast chromatography. Increased baseline noise during over sampling can alter qualitative and quantitative detection limits during trace analysis. Therefore, the determination of the right sampling frequency is crucial in any analysis.

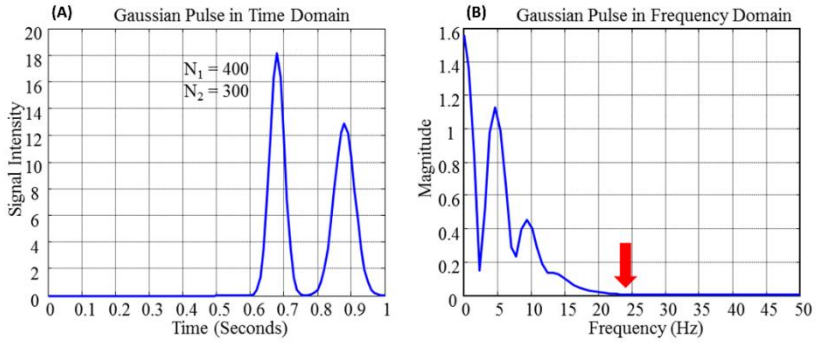

Figure 1.3 Computer simulation of a hypothetical separation under a second in (A) time domain and (B) frequency domain via Fourier analysis.

Sampling frequencies and efficiencies required for sub-second separation can be studied via computer simulations as shown in Figure 1.3 (MATLAB version 7.110.854 (Mathworks, Natick, MA)). Fourier analysis of the signal (Figure 1.3.B) discloses the

maximum frequency component of the original signal (sub-second chromatogram shown in Figure 1.3.A) to be 25 Hz. Therefore, according to the sampling theorem minimum of 50 Hz (25 Hz x 2) sampling frequency must be acquired in ultrafast chromatography. State of the art HPLC/UHPLCs provide a range of sampling frequencies, mostly sampling frequency up to 160 Hz – 250 Hz. Some instrumentation designs allow the user to choose sampling frequency and rise time/response time independently (e.g., Thermo, Shimadzu) while others offer a pre-defined combination of sampling frequency and response time (e.g., Agilent). The effect of two very different sampling frequency and response time combinations on signal detection is demonstrated below (Figure 1.4). As a rule of thumb, the smaller response time, better the signal.

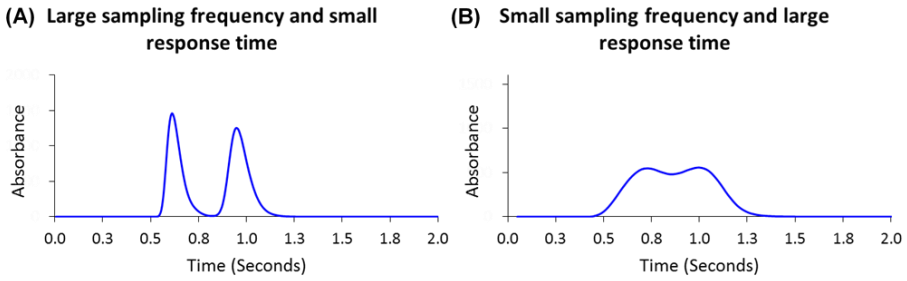

Figure 1.4 An schematic example of the effect of the choice of sampling frequency-response time

1.1.3 Applications of Ultrafast Chromatography

There are at least two important applications that require ultrafast chromatography. One is as the second dimension of two dimensional liquid chromatography (2D-LC) and another is high throughput screening for method development.

1.1.3.1 As the second dimension of 2D-LC

Two dimensional liquid chromatography is a powerful tool in separation sciences as it provides convenience to complex sample analysis. A typical 2D-LC instrumentation setup is shown in Figure 1.5

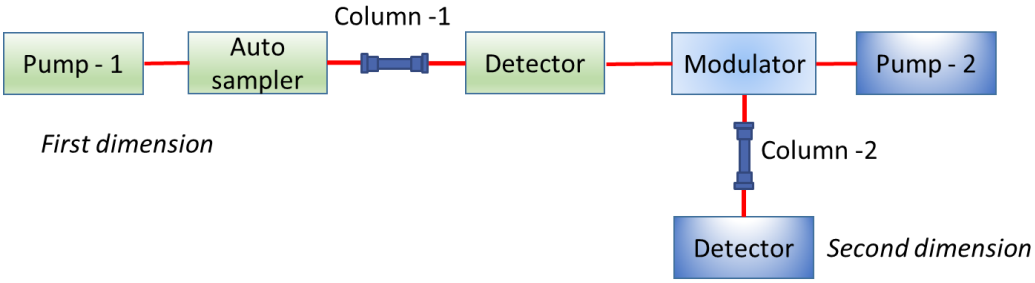

Figure 1.5 Conventional two dimensional liquid chromatography setup

Peak purity analysis is one of the main applications of 2D-LC. Samples of biological origin such as proteins are complex by nature. Most of the time single dimension separations do not provide enough resolution for successful analysis of complex samples. Therefore, comprehensive 2D-LC is utilized in most of the complex biological sample analysis. In comprehensive 2D-LC, the first dimension effluent is sequentially sampled and injected into the second dimension as sharp pulses by a modulator. This process is called modulation. In practice, the modulation period is limited to a few seconds. Usually, with higher the modulation rates, the quality of the separation increases. However, the second dimension run time should be less than the modulation period to avoid the occurrence of wrap round peaks.[24] Therefore, the second dimension should be able to provide extremely fast separations. Hence the proposed ultra-high efficiency columns will be an ideal choice for the comprehensive 2D-LC 2nd dimension.

1.1.3.2 High Throughput Screening

Achiral and chiral method development play a major role in screening and impurity profiling in drug discovery and product development processes. In most cases, classic separation methods are utilized such that the analysis times range from several minutes to hours. As the number of samples increases, the time required to complete the analysis also increases tremendously. Ultrafast chromatography is a great tool to increase the throughput as it increases the number of samples analyzed per unit time compared to traditional method development protocols. Its implementation is more economical compared to traditional techniques as much less solvent is consumed.

1.2 Development of Geopolymer Based Base-Stable Stationary Phase Media

Separation scientists continue to develop of new stationary phases with improved chromatographic figures of merits such as hydrolytic stability, different selectivity, higher efficiency, etc. to address some common issues in routine chromatographic method development. As shown in the schematic (Figure 1.6) when the peaks of interest (impurities) reside on the tail of the main peak, accurate quantitation is challenging as it is difficult to define the true baseline. (Figure 1.6A). Also, scaling the analytical HPLC method to a preparative liquid chromatography method to separate and isolate impurities is not facile with the separation shown in Figure 1.6.A. As an alternate, the separation can be obtained on a stationary phase with different selectivity as shown in Figure 1.6B where the small impurity peaks elute before the main peak.

Also, the HPLC result shown in Figure 1.6B is more easily transferred and scaled to preparative liquid chromatography for separation and isolation of impurities. Therefore,

availability of stationary phases with distinct selectivities is advantageous in addressing the above mentioned issues. Further, in 2D-LC orthogonality is one of the main measures of the quality of the separation. To maintain the orthogonality, distinct selectivities of the first dimension and the second dimension stationary phases are important. Availability of the stationary phases with distinct selectivities expands the method development capabilities in 2D-LC.

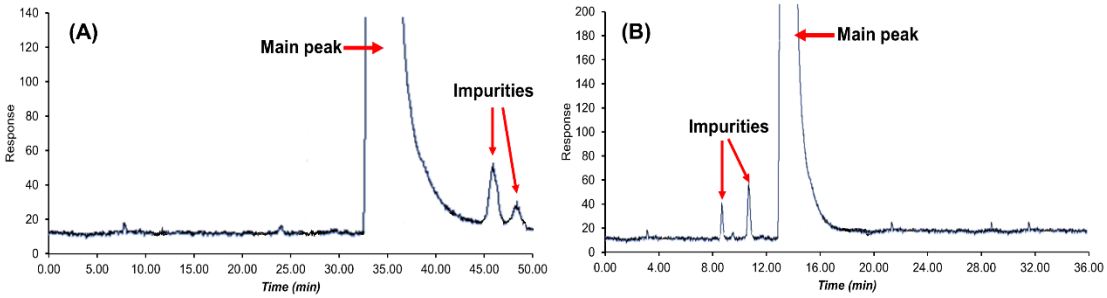

Figure 1.6 Baseline separation of impurities by utilizing stationary phases with different selectivity (Schematic representation)

1.2.1 What are Geopolymers?

Geopolymers are X-ray amorphous polycondensed aluminosilicates[25] with an array of interesting and unique chemical and physical properties such as excellent mechanical strength, chemical resistance, heat resistance etc.[26] Geopolymers have been used as construction materials, fire resistant materials, and sorbents for many years. [27] Due to their physicochemical nature, geopolymers make a promising chromatography stationary phase material. Although their comprehensive applications in separation

sciences has not been reported. One reason could be the fabrication of spherical geopolymer particles with micron level particle size has been extremely challenging. We report the first successful synthesis of spherical geopolymer micron size range particles and demonstrate their utilization in high performance liquid chromatography.

The reaction of solid aluminosilicate with concentrated aqueous alkali followed by a polycondensation reaction, results in solid geopolymers.[25] They consist of 3D polymeric network of -Si-O-Al- bonds.[28,29] The Al/Si ratio determines the microstructure and surface chemistry of the geopolymers.[28] Aluminum and silicon can be found as tetrahedrally coordinated Al^{3+} and Si^{4+}.[26,30,31] The overall negative charge arises from aluminates in the polymeric network and they are charge-balanced by the alkali metal counterions. [26,30,31]

1.2.2 Synthesis Aspects of Geopolymer Particles

There are multiple categories of geopolymers based on their starting materials such as metakaolin geopolymers and fly ash geopolymers. As its name implies, most of the starting materials arise from natural sources. Metakaolin is dehydroxylated kaolin while fly ash is an industrial waste. Since the composition of fly ash is not well defined,[28] we prefer metakaolin as starting material. The factors affecting the physiochemical properties of final geopolymer material are explained below.

Al/Si ratio – The elemental ratio of Al and Si in the geopolymer reaction mixture is crucial in controlling the mechanical strength of the final product. When higher Si/Al ratios are utilized, mechanical strength of the final material increased (Si/Al ratios of 1.15 to 2.15 have been reported in the literature). [29] The reason being Si-O bonds are stronger than Al-O bonds, when more Si is present, the population of Si-O is greater than Al-O bonds. [32]

Type of alkali – The most common types of alkali are sodium and potassium hydroxide. Potassium geopolymers are known to show better mechanical strength than sodium geopolymers.[32] When the geopolymers are synthesized using mixed alkali a remarkable change in the Al and Si ordering in the polymeric network is found.[29]

Temperature – Curing temperature also is an essential factor in tailoring physicochemical properties of geopolymers. The kinetics of geopolymerization reaction can be accelerated by higher curing temperatures which also enhances the mechanical strength. Typical curing temperatures vary from 35 ℃ – 100 ℃.[32,33] Based on our experimental observations sintering at high temperatures (≈ 500 ℃) via subjecting to slow temperature ramps can further increase the mechanical strength. Usually, geopolymers are synthesized in block form using a desired type of mold if necessary (Figure 1.7).

Figure 1.7 Metakaolin geopolymers synthesized in block form

A few attempts at geopolymer particle fabrication has been reported in the literature utilizing techniques such as thermal spray drying and ball milling geopolymer solid blocks.[30,34] They resulted in irregular particles or spherical particles in the millimeter size range making them less useful in chromatography. In this work, a novel synthetic scheme

has been implemented based on “reverse emulsion templating.” An edible oil has been utilized as the continuous phase, and the aqueous geopolymer mixture was used as the dispersed phase. The aqueous geopolymer reaction mixture contains an aluminosilicate source, fumed silica, and concentrated alkali such as KOH or NaOH. Excess base in the geopolymer reaction mixture reacts with the oil and produces glycerol and soap molecules. Therefore, the emulsion system is stabilized. Each aqueous droplet corresponds to a geopolymer particle. After the geopolymerization reaction reaches completion (≈ 8-72 hours), particles are extracted into water. Sintering at high temperatures increases the mechanical strength of the particles. Powder X-ray diffraction (Broad “structure” around 2θ) and energy dispersive spectroscopy analysis are confirmatory tests of the geopolymerization. Further characterization has been done using scanning electron microscopy, laser diffraction particle size analysis and pH titrations.

1.2.3 Chromatographic Performance

Given the hydrophilic nature of the geopolymers, they can be utilized in hydrophilic interaction liquid chromatography (HILIC), normal phase chromatography (NP), and supercritical fluid chromatography (SFC). In this work, we report the first comprehensive chromatographic assessment of geopolymers as a stationary phase media. Chromatographic features such as selectivity, hydrolytic stability, and efficiency of geopolymers are compared to silica, the most common chromatographic support. The geopolymer phases showed excellent pH stability (at basic pHs) and unique selectivity for a broad range of compounds compared to silica and other HILIC phases (Chapter 6).

1.2.4 Future Work

Geopolymers have a significant potential to be utilized in chromatography and as well as in different branches of the separation science. Different types of geopolymers can be synthesized utilizing various starting material. For instance, synthetic kaolin/metakaolin based geopolymers can be utilized to synthesize trace metal free geopolymers (Figure 1.8, Table 1.1). This is expected to produce improved peak shapes especially for nitrogen containing compounds.

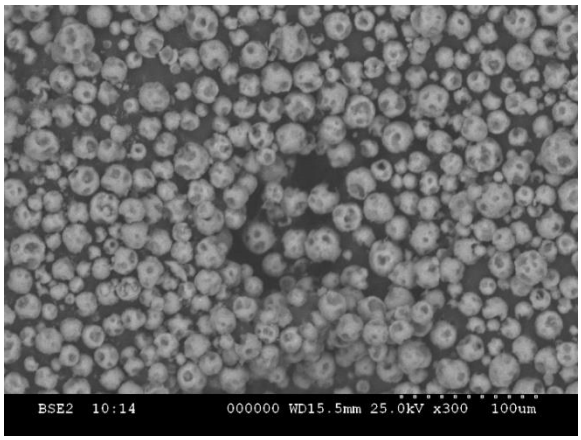

Figure 1.8 Scanning electron micrograph of geopolymer particles synthesized from high purity metakaolin form synthetic kaolin

As expected trace metal impurities were not observed in geopolymers synthesized from high pure metakaolin from synthetic kaolin. This topic is the subject of future work in our laboratory.

Table 1.1 Comparison of elemental composition of geopolymers synthesized from natural and synthetic starting material from energy dispersive X-ray spectroscopy

Element	Geopolymer from natural metakaolin Atom weight %	Metakaolin from high purity kaolin Atom weight %
O	50.05 ± 0.56	49.61 ± 0.56
Al	11.3 ± 0.19	12.97 ± 0.20
Si	27.07 ± 0.26	26.34 ± 0.26
K	10.03 ± 0.18	11.08 ± 0.20
Ti	0.54 ± 0.07	_
Fe	1.01 ± 0.11	_

1.3 Organization of Dissertation

The first section of this thesis will be related to fundamental studies of ultrafast chromatography. All the theory, practical implementations and recent advances in ultrafast chromatography will be discussed. Chapter 2 will be dedicated to addressing fundamentals behind HPLC column packing. In Chapter 3, high throughput and ultrafast separations in

hydrophilic interaction liquid chromatography are discussed. Hydroxypropyl β-cyclodextrin bonded SPP stationary phases have been evaluated in this regard. Chapter 4 examines the concept of high throughput and ultrafast separations in the septation of small biological molecules. Macrocyclic glycopeptide bonded SPP stationary phases have been evaluated, and development of fast tryptic peptide separation protocols have been discussed. In Chapter 5, liquid chromatographic separations under a second are discussed including instrument modifications and data processing.

The second part of this thesis will be related to the development of base-stable geopolymer chromatographic stationary phases. The novel geopolymer particle synthesis approaches will be discussed. Complete characterization of the material and chromatographic evaluations will be presented.

Chapter 2

FUNDAMENTAL AND PRACTICAL INSIGHTS ON THE PACKING OF MODERN HIGH-EFFICIENCY ANALYTICAL AND CAPILLARY COLUMNS

2.1 Abstract

New stationary phases are continuously developed for achieving higher efficiencies and unique selectivities. The performance of any new phase can only be assessed when the columns are effectively packed under high pressure to achieve a stable bed. The science of packing columns with stationary phases is one of the most crucial steps to achieve consistent and reproducible high-resolution separations. A poorly packed column can produce non-Gaussian peak shapes and lower detection sensitivities. Given the ever larger number of stationary phases, it is impossible to arrive at a single successful approach. Thecolumn packing process can be treated as science whose unified principles remain true regardless of the stationary phase chemistry. Phenomenologically, the column packing process can be considered as a constant pressure or constant flow high-pressure filtration of a suspension inside a column with a frit at the end. This process is dependent on the non-Newtonian suspension rheology of the slurry in which the particles are dispersed. This perspective lays out the basic principles and presents examples for researchers engaged in stationary phase development. This perspective provides an extensive set of slurry solvents, hardware designs, and a flowchart, a logical approach to optimal column packing, thus eliminating the trial and error approach commonly practiced today. In general, non-aggregating but high slurry concentrations of stationary phases tend

to produce well packed analytical columns with small particles. Conversely, C18 packed capillary columns are best packed using agglomerating solvents.

2.2 Introduction

Stationary phase development in separation science is an active and prolific research area. Once the stationary phase has been developed, the particles must be packed into columns to perform separations. A frustrating situation for a researcher arises when the desired selectivity is achieved but the column efficiency, measured as the reduced plate height h (plate height H/particle diameter dp), turns out to be greater than 2 along with a non-Gaussian peak shape. A range of chromatographic materials have been developed such as bare silica, modified silica, non-porous or macroporous polymers, inorganic oxides (TiO2, Al2O3, and ZrO2),[35-37] carbon coated silica,[38,39] diamonds, boron doped diamonds,[40] and porous graphitic carbon.[41,42]In Figure 2.1, we show the scanning electron micrographs (SEM) of several particle morphologies namely, fully porous sub-2 µm silica (FPP), 2.7 µm superficially porous silica (SPP), latex coated sulfonated polymer, and 5 µm porous graphitic carbon.[43] To overcome packing challenges, a thorough understanding of the properties of suspensions and hardware design is required. Several properties are desirable for a packed column such as Gaussian peaks with $h \leq 2$, and a mechanically stable bed which can survive 500-1000 injections. This perspective highlights the current scientific understanding along with our own experience with 20 different stationary phases (the list appears in the SI), provides insights in packing small particles of various polar and non-polar chemistries from the literature and from other practitioners.

These approaches were developed over the course of packing several hundreds of columns in various dimensions

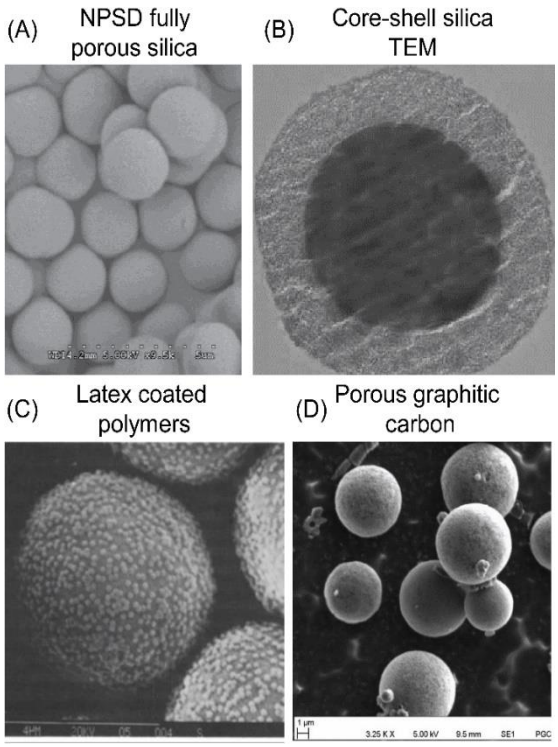

.

Figure 2.1 Scanning (SEM) and transmission (TEM) electron micrographs of various stationary phases (A) SEM of narrow particle size distribution (NPSD) 1.9 µm fully porous silica (9500x), (B) TEM of 3.6 µm superficially porous silica (shell thickness 0.5 µm) adapted from ref 99 with permission from Phenomenex, (C) 5 µm latex coated sulfonated styrene divinylbenzene (9000x) adapted from ref with permission from Elsevier, (D) 5 µm porous graphitic carbon (3250x), adapted from ref Copyright 2013 American Chemical Society.

2.3 Experimental, Results and Discussion

2.3.1 Phenomenological Understanding of the Slurry Packing Process.

The column packing process is a pressure filtration of a suspension into a cylindrical mirror polished tube with a frit at the end (Figure 2.2).

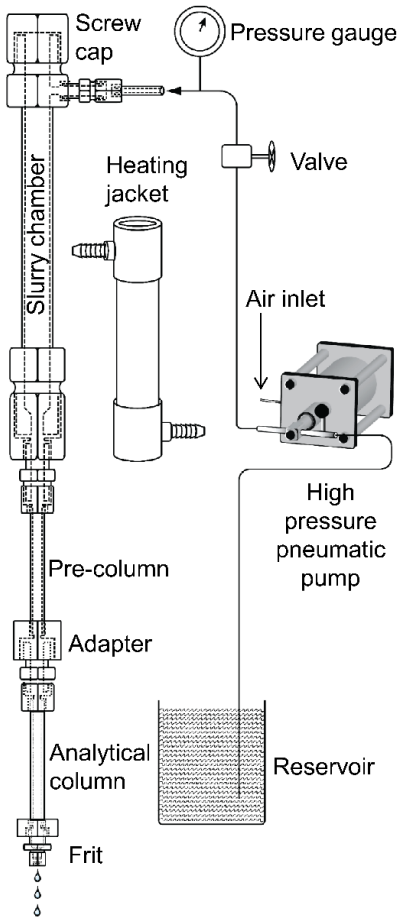

Figure 2. A downward slurry packing system for packing analytical columns (up to 20,000 psi). The connection tubings are connected by a collar and gland type or Swagelok fittings. The pre-column should be at least 5-10 cm long with the same i.d. as the column being packed.

The force of filtration is obtained from a pump which can operate in a constant pressure or constant flow mode. The current understanding of the slurry packing process of columns is far from complete because it is difficult to model suspension rheology, particle to wall friction, and behavior of the particle solvent interface under extreme pressures ranging from 4000 to 30,000 psi. As the bed of particles is formed, the secondary consolidation processes take place to make a tighter bed under pressure.[44] The pressure is such that it is 2-3 times the expected pressure on the chromatograph. After the column is packed, the pressure is removed and the column is capped. There are numerous column geometries with the options of construction materials such as stainless steel, polyether ether ketone (PEEK), and PEEK or glass lined stainless steel tubes. The column nomenclature is typically classified as capillaries (20 μm to < 1 mm i.d.), microbore (1 - < 2.1 mm i.d.), narrow bore (> 2.1 - 3.9 mm i.d.), and normal bore columns (3.9 - 5 mm i.d.). Preparative columns employ slurry packing or mechanical approaches such as dynamic axial packing or radial compression to obtain high efficiency preparative columns and will not be considered here.[45]

2.3.2 Hardware Design Considerations.

Well-designed column packing hardware is critical to achieve high efficiency columns in any format. Figure 2.2 is a schematic of the hardware: a solvent reservoir connects to an ultrahigh pressure pump which pushes the suspension of particles held in a slurry chamber attached to a pre-column and an empty column. Under pressure, a tightly packed bed builds up in a dynamic fashion (with an axial density gradient of particle concentration). We prefer pneumatically driven pumps (30,000 psi max.) which operate in a constant pressure mode. The main drawback of penumatic pumps is the large pressure pulsations during the “breathing cycle” of piston strokes. Electrically driven piston pumps

(up to 18,000-25,000 psi) can also used either in constant flow or constant pressure mode. If accurate flow rates are required, up to 30,000 psi, specially designed syringe pumps can be used. Typically 10, 20, 40, and 80 mL slurry chambers with 1.4 cm (or narrower) i.d. are employed for 2.1 to 4.6 mm i.d. columns. Verzele[46] achieved maximum efficiency when the geometries of the slurry chamber and the column matched. It is important to match the pre-column diameter extending from the slurry chamber with the column for a smooth transition of the suspension into the column. Any disturbance by a poor design/bent tubing, damaged seals usually leads to a failed column.

The slurry chamber can be externally heated by circulating hot water as shown in Figure 2.2 using a heating jacket.[43] For the slurry chamber design, the pushing liquid can be made to enter the chamber at a 90^{o} angle rather than vertically. If vertical entrance is preferred, a flow distributor which distributes the liquid in horizontal directions is used. The logic behind this design is to prevent rapid mixing of the suspension with the pushing solvent. The outlet frit retains the stationary phase inside the column during packing. Frits should be chosen to withstand pressures (4000-30,000 psi) during column packing. The theoretical importance of frit designs and flow distribution properties is discussed elsewhere and it should be ensured to use high quality frits made from small sintered particles.[47]

The packing methods for capillaries usually involves high pressures (5,000-40,000 psi) using pneumatically driven pumps.[48] Alternatively, for capillary packing, a high pressure generator is a manually operated piston screw pump can also be employed (High Pressure Equipment Company, PA). These pumps can compress small volumes of liquids (< 100 mL) to extremely high pressures without producing pressure pulses. A schematic

of a custom designed system is shown in Figure 2.3 which is based on the system designed by Jorgenson.[49]

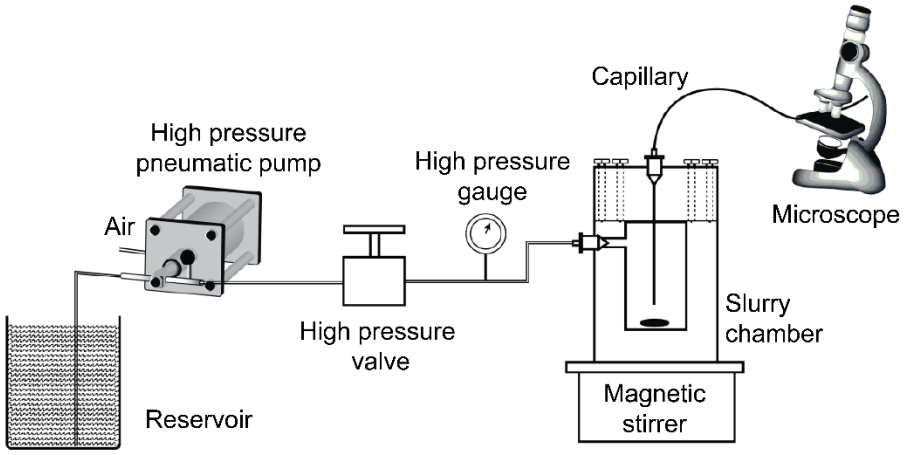

Figure 2.3 A high-pressure upward slurry packing system for capillaries (up to 30,000-60,000 psi). The microscope can be used for examining the bed as the capillary is being packed.

The capillary is placed in a small suspension chamber (stirred with a small magnetic bead), and high pressure is applied from a pneumatic pump directly to a bolted chamber. The packing behavior can be monitored by an optical microscope. For packing capillary columns, the column frits are often prepared in-house by the Kasil frit method and other techniques.[50] Additionally, the capillaries can also be packed in a downward fashion without a stir bar just like an analytical column. The key requirement in such design is to have a precision engineered bore in the outlet, matching the i.d. of the capillary. This allows smooth transition of the suspension of the particles into the capillary rather than clogging the capillary head (a common problem). Capillaries are often sonicated during packing. Several commercial slurry chamber designs have pressure limitations of 9000 psi and

utilize He gas to push the solvent through capillaries. The readers can consult the classic work on high pressure hardware design by Spain and Paauwe.[51]

2.3.3 Fundamental Insights into the Slurry Packing Process.

The following sections describe the theoretical considerations in the column packing process to achieve good results.

2.3.3.1 Particle Size Distribution and its Role in Column Performance.

The concept of "reported" particle diameter is rather complex and there are several ways to express the particle size. To theoretically estimate h, the true particle diameter must be known for making any judgements on the packing procedure. The Sauter diameter d_{Sauter} is commonly used for quoting chromatographic particle sizes. It represents the diameter of a sphere that has the same volume to surface area ratio as a particle and it is defined as:[52]

$$d_{Sauter} = \frac{\sum n_i d_{p,i}^3}{\sum n_i d_{p,i}^2} \quad \text{.....Equation 2.1}$$

Where n is the number of particles and d_p is the particle diameter. The Sauter diameter is easily determined by Coulter-counter techniques.[52] One may employ scanning electron microscopy (SEM) and measure the particle diameter, e.g. by using ImageJ software for n >500 followed by using the equation (2.1).[53] It will be clear from Figure 1 that there is no "unique" particle size and, at times, there is a significant departure from the nominal particle size. Another specification for size distribution is the percentile ratio, d_{90}/d_{10}; where d_{90} and d_{10} are the particle diameter at 90th and 10th percentile of the particle size distribution (PSD),

respectively. The closer the value of d_{90}/d_{10} is to unity, the narrower is the particle size distribution. Commercial stationary phase particles rarely come close to d_{90}/d_{10} of unity. Titan particles (1.9 µm , Supelco, Sigma-Aldrich) marketed as “monodisperse” silica have a d_{90}/d_{10} ~ 1.3, while other suppliers for sub-2 µm silica have even higher ratios.[54] The larger size distribution can have a very significant effect on the bed density and affect the efficiency in deleterious ways (as per recent reports)[55,56] or beneficial ways (e.g. having a small percentage of large particles).[57] Sometimes adding 5-10% of larger particles than the nominal size being packed implemented in practice to ease the packing process.[49]

2.3.3.2 Role of Stationary Phase Fines in a Column Performance.

Fines refer to very small spherical or irregular particles found in particulate materials (e.g. in Figure 2.1D). The problems in particle size distribution mainly arise if smaller particles (and fines) are the major cause of size distribution rather than larger particles. Higher back-pressure than expected from the nominal size is observed in such cases. A study on fines concluded that “*it is not so much the width or span of the particle size distribution, but rather the presence of fines that greatly determines the chromatographic performance of particulate columns*.”[55] SEM will reveal the quality of the particles, presence of debris or foreign material before and after synthesis. If magnetic bars are used for small scale synthesis, some particles may be crushed by mechanical/grinding forces. This is true for soft materials or silica of low mechanical strength, porous graphitic carbon, or coated particles such as carbon clad zirconia etc.

2.3.3.4 Picking Suspension Solvents for a Given Stationary Phase.

Choosing the right and stable suspension medium for given particles is very important for successful packing. The term “stable” suspension refers to the fact that the critical suspension properties do not change significantly in a given time-frame of the column packing process. All suspensions are thermodynamically unstable but may be kinetically resistant to settling (compare the stability of colloids).[58] Table 1 shows an extensive summary of slurry solvents utilized in packing for various surface chemistries. It is also useful to consider wettability, dispersion state, viscosity, density of the solvent, and shear thickening/ thinning properties before finalizing the choices (*vide infra*).

Table 2.1 A guide to choosing slurry solvents for capillary and analytical columns. Suspension with chosen solvent should be examined by optical microscopy.

(a)	**Silica**: MeOH[59,60], IPA[61-63], Acetone,[61,64,65] 70:30 IPA:MeOH, 1:1 5% Tween 20:ethylene glycol,[66] 50/2.5/47.5 ethylene glycol/Tween 20/Water,[67] IPA:CCl_4
(b)	**Cyano Silica Phases**: Anhydrous EtOH[61], (50:50) → (90:10) Toluene:IPA,[61]
(c)	**Reversed Phase Silica Phases (C18 type)**: 50:50 MeOH:IPA[68,69], 1:1 paraffin:CCl_4,[69-71] Acetone,[72-75] 1:2 acetone:hexane,[76] $CHCl_3$,[72,77] 80:20 $CHCl_3$:MeOH (with acidic additives), 95% EtOH:n-propanol:toluene 1:1:1(v/v) **Reversed Phase Silica Phases (C4/C8 type)**: Anhydrous EtOH[61], Anhydrous IPA,[61,71,72] 50:50 Acetone: IPA,[61] (50:50) → (90:10) THF:IPA[61]
(d)	**Silica based HILIC Phases including Amino Silica and Sugar Bonded Phases**: 98:2 ACN: 1M NH_4NO_3, 70:30 Dichloromethane:MeOH, (50:50 → 90:10) Toluene/IPA[61]

(e)	**Polymeric Ion-Exchangers/ Stationary Phases**: Pure deionized water (heated slurries),[43,78] 2:1 Acetone:H_2O,[79] Acetic acid/ethylene diamine/polyethylene glycol/mono(nonylphenyl)ether in DI water[80], Note: *Polymeric phases usually swell in organic solvents unless highly cross-linked*
(f)	**Carbon Based Phases including Porous Graphitic Carbon**: MeOH[81], dichloromethane[82], neutral surfactants such as Igepal in water **Modified hydrophilic PGC**: Pure deionized water[81]
(g)	**Hybrid Materials:** Carbon coated zirconia (IPA), Carbon coated silica (N-methylpyrrolidone), Polymer coated zirconia (IPA, 50:50 IPA:THF), Core-shell diamonds (50:50 acetone:water)
(f)	**Additional Successful Blends for Dispersing Stationary Phases**: 50:50 IPA:THF, 50:50 IPA:acetone, 50:50 MeOH:acetone, 50:50 IPA:chloroform with organic acid additives such as formic acid, 80:20 MeOH:cyclohexanol, 80:20 MeOH:glycerol, 80:20 EtOH-cyclohexanol, 80:20 1-butanol cyclohexanol, 80:20 EtOH-anhydrous dimethylsulfoxide, 50:50 MeOH:dioxane, 85:15 Dichloromethane: MeOH, Acetone:Dichloromethane, butanol:dimethylsufoxide, pure acetone (the ratios can be varied depending on achieving a dispersed state)

2.3.3.5 Wettability and Surface Energies.

One of the most obvious requirements is to choose a solvent which will wet the stationary phase surfaces. An incorrect match leads to “creaming” i.e. the stationary phase

rises to the surface. For example, water will not wet C18 silica, or a carbonaceous phase (see pictures in SI); the stationary phases keeps floating on the surface despite having higher densities than water. The wetting process originates from a balance of surface forces. Thermodynamically, if the spreading coefficient *S*, as defined in equation (2)[83,84], is positive, then wetting will occur spontaneously. Here γ represents surface energies, the subscripts *S* refers to solid and *L* refers to liquid phases, and LS represents the liquid-solid interface.

$$S = \gamma_S - (\gamma_L + \gamma_{LS}) \quad \text{.....Equation 2.2}$$

Harkins and Feldman[83] noted that free surface energy of solids is usually larger than liquids e.g. silica has a surface energy (γ_S) of 287 mJ/m^2, whereas water has surface energy of 72.2 mJ/m^2, the spreading coefficient is likely to be positive assuming γ_{LS} to be small.[85] Silica is indeed thoroughly wetted by water. Organic materials such as polymeric phases have usually lower surface energies than inorganic materials. In other cases, especially for aqueous dispersions, wetting agents such as neutral, cationic, or anionic surfactants will usually lower γ_L and γ_{LS}. For instance, porous graphitic carbon phase (PGC), which is not wettable by water at all, forms a stable suspension in the presence of neutral surfactants such as Igepal. As Table 2.1 shows, surfactants such as Tween 20 (polyoxyethylene-sorbitan monolaurate), Igepal DM-970, sodium lauryl sulfate, and polyethyleneglycol mono(nonylphenyl) ether have led to significant improvement for packing C18 silica, bare silica, and ion-exchange resins in narrow bore tubes as well as capillaries.[66,67,80] Note that adding the surfactants may not be the first priority, since wetting agents not only affect the surface tension and viscosity but can also lead to an unstable suspension. Kirkland pointed out a very interesting solvent: hexafluoro-2-propanol (HFIP) which he termed as a "universal" slurry medium.[86] He postulated that the reason for the capability of HFIP to

handle a wide variety of stationary phase types is that the molecule has low surface energy at one end from the halogen atoms, and high surface energy (hydroxyl groups) at the other side of HFIP. Thus, HFIP can "energy match" various stationary phase chemistries. Thus, Kirkland concluded "*high surface energy, polar unmodified silica requires methanol or some other high surface energy or polar solvent. Modified particles with much lower surface energy, such as C8 or C18 (which still contains many polar unreacted silanol groups), should be packed with a lower surface energy, less polar solvent such as tetrahydrofuran, methyl-t-butyl ether, or mixtures such as acetonitrile/chloroform*."[86]

2.3.3.6 Viscosity and Density Considerations of Solvents and the Suspension.

The viscosity and density of the solvent(s) both contribute to the suspension stability as predicted by the Stokes law on settling velocity *v*. For a suspension of porous particles of finite concentration, the settling velocity *v* is:

$$v = \frac{(1-\varphi)^{-\kappa}\, d_p^2\{\varrho_p(1-\varepsilon_i)+\varrho_l(\varepsilon_f-1)\}g}{18\eta} \quad \text{.....Equation 2.3}$$

Where $(1-\varphi)^{-\kappa}$ a hindered settling is function of particles in suspension of volume fraction φ, ϱ_p and ϱ_l are the densities of the particle skeleton and the liquid, η is the viscosity of the liquid, and g is the gravitational constant. The ε_i is the particle porosity and ε_f is the fraction of a total particle volume.[87] The particle skeleton densities can be measured with a He based stereopycnometer.[87] The skeleton density of porous silica is 1.98-2.19 gm/cm^3.[87] From an examination of the modified Stokes law (equation 2.3) for the settling of porous particles, it is clear that a lower particle density and a higher solvent viscosity will prevent settling. This concept led to use of balanced density methods (now obsolete because of toxicity concerns of brominated solvents). A better metric for choosing solvents systems is their kinematic viscosity $\frac{\eta}{\rho}$ rather than individual density or viscosity values e.g. acetone,

chloroform, methanol, and isopropanol (IPA) have kinematic viscosities of 0.41, 0.38, 0.745, and 2.7 cSt, respectively. Thus, a suspension made in pure IPA will settle very slowly, but it will also be very viscous and will pack extremely slowly with small particles. Often peak shoulders are observed in very viscous suspensions when packed at medium pressures of 10,000 psi. Binary solvent mixtures offer greater flexibility in tuning the density, viscosity and surface energies of the slurry system. For example, adding acetone to IPA in 1:1 ratio would bring its viscosity from 2.6 down to ~ 0.6 cSt which can offer higher flow rates under constant pressure packing. Perhaps, the "universal" nature of hexafluoro-2-propanol (HFIP) as a suspension medium is due to its high density 1.596 g/mL which is closer to silica and low viscosity 1.03 cP (compare from water 1 cP).

2.3.3.7 Non-Newtonian Behavior of Suspensions.

In the previous section, the physicochemical properties of neat solvents or their mixtures were highlighted. The particle concentration affects the surface tension as well as the viscosity of the suspension.[88] If we express volume fraction ϕ of particles in a suspension as the $volume\ occupied\ by\ particles/total\ supension\ volume$, then the relative viscosity η_{rel} (compared with the pure solvent system), as the particle concentration increases, the relative viscosity of suspension becomes a higher order polynomial function as shown in equation 4.[89]

$$\eta_{rel}=1+B\phi+B_1\phi^2+\ldots\ldots\ldots\ldots\ldots\ldots\ldots\ldots\ldots\ldots\ldots\ldots\ldots\ldots\ldots\ldots\text{Equation 2.4}$$

Where, B is a constant. This relationship shows a faster viscosity increase as the particle concentration is increased. In reality, most suspensions are non-Newtonian which implies that their viscosity is dependent on the flow rate (or shear rate). One can estimate the shear

stress τ and the wall shear rate $\dot{\gamma}$ under constant velocity conditions with a pressure drop ΔP in a tube of radius *r* and flow rate of *V/t*.:[90]

$$\tau = \frac{\Delta P r}{2L} \qquad \dot{\gamma} = \frac{4}{\pi r^3}\left(\frac{V}{t}\right) \quad \text{.....Equation 2.5}$$

Only three papers have paid attention to practical rheology, in detail, in column packing and with non-Newtonian suspension behavior.[43,67,90] The suspensions which become very viscous with flow rate are shear thickening and the ones which drop the viscosity are shear thinning (Figure 2.4).

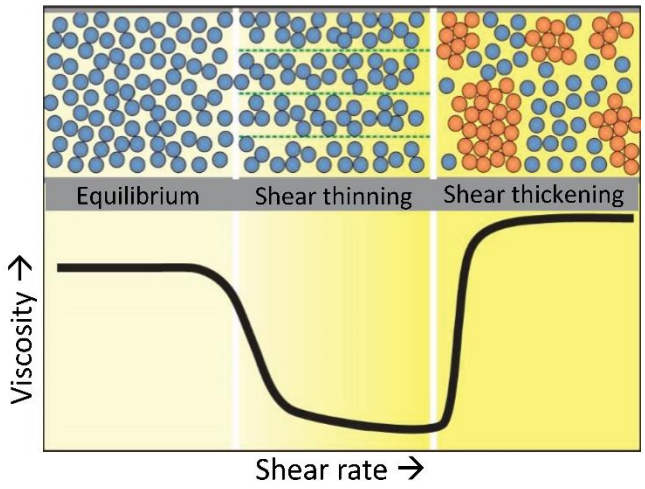

Figure 4. The change in the microstructure of a suspension explains the transition to shear thinning and shear thickening. In equilibrium, random collisions among particles make them naturally resistant to flow. But as the shear rate increases, particles become organized in the flow, which lowers their viscosity (shear thinning). At yet higher shear rates, hydrodynamic interactions between particles dominate over random collisions and the viscosity increases significantly (shear thickening). Adapted from ref [91] with permission from the American Institute of Physics.

Paradoxically, *all* non-aggregating solid suspensions, which often produce the highest plates, display reversible shear thickening under the right conditions.[92] These conditions are dependent on particle properties (size distribution, shape, particle-particle interactions), continuous phase viscosity and the nature of suspension deformation (extensional or shear type).[92] On the other hand, agglomerated suspensions can have permanent clusters (flocculates), and are typically shear thinning. Light scattering experiments (using Bragg diffraction) have shown that there is microstructural changes when suspensions make transitions from Newtonian to non-Newtonian behavior; these changes are referred to flow induced order-disorder transitions (Figure 3.4).[89] The term hydroclusters is used to describe this localized flow induced suspension density variations (which can form in protic/aprotic solvents). These rheological ideas are summarized by Barnes.[92]

2.3.3.8 Fundamental Problems with Narrow Diameter Columns.

Herein a fundamental issue with narrow diameter columns is highlighted, which are increasingly becoming popular because of LC-MS compatibility. Improved detection sensitivity (less dilution of the injected band) when operated at the same linear velocity as a wider bore column, saving of solvent and expensive stationary phase are additional benefits. Unfortunately, narrow bore columns present significant theoretical and practical challenges. From the following equation (6) obtained from solving the diffusion problem in 3 dimensions in an empty tube, two critical problems in narrow bore columns are discussed.[93]

$$C(r,z,t)=\frac{M}{(4\pi t)^{3/2}D_t\sqrt{D_a}}\exp\left[\frac{-(z-ut)^2}{4D_a t}-\frac{r^2}{4D_t t}\right] \quad \text{.....Equation 2.6}$$

Where *C* is the analyte concentration, *r, z* are radial and axial coordinates at time *t*, *M* is injected mass, D_t is the dispersion coefficient in the radial direction and D_a is the dispersion coefficient in the axial direction, *u* is the linear velocity. The first problem pertains to the limiting case of the last term in the equation 6, $(4D_t * dead\ time) \ll r_c^2$, where r_c is the column radius. This situation corresponds to the elution time being smaller than the time to "see and explore" the total radius of the column. Herein, the influence of packing heterogeneities near the wall is negligible but the flow path distribution at the inlet and the outlet of the column is not (hence the importance of frits). The problem is clearly illustrated in Figure 2.5, where the low retention band traveling in center has a separate velocity as well as a separate band shape compared to the wall.

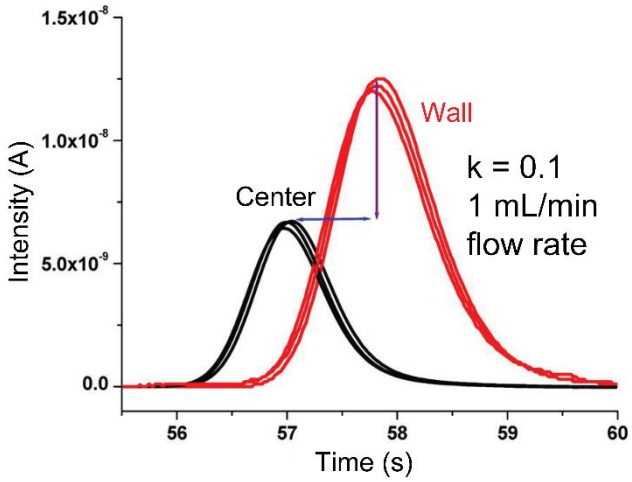

Figure 2.5 The velocity bias between the wall region and the center of a radially heterogeneous packed bed (packed by the manufacturer). Sample: *p*-benzoquinone, recorded by electrochemical detection at the center and the wall of the outlet frit. Column: 10x0.46 cm i.d. Kinetex-C18 2.6 µm SPP. MP: 30/70 water/methanol, k = 0.1. Adapted from reference [93]. Copyright 2013 American Chemical Society

It is now well established as to why a non-Gaussian peak shapes arise due to velocity bias around the column walls.[94] It can be shown that there is significant velocity bias in the center and the wall by implanting electrochemical detectors at radial positions on the column outlet.[93] Such wall effects were well known in chemical engineering 50 years ago.[95] The "wall region" extends to 30-50 particle diameters. Conversely, if $(4D_t * dead\ time) > > r_c^2$, this implies that solute spends enough time in the column to reach radial equilibration and “see and explore” the walls. This case pertains to narrow (capillary like) columns. Counterintuitively, one rarely sees fronting or tailing in packed capillaries, rather the peaks are symmetrically broad.[49] Any distortion introduced by the heterogeneity near the walls is compensated by the trans-column diffusion. Two types of wall effects were recognized and understood much later in chromatography.[96] The first is the geometrical wall effect just because the particles cannot penetrate the walls; the second wall effect is the oscillation in the porosity of the bed as one goes from wall towards the center.[97,98]

2.3.4 Practical Insights into Packing High Efficiency Analytical and Capillary Columns.

This section will discuss the practical considerations in slurry packing of capillary and analytical columns while providing a useful set of guidelines. These concepts have been developed after an experience of packing of over 17 different surface chemistries. The chemistries comprise chiral, HILIC, polymeric, reverse phases, silica based ion-exchangers, zwitterionic phases, porous graphitic carbon, and carbon clad zirconia particles in analytical/narrow bore formats. The flow chart in Figure 2.6 is a general outline for packing when starting with a new stationary phase. If *a priori* information on the packing procedure is not available, one can start by picking 5 slurry solvents (use HPLC grade/anhydrous solvents) from Table 2.1 after thoroughly cleaning, defining, and drying

(if applicable) the stationary phase and the hardware. It may be useful to determine the charge on the stationary phase, if dealing with hydrophilic chemistries or polar chemistries by zeta potential measurements. Fines, if visible in the SEM, can be removed by suspending the stationary phase in a low viscosity solvent. ***A note of caution*:** Presence of moisture in the stationary phase, high humidity, or moisture in the hardware can result in poor efficiency especially with halogenated solvents because of particle aggregation.[99] For some charged polymeric phases, organic solvents cannot be employed (because of swelling), there even pure deionized water as suspension medium can produce reduced plate heights of < 2.[43]

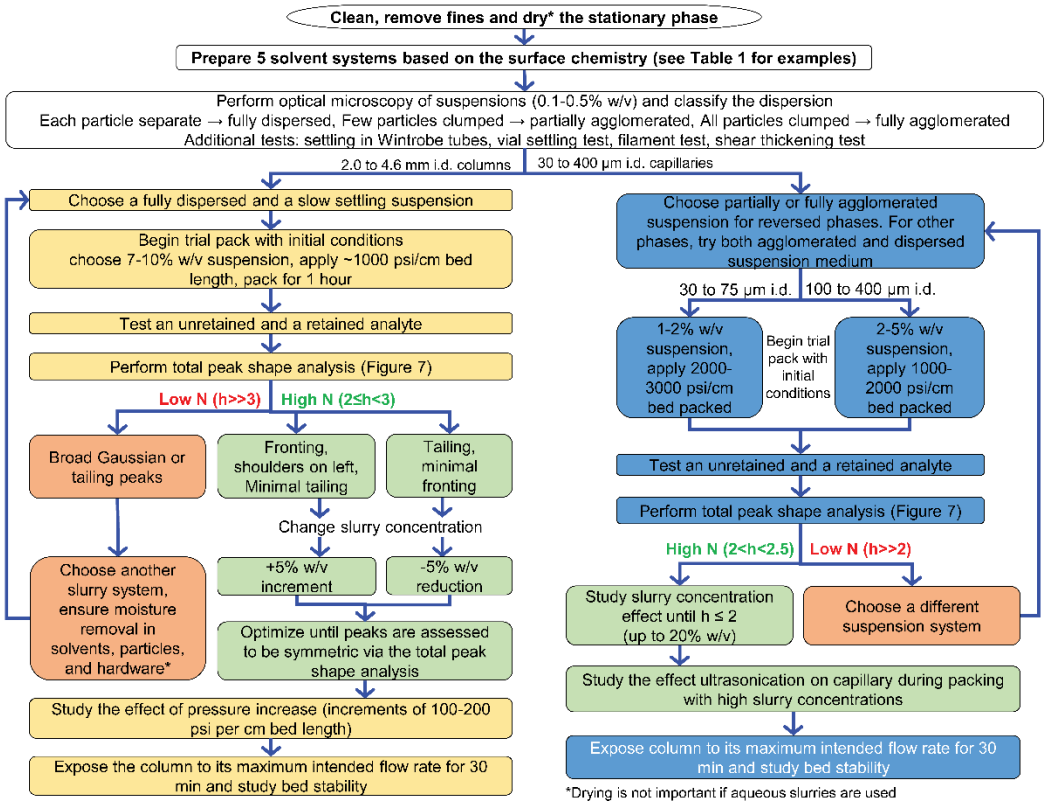

Figure 2.6 The flow chart for logical optimization of slurry packing.

Once a suitable choice of the solvent system is made from preliminary judgements of density, viscosity, and wettability; optical microscopy of the suspensions should be performed. It is the most useful qualitative predictor of packed column's performance. Figure 2.7 shows a comparison of microscopic images of two silica and a polymeric stationary phase in dispersed and agglomerated forms.

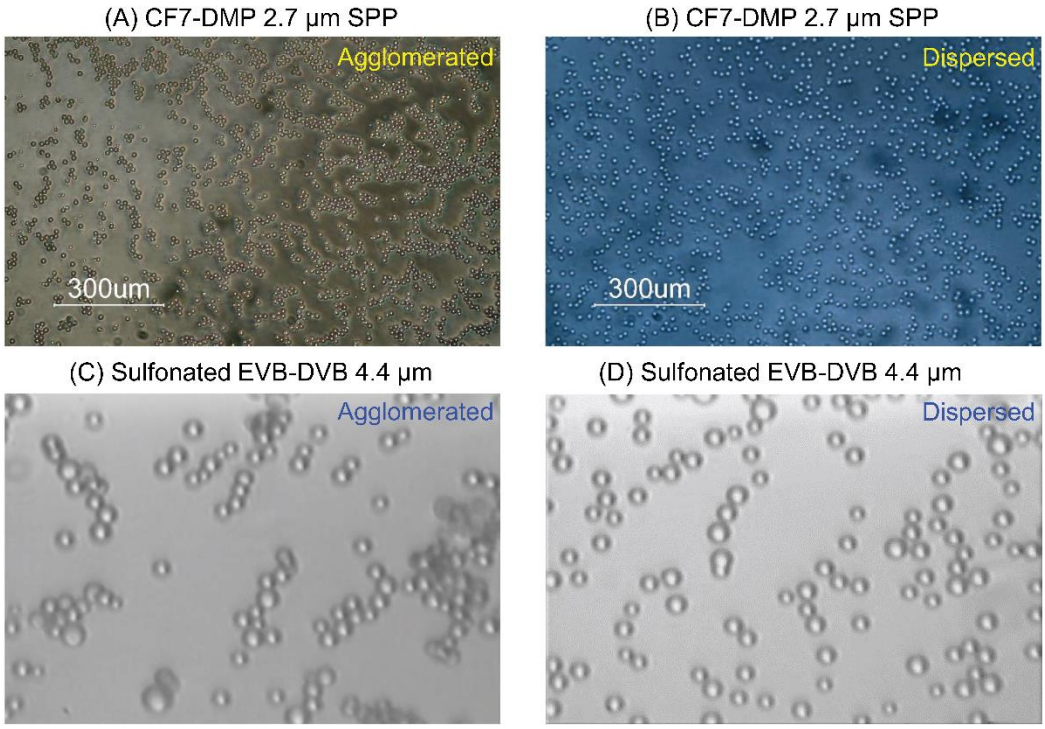

Figure 6. Optical microscopy of stationary phase suspensions. Derivatized cyclofructan-7 bonded to 2.7 µm SPP in (A) 98:2 methanol: 1M NH_4OAc – agglomerated slurry and (B) 1:1 $CHCl_3$:IPA – dispersed slurry. A suspension of 4.4 µm non-porous sulfonated ethylvinylbenzene-divinylbenzene in (C) 0.1M $MgCl_2$ – agglomerated slurry and (D) Deionized water – dispersed slurry.

To perform optical microscopy, place few drops of a dilute suspension and observe the suspension near the edges of the cover slip. The evaporating liquid (at the air interface)

causes motion in the suspension and one can easily see how the particles would travel during the column packing process. One major problem occurs when the solvent's refractive index matches with that of silica (e.g. CCl_4 + silica). In such cases, small amounts of other solvents can be added until the particles are visible. A slurry that promotes dispersion of particles would pack in a "layer by layer" fashion forming a random closed packed structure and resulting in a tightly packed high-efficiency column at high flow rates. Oppositely, an agglomerated slurry can induce packing of stationary phase particles in clusters leading voids in the beds. For capillaries, we wish to point out a stark difference for C18, where agglomerated suspensions followed by sonication have produced the best results.[48,60] Unfortunately, there are very few packing details published on other stationary phase chemistries in capillaries. For now, it may be useful to keep the "world" of capillaries separate from the narrow bore and analytical columns.

A settling test or vial test,[43] should be performed by letting a sonicated suspension settle and monitoring the nature of the bed so formed in small vials or better in Wintrobe tubes (narrow test tubes with a length scale, see SI). A loose bed (or lager height in a Wintrobe tube) is an excellent test of a poor solvent system. As a caveat, very dispersive suspensions but in a low viscosity solvent (acetone/dichloromethane system) may settle very fast yet yield excellent columns. Settling speed alone is not a good predictor. A simple rheological test to determine shear thickening in a given solvent, referred as "the filament test" or "test on a spatula", can be done as follows. One can make a very concentrated suspension by adding few drops of slurry solvent on the stationary phase in a vial. Quickly moving a thin spatula, one can notice the resistance offered by suspension in the motion of the spatula, followed by drying/cracking. As the motion is stopped, the suspension becomes *wet and shiny* (from the so-called dilatancy effect). Lifting the spatula from such suspensions forms a flowing filament.

After choosing the slurry, carefully pour the sonicated suspension into the slurry chamber (*e.g.* with a syringe), the top-up solvent should be very carefully trickled into chamber without disturbing the slurry concentration. The first column can be packed as a trial based on the initial parameters suggested in Figure 2.6. The criteria for choosing a push solvent are given in Table 2.2.

Table 2. Criteria for choosing push solvents

(a) Degassed solvents with relatively low compressibility at high pressures (> 10,000 psi) and low viscosity e.g. acetonitrile, MeOH, isooctane, toluene, hexane, acetone, hexane:IPA, or in some cases with aqueous slurries, pure water can be used.
(b) Ideally, agglomerating solvent for the stationary phase
(c) Density should be lower than the solvent blend used in the chamber so that the push solvent floats on the suspension

It should not be very compressible at the packing pressures nor denser than the slurry itself. For instance, if hexane is chosen, at 10,000 psi, it will be compressed as 158×10^{-6}/bar. We prefer a pressure ramp starting from 0 psi to the final pressure (in 10-20 seconds) for safety and improved reproducibility. The packing pressure is typically chosen to be at least twice (or thrice) the operating pressures. We consistently see a significant efficiency loss, if the packing pressure is similar to the operating pressure especially in short columns. In general, for 4.6 mm i.d. columns, 10,000 to 12,000 psi is sufficient, whereas narrow bore columns are typically packed at 16,000 psi to 30,000 psi for particle sizes < 5 µm silica or other inorganic oxides. Polymeric/carbonaceous materials cannot handle this pressure. Once the column is packed, the system should be allowed to come to the atmospheric pressure and the column should be removed as soon as possible, flattened with a blade

knife, and fitted with a frit. An unretained solute peak and a well retained solute peak should be analyzed for plate count and a total peak shape assessment should be performed.[100]

2.3.4.1 Total Peak Shape Analysis after Packing Experiments.

During packing experiments, one may obtain non-Gaussian peak shapes. The departure from Gaussian shape of an unretained analyte is a manifestation of flow heterogeneity problems from poor velocity distribution in the packed bed (Figure 2.8).

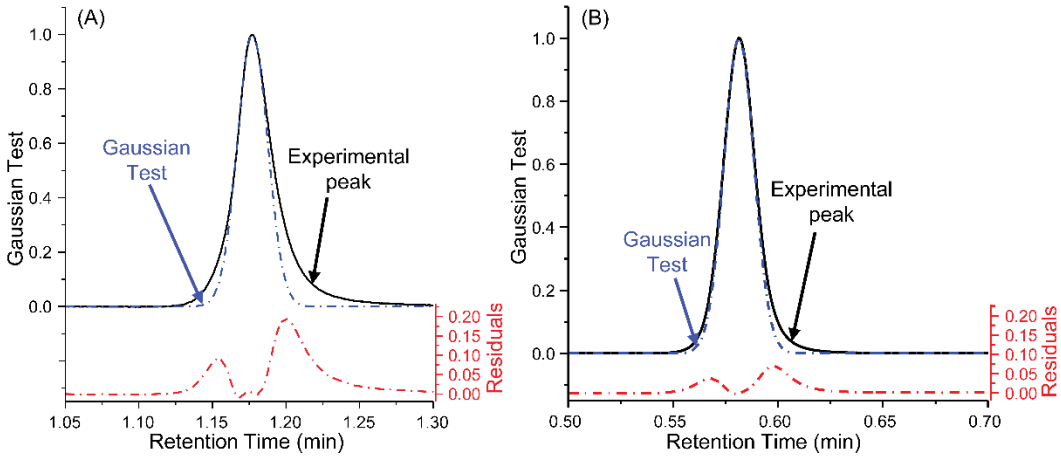

Figure 2.8 Gaussian test applied to experimental peaks for testing a peak shape after column packing. The peaks show concurrent fronting and tailing which remain undetected by the USP tailing factor. The residuals here show the problematic regions of the peaks (A) Column: teicoplanin bonded 2.7 µm SPP (15x0.21 cm i.d.). Analyte: 1st eluting enantiomer of 5-methyl-5-phenylhydantoin, (B) the bottom 5 cm section of a long column packed with 2.7 µm SPP silica in IPA slurry. Analyte: uracil. Retrieve the total peak shape analysis template from ref [100].

In Figure 2.8A, a peak with concurrent fronting and tailing is shown, the asymmetry of which is not identifiable by asymmetry factors such as USP tailing factor A_S.[100] However, with use

of Gaussian superimposition at the peak top, one can detect concurrent fronting and tailing. The example shown in Figure 2.8B is a seemingly symmetric peak which only shows its concurrent slight fronting in addition to tailing when analyzed with Gaussian superimposition. See free Excel based template provided as a SI which automates the total peak shape analysis.[100]

2.3.4.2 Practical Insights with Illustrative Examples.

Illustrative examples based on fundamentals discussed above will be demonstrated below. The general principles are straightforward and applicable to virtually all stationary phases. All columns were packed with a pneumatically driven Haskel (DSHF-202) pump using slurry chambers (10, 20, 40, 80 mL) from Scientific Systems Inc. (USA) and pushed with either methanol or acetonitrile. The packing hardware utilized in all experiments was similar to that shown in Figure 2.2, except that the push solvent entered vertically through a flow distributor. The glassware/ apparatus was oven dried and disposable Norm-Ject syringes (Henke Sass Wolf) were used for volume measurements of solvents. All slurry concentrations reported in this work are %w/v as g/mL. Chromatography was performed on an optimized Agilent 1290 Infinity series UHPLC.[2,11] As suggested in the flow chart, the SEMs revealed the absence of fines or broken/cracked particles in the silica used in the following experiments. The efficiencies of the peaks were calculated by the half-method whereas distorted peak efficiencies were determined by the second moments (Agilent OpenLab). The peak asymmetries (A_s) are based on the USP tailing $w_{0.05}/2f_{0.05}$, where $w_{0.05}$ is the width at 5% peak height and $f_{0.05}$ is the distance from the leading edge to the peak maximum at 5% peak height. The results and phenomenon illustrated below are reproducible as shown in the Figure 2.9E.

2.3.4.3 Dispersed Slurries Produce Better Columns.

Figure 2.9 shows a very important and general phenomenon that has a profound effect on the column performance.

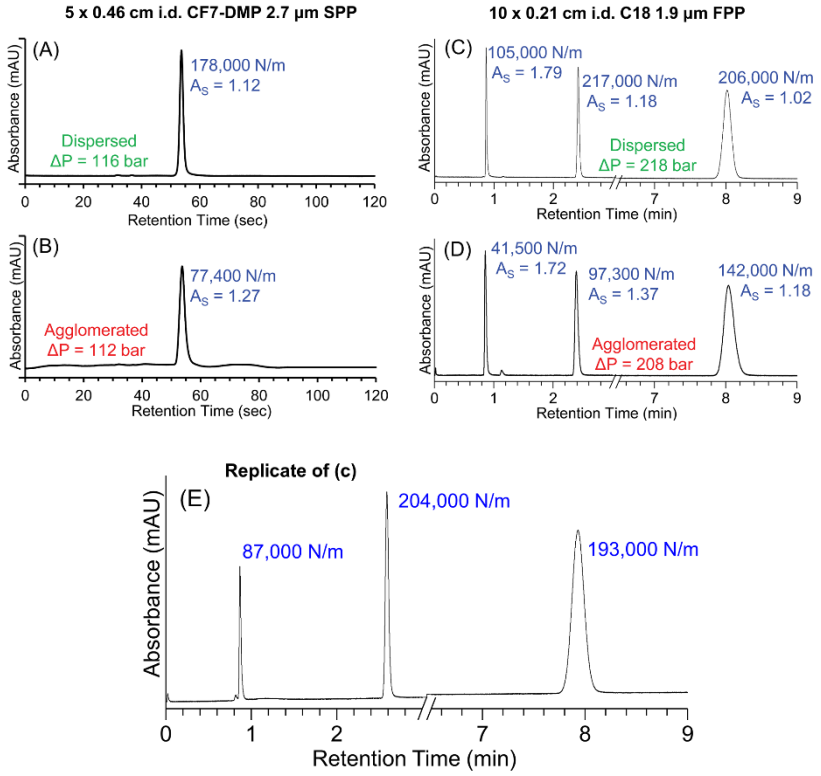

Figure 2.9 Performance comparison of dispersed vs. agglomerated slurries on analytical and narrow bore columns with different surface chemistries. (A) and (B) show the 5 x 0.46 i.d. columns packed with 2.7 µm SPPs bonded to cyclofructan-7 dimethylphenyl carbamate (CF7-DMP) analyzed with 1,3-dinitrobenzene using 70/30 heptane/EtOH at 1.0 mL/min. (C) and (D) show the 10x0.21 cm i.d. columns packed with C18 bonded 1.9 µm FPP silica analyzed using a mixture of uracil, 1,3-dinitrobenzene, and biphenyl (in order of elution) using 60/40 ACN/Water at 0.2 mL/min. (E) is the replicate of (C) to demonstrate the reproducibility of the phenomena and results.

It is postulated that dispersed suspensions should pack “layer by layer” producing a uniform bed without channeling or voids resulting in high efficiency columns. On the other hand, agglomerated suspensions can pack as “loose clumps” piling up on each other resulting in a loose bed. Intuitively, one would expect to have more voids in such a bed structure. These concepts are shown using a 2.7 µm SPP dimethyl phenyl cyclofructan-7 bonded chiral (polar) stationary phase and a 1.9 µm FPP bonded C18 silica (Figure 2.9). Additionally, two different column geometries were chosen to illustrate the key differences between agglomerated and dispersed suspensions. As pointed out earlier, a dispersed and agglomerated suspension will have the opposite rheological behaviors, shear thickening and shear thinning, respectively.[101] To obtain a dispersed suspension, various combinations of several organic solvents (chosen from Table 2.1) were assessed via microscopy (Figure 2.7 A-B), sedimentation, and shear thickening test. It was found that a mixture of 1:1 chloroform: IPA provided a dispersed slurry and 98:2 MeOH: H_2O (ammonium acetate) agglomerated the particles. The kinematic viscosities of 1:1 Chlorofom:IPA and 98:2 MeOH-H_2O are 0.58 and 0.76 cSt, respectively.[102,103] A trial packing was performed with 5 %w/v concentration at 10,000 psi in a 5x0.46 cm i.d. column. Figure 2.9A and 2.9B show the peak profiles from a dispersed and agglomerated slurry, respectively. Although identically packed otherwise, a change of slurry dispersion state provided more symmetric peaks with 178,000 N/m and h = 2 (Figure 2.9A) while the agglomerated slurry produced only 77,400 N/m (Figure 2.9B) and h = 4.8 which is a ~ 60% decrease in efficiency.[2] The lower backpressure of the agglomerated slurry column also indicates a more loosely packed bed.

For an achiral example, a 1.9 µm FPP silica C18 was packed in 10x0.21 cm i.d. columns. Using a procedure similar to that described for 4.6 mm i.d. columns; two slurry mediums were used that provided a dispersed slurry (85/15/0.1 $CHCl_3$/MeOH/formic acid;

literature value of kinematic viscosity of 85/15 $CHCl_3$/MeOH[104] is 0.38 cSt) and an agglomerated slurry (absolute EtOH, kinematic viscosity 1.51 cSt) under an optical microscope. Using 8% w/v slurries, two 10x0.21 cm i.d. columns were packed at 12,000 psi and their performance comparison is shown in Figure 2.9C and 2.9D. The dispersed slurry produced far greater number of plates (217,000 N/m) as compared to the agglomerated slurry (142,000 N/m, a ~35% decrease). Also apparent are the significantly enhanced peak asymmetries for dispersed slurries while the agglomerated slurry shows more tailing. The remarkable efficiencies seen in Figure 2.9C far outperform the specifications of many 10x0.21 cm i.d. C18 columns from major manufacturers (170,000 N/m). Consistent with our postulate on agglomerated suspensions forming a loose bed, the agglomerated slurry column showed a 10 bar lower (~5%) backpressure.

Note that in each successful case of dispersed suspensions, the *additional benefit* comes from the low kinematic viscosities of chloroform-2 propanol and chloroform methanol (<1 cSt) with relatively high densities which is consistent with our discussion on choosing appropriate solvent systems. In contrast, simply choosing a low kinematic viscosity solvent such as hexane/pentane/acetone will not produce a good column. Additionally, our previous experience with Hypercarb, polymeric cation exchangers, fully porous (1.9 to 5 µm) and core-shell particles of various sizes (1.5 to 2.7 µm) convincingly illustrate the advantages of using dispersed suspensions producing near theoretical plate height of two particle diameters.[2,43,54,105-107]

2.3.4.4 Can Agglomerated Slurries Ever Produce Good Columns in Analytical or Narrow Bore Formats?

In our experience[2,43] and that of others,[108] analytical and narrow bore columns packed with agglomerated suspensions of particles have invariably performed poorly (as

shown in Figure 2.9), regardless of the stationary phase chemistry. The failure rate is very high but occasionally one might obtain acceptable efficiency. However, reproducibility of such experiments is very low. For example, aqueous slurries of 4.4 µm sulfonated ethylvinylbenzene-divinylbenzene in presence of Al^{3+}, Mg^{2+}, and Na^{+} ions which caused particle agglomeration (Figure 2.7C) always produced very low efficiency columns. When pure DI water was used, it dispersed the particles because of their high negative zeta potential (-52 mV) and produced high efficiencies.[43] Silica has a very negative zeta potential in water (-56 mV) implying a highly charged surface hence it is difficult to agglomerate. For the native 1.9 µm FPP silica, no suitable slurry solvents could fully agglomerate the silica particles except toluene, which produced permanent flocculates. Similarly, 1.9 µm fully porous silica when packed using pure THF (~ 23% w/v slurry conc., agglomerated) into 5x0.3 cm i.d. columns produced very low plate counts (83,800 plates/m). A mixture of oleylamine and hexadecyl-trimethyl-ammonium bromide, when added in EtOH, *partially* agglomerated the silica particles. The adsorption of the surfactant and amine on the surface can produce a pseudo-C18 like phase. A 5x0.21 cm i.d. column packed with this 18 % w/v slurry at 8000 psi produced 200,000 N/m in a 2.1 mm i.d. column with slight tailing (See Figure 2.10). A similar attempt for a positively charged phase hydrosilylated quinine (2.7 µm SPPs) failed in agglomerated suspensions. This stationary phase provided high efficiencies (180,000 N/m), when packed with a dispersive suspension of chloroform:IPA.[107] Our recommendation is to start with dispersed slurries for quickly optimizing column packing processes. Partially agglomerated suspensions, especially of ion-exchangers, may produce good columns. For the capillaries, researchers have shared with us,[49] that partially dispersed or high concentration suspensions produce very high efficiencies with theoretically expected plate heights $H= 2d_p$ (see more discussion in the following capillary sections).

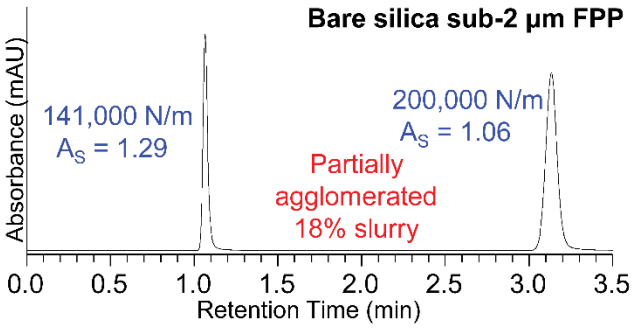

Figure 2.10 Performance of agglomerated slurries for polar 1.9 µm bare silica packed in 5x0.21 cm i.d. column with 18% w/v/w 100/0.1/0.075 EtOH/oleylamine (assay: 80-90% C18 content)/hexadecyl-trimethyl-ammonium bromide slurry. Analyzed using a mixture of uracil and cytosine (in order of elution) with 90/10 ACN/100mM NH_4OAc at 0.2 mL/min.

2.3.4.5 No Column is Axially or Radially Homogeneous.

Figure 2.11 shows interesting examples of a long 0.46 cm i.d. column packed with 2.7 µm bare SPP silica. The IPA slurry was chosen because it dispersed the particles; however, it does have a high viscosity to density ratio (2.7 cSt). Three 5x0.46 cm i.d. columns, connected in series, with unions were packed at 10,500 psi using a 4.3% w/v suspension. In general, high viscosity and dispersive suspensions are shear thickening and often produce fronting peaks due to high shear rate at the column walls. IPA suspension of SPP particles displays shear thickening effect. The question arises if a column performs poorly, is the entire column bad or are only certain sections of it. Figure 2.11 shows the chromatographic performance of three sections. There are several remarkable features in the figure: (a) the bottom column section shows the highest back-

pressure and poorest column efficiency (b) and the top column shows (generally lower pressure) and comparable efficiency (within error) to the middle section.

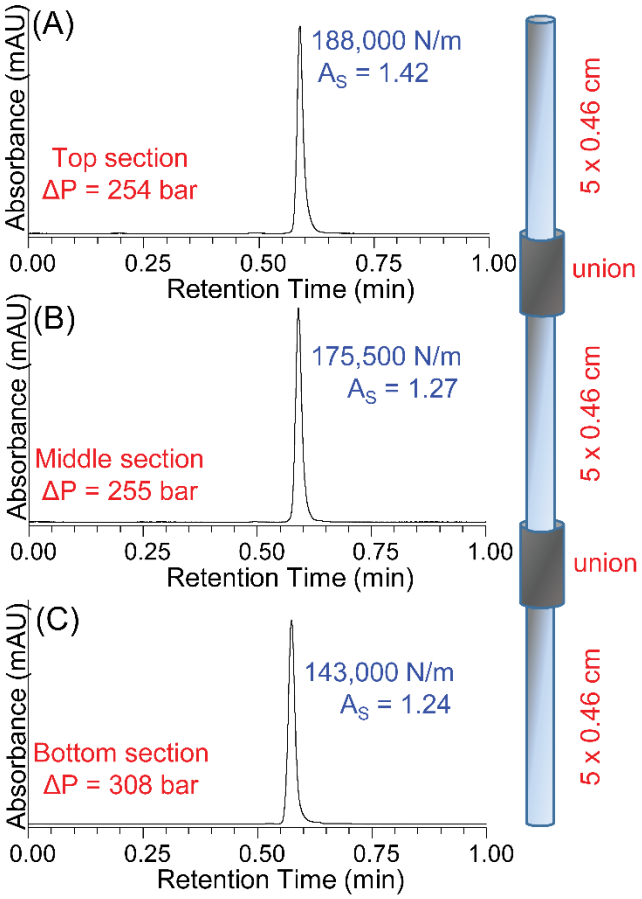

Figure 2.11 Packing homogeneity of various parts of a column investigated through packing of 2.7 µm SPPs in 5x0.46 cm i.d. columns in series using a 4.4% w/v IPA slurry at 0-10,500 psi final pressure and evaluated chromatographically individually. Sample: uracil. Mobile phase: 1:1 MeOH:Deionized Water, 1.0 mL/min, 254 nm.

We also observed that the top section is metastable i.e. high efficiency but settles with time. This is consistent with the fact the top column section experiences the least force under constant pressure mode. In fact, the total column length dictates which sections of a column will perform the best e.g. for a 15 cm column, the bottom and the middle sections were the best as shown previously.[74] However, the authors employed 10 µm C18 silica particles using acetone suspensions. Our studies with 2.7 µm SPPs (bonded or non-bonded) showed that bottom sections always perform poorly regardless of chosen slurry solvent than the middle or top sections for 15 cm formats. In the constant pressure mode, the initial flow is very fast but drastically decreases as the hydraulic resistance increases from the packed bed. In a constant flow mode, the pressure builds up as the bed is formed while the flow remains constant. In each case, the entire column does not experience the same pressure drop. The smaller asymmetry of the bottom section (A_s=1.2) is *deceptive* because the peak is both fronting and tailing as revealed by the total peak shape analysis (Figure 2.8B).[100] Performing the total peak shape analysis reveals interesting properties of the sections. The bottom section, which packs the fastest in the constant pressure mode, has the highest contribution from fronting to the overall peak distortion. This contribution decreases with middle section and is the lowest for the top section. This trend is consistent with the equation 5 ($\dot{\gamma} = 4V/ \pi r^3 t$), which shows that the shear rate will be highest at the walls and high shear rate (high flow) will produce shear thickening effects in a viscous suspension, such as IPA. This implies that the wall region is different from the bulk packed region making it radially heterogeneous as well. Alternatively, instead of section packing, one can do peak parking experiments to assess which part of a column is “bad” along its entire length from the shape of the distorted peak.[109]

2.3.4.6 Narrow Bore Columns are Not Easy to Pack.

In narrow bore columns, the wall effects can easily affect the column efficiency resulting from the proximity of the column wall to the injected band. One can roughly estimate the time it takes for radial equilibration as $(d_c^2/4D_t)$. It can be shown,[93] with L/u of < 50 s, in a 2.1 mm i.d. column, it will take 1000 s for an analyte to reach the walls, whereas for a 4.6 mm i.d. column, it will take 5000 s. Since the wall region, is "different or heterogeneous" in the packing structure than the rest of the bulk, narrow bore columns usually offer lower plates than their 4.6 mm i.d. counterparts.

From a practical perspective, narrow bore column typically show two major problems namely, higher permeability (which implies loose packing), and up to 40% lower plates as compared to their wider bore counterparts (3 or 4.6 mm i.d.), even in the absence of extra-column effects. Note that the all the packing phenomena in going from a 4.6 i.d. to 2.1 mm i.d. remain the same. As we decrease the diameter, for the same pressure, the *absolute* force decreases since *force = pressure x area*. Not only the absolute force, but linear velocity changes with the column diameter. Thus, narrow bore columns with sub-2 µm particles are often packed at 15,000-30,000 psi in industrial settings. However, this might be an "overkill" situation since medium pressures with the right slurry choice may be adequate to form a random closed packing and further pressurizing may simply decrease the permeability. Figure 2.12, shows the difference in peak shape distortion as the column diameter changes from 4.6 mm to 3 mm i.d. after being packed with 1.9 µm FPP silica using the same conditions (3.4-3.5 % w/v, 80:20 IPA: $CHCl_3$). It is clear, that the 3 mm i.d. column shows significantly more distortion (what we refer to as a "foot" in the chromatographic peak) as seen from lower efficiency and USP tailing.

Note that in this case, although the slurries were fully dispersed, the kinematic viscosity of 80:20 IPA:$CHCl_3$ is 1.9 cSt.[103] The density of the solvent system is 0.83 g/mL. As we stated in the theory section, high kinematic viscosity solvents can lead to fronting or peaks with “foot” on the leading edge. This is a consistent effect seen with many stationary phases and it is most likely a rheological phenomenon rather than stationary phase chemistry related issue. The cure is described in the next section.

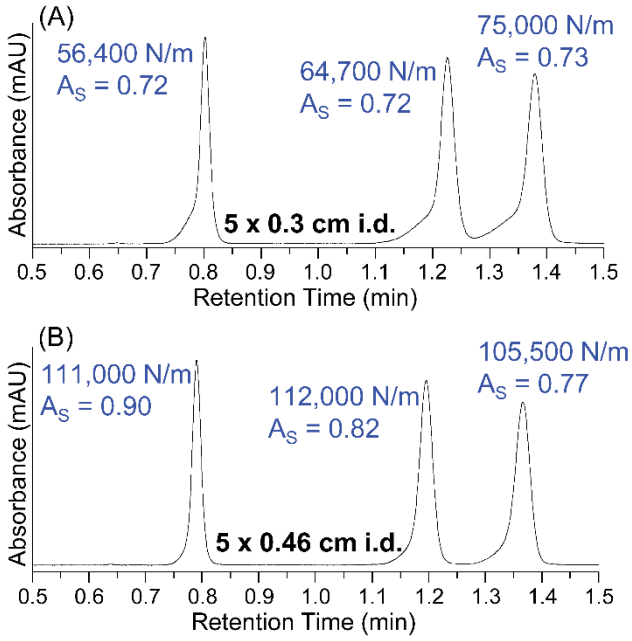

Figure 11. Enhancement of wall effects in a narrow and analytical bore column packed identically with bare 1.9 µm FPP silica at 11,000 psi final consolidation pressure. (A) 5x0.3 cm i.d. column, 0.425 mL/min. (B) 5x 0.46 cm i.d. column, 1.0 mL/min. Mobile phase for both chromatograms was 80/20 ACN/25mM NH4OAc. Sample: uracil, adenine, and cytosine (in the order of elution). Efficiency is calculated by statistical moments to account for peak shapes that strongly depart from the Gaussian profile.

2.3.4.7 Shear Thickening is a Kinetic Process: The Influence of Slurry Concentration on Column Performance.

Often dispersed suspensions produce a so-called “foot” on the front side of otherwise narrow of the peaks which probably arises from the shear thickening effects. The peak efficiency in such cases, if calculated by half-height method in Figure 11, gives 226,000 N/m (h = 1.6). Shear thickening suspensions (dispersed) may lead to channeling (thick suspension tend to crack), if given sufficient time during packing. Figure 2.13 shows a comparison of three different slurry concentrations on the performance of 5x0.3 cm i.d. columns packed with 1.9 µm FPP silica using a dispersed slurry.

It is apparent that the lower slurry concentrations (3.5 and 10% w/v) led to low efficiencies (75000-89,200 N/m) along with a distinct foot on the leading edge of every peak. This systematic behavior is an indication of channeling or cracks in the packed bed. Increasing the slurry concentration is known to prevent formation of large voids in packed bed and, accordingly, as the slurry concentration is increased to 23% w/v, significantly higher efficiencies (206,000 N/m) along with improved peak symmetries are noted. Our hypothesis is that since shear thickening is a kinetic effect, a 23 % w/v suspension packs the column very fast as compared to more dilute slurry concentrations, thus mitigates the non-Newtonian behavior. This phenomenon is reproducible and general rather than stationary phase specific. As indicated in the flow chart, Figure 2.6, it is recommended to start with a 7-10% w/v slurry concentration for columns and further tune the peak shape to make it symmetrical. If tailing is seen instead of fronting, the slurry concentration can be lowered to prevent particle agglomeration. A question often brought up is that whether by increasing slurry concentration in a dispersive medium, are we essentially agglomerating the particles? This is a misconception because even with high slurry concentration, optical

microscopy shows that the particles are indeed separate from each other. The particles are close, but not flocculated (clumped); this criterion still differentiates this concentrated suspension in a dispersive medium from an agglomerated one.

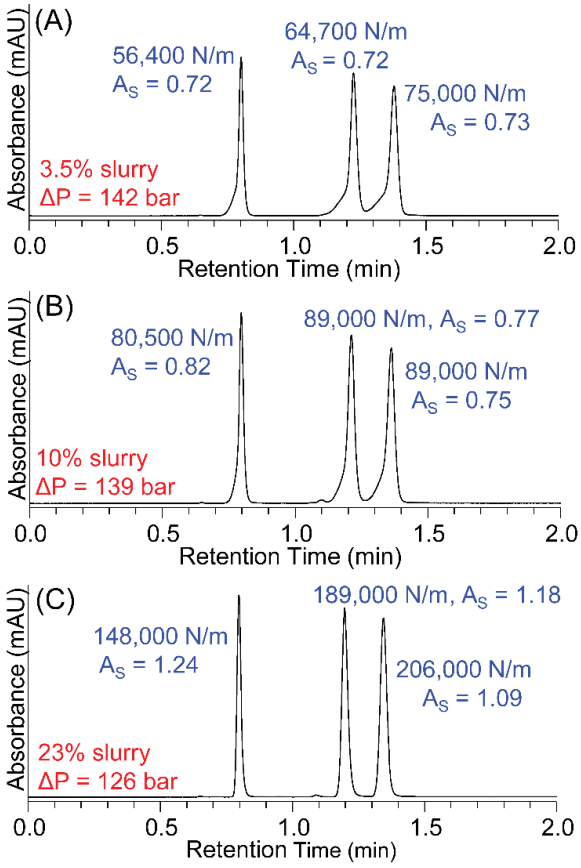

Figure 2.13. Effect of varying slurry concentrations on 5x0.3 cm i.d. columns packed with 1.9 µm fully porous native silica using a dispersed slurry of $CHCl_3$/IPA using a pressure gradient 0-8,000 psi followed by 8,000-11,000 psi for 15 min each. Sample: mixture of uracil, adenine, and cytosine (in the order of elution). Mobile phase: 80/20 ACN/25 mM NH_4OAc, 0.425 mL/min, 254 nm. (A) 3.5% w/v slurry concentration (B) 10% w/v slurry concentration (C) 23% w/v slurry concentration, N obtained using statistical moments.

2.3.4.8 Influence of Packing Pressure in Short Analytical Columns.

The packing pressure is a factor that can be altered to affect the rate of bed formation and the performance of the column as indicated in Scheme 1. Besides column efficiency, a packed bed should be stable to >1000 injections and the pressure shocks it receives at every injection from valve switching.

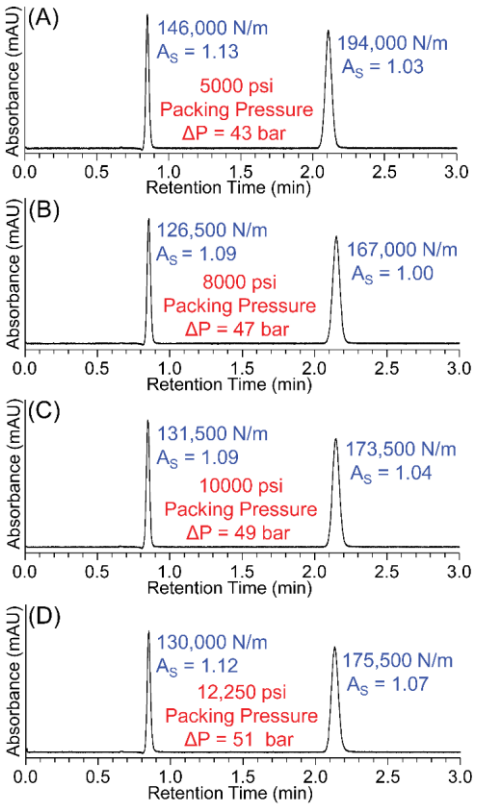

Figure 2.14 Effect of packing pressure on the chromatographic performance of 5x0.3 cm i.d. columns packed with 2.8 µm native SPP silica using dispersed slurry 1:1 acetone: IPA slurry (ca. 16% w/v concentration). Sample: uracil and cytosine (in order of elution). Method: 90/10 ACN/100mM NH_4OAc, 0.425 mL/min, 254 nm. (A) 5000 psi, (B) 8000 psi, (C) 10,000 psi, and (D) 12,250 psi packing pressure. Pressure ramp was from 0 to the final pressure

A dispersed slurry of 1:1 acetone:IPA (found using the approach in Figure 2.6 and solvents from Table 2.1) was used to pack bare 2.8 µm SPP silica in 5x0.3 cm i.d. column at 5000, 8000, 10000, and 12250 psi, respectively. The column packed at 5000 psi performed the best with 194,000 N/m followed closely by the columns packed at 10000 and 12250 psi which produced about 175,000 N/m (Figure 2.14). This experiment shows that very high packing pressures may not be necessary for packing narrow-bore columns and even pressures as low as 5000 psi can be adequate for a 5-cm column, since pressure drop per unit length is what matters rather than the absolute pressure value. However, if the short column is to be used at high flow rates, higher packing pressure should be employed. For example, a 5000 psi packed column should not be employed if the working pressures are ≥ 5000 psi. One practical exception for very high pressure packing is the guard columns (0.5 to 1 cm) which we still pack at 10,000 psi for 2 µm silica SPP or FPP (considering the length including the bed packed in the pre-column).

2.3.5 Packing of Capillary Columns.

Capillaries, like narrow bore columns, save solvent and expensive stationary phase, and provide high detection sensitivity. Unlike the analytical bore columns, there is no fronting or tailing in capillaries because of fast lateral diffusional relaxation provided the capillaries are long enough to satisfy the Aris-Taylor dispersion requirements.[49] Capillaries have produced phenomenal efficiencies (h as low as 1.0) which have never been observed in analytical or narrow bore columns.[48] As the trend of moving to smaller particle size continues, this work only covers packing methods for capillary packed with sub-2 µm SPP and FPP, largely derived from the work of Jorgenson on C18 chemistries.[48,49,60,76,110-114] When choosing to pack a capillary column, the same principles apply-optical microscopy is the best predictor of the packed capillary. Figure 2.15A shows a comparison of slurry

solvents on the performance of capillary columns packed with 1.1 µm C18 SPPs. The proprietary solvent is very dispersive, whereas acetone and hexane are partially agglomerating, and MeOH produced large aggregates. It is clear from the van Deemter curve that a flocculated suspension is beneficial in producing higher efficiencies for reversed phases in capillaries. The logic behind choosing agglomerated suspension is that snow-ball effect, where a clump containing large number of particles simply piles up on the bed reducing the size discrimination between the wall and the central region.[49] Microscopy videos of capillaries being packed clearly show this effect, whereas dispersed dilute suspensions pack in the center as a pile and the particles roll-off towards the walls.[49,98] Following the guidelines in Figure 2.6, next the slurry concentration should be optimized. Figure 2.15B shows that increasing the slurry concentration from 0.3 to 2.5% w/v drastically enhances the capillary performance (173,000 to 318,000 N/m). Through studies of capillary bed structure with confocal laser scanning microscopy, it was discovered that the bed heterogeneity between the capillary column's wall region and the bulk packed region is the key contributor to poor performance and so is the presence of voids.[98,115,116] This heterogeneity can be influenced with changes in slurry concentration as increasing the slurry concentration leads to an even distribution of voids across the bed improving its uniformity.[97,112]

Increasing the slurry concentration also leads to an increased number of voids in the packed bed, eventually resulting in diminishing returns.[97,112] Figure 2.15C shows a recent study that demonstrated performance improvement from ultrasonication during packing with concentrated slurries (20% w/v) and achieved an impressive reduced plate height of 1.05 for capillary packed with 2.0 µm C18 bridged ethyl hybrid (BEH) FPPs.[48]

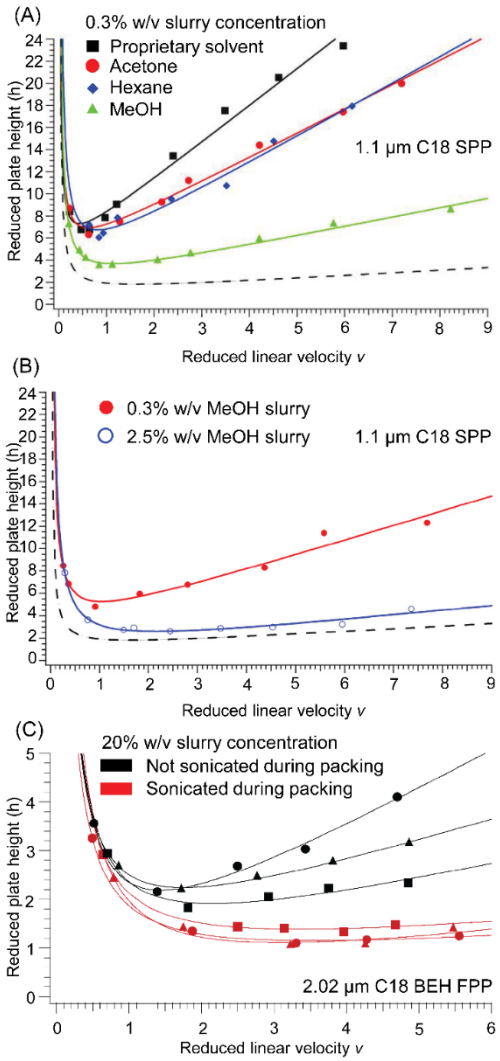

Figure 2.15. The van Deemter plots (h vs. reduced velocity v) of packed capillaries which show the effect of packing C18 SPP particles in (A) various slurry solvents and (B) various slurry concentrations in an agglomerating solvent in 30 µm i.d. capillaries. Dashed black lines represents ideal limits in (A) and (B). The effect of ultrasonication during packing with high slurry concentration (20% w/v) with C18 FPP in 1 mx75 µm i.d. is shown in (C).

Compared to this, the columns not sonicated during packing but packed identically otherwise, produced *h* in the range of 1.8-2.2. It was reported that the use of ultrasonication (at 80 kHz) during packing prevented formation of large voids typically formed when using high concentration slurries.[48] To the best of our knowledge, first use of ultrasonication during packing of analytical and capillary columns was reported by Light[71] and Novotny[117], respectively. For metallic analytical columns, the metal can absorb the ultrasonic energy (typical sonic bath), and we have seen poor packing results in doing so. It is highly desirable to learn whether there are any drawbacks of ultrasonication on column stability and lifetime. In this publication and many others from the past decade, there are no systematic results on long term bed stability with agglomerated slurries, because such beds, may be metastable because of their high permeability. In packing capillary using supercritical fluids, stable beds have been reported after 6 months of use.[118]

2.3.6 Future Directions for Column Packing and Improving Chromatographic Efficiency

It is apparent that emerging techniques in improving column efficiencies will try to circumvent the problems of axial and radial heterogeneities of the packed beds; which are main causes of poor column performance.

2.3.6.1 Colloidal Crystals as Chromatographic Beds.

One of the most interesting directions in enhancing column efficiencies using monodisperse colloids which organize themselves in long-range-ordered crystals.[119] This arrangement is excellent for any chromatographic columns since simulations have shown that a crystalline bed can provide extremely high efficiencies ($h < 1$).[120] The authors tested simple cubic (sc), body-centered cubic (bcc), and face-centered cubic (fcc) arrangement of particles, and concluded that zone broadening is less for the fcc structure than the sc and bcc structures at the van Deemter minimum. Surprisingly, the random packed bed,

outperformed at higher flow velocities. It is known that uniformly sized silica particles can self-assemble into highly ordered fcc crystals.[121] Reproducible packing studies and packing procedures are yet to be demonstrated for making crystalline packed capillaries from colloidal crystals.

2.3.6.2 3D printing of columns and Wall Patterning.

Three dimensional (3D) printing can possibly bring a paradigm shift in separation science, where 3D printed columns will circumvent many packing problems and wall effects. It is possible to obtain crystalline packing in simulations which can be 3D printed to obtain an ideal packed bed. In the first proof of concept of a 3D printed column, the researchers simulated perfectly ordered beds with octahedral beads (115 μm apothem) packed in a simple cubic configuration.[122] The models were then printed by UV curing of acrylonitrile-butadiene-styrene powder layers. A complete column including a bed, flow connectors, and flow distributors were printed. An interesting capability of 3D printing is the possibility to embed the particles in the wall. This approach will break the geometrical discontinuities which occur near the walls of all existing capillary and analytical columns. In 2016, Agilent Technologies (Santa Clara, CA) patented a technology of creating spiral patterns on the column walls referred to as “structured walls” to potentially circumvent these geometrical constraints.[123] However, no supporting chromatography was provided. Of course, for chromatographic purposes, a 3D-column must be able to withstand high pressures and provide high surface area. Other alternatives such as pillar-array columns have emerged as ordered separation media which can also provide very high efficiencies.[124]

2.3.7 Non-Conventional Column Packing Approaches.

Although the slurry packing at high pressures has remained a preferred method of packing columns, other methods such as packing using supercritical fluids,[118,125,126] electro-kinetic packing,[127] and packing by centripetal forces have been tested with mixed results.[125,128,129] Packing capillaries using supercritical CO_2 has also been considered a viable alternative to the traditional slurry packing.[118] Packing capillaries using centripetal forces uses acceleration of particles with an in-house designed apparatus that can spin the columns during packing.[128,129] This approach could significantly improve the productivity due to the possibility of packing multiple columns simultaneously as well as rapid speed of packing.[130]

2.3.7.1 Active Flow Management (AFM).

AFM is not a column packing approach; however, it is a clever way to circumvent the radial heterogeneities of the packed bed as highlighted in the limiting cases of equation 6. In AFM, the analyte is introduced into the center of the column. A “curtain flow” of mobile phase prevents the solute from seeing and exploring the wall region of the column.[131] A segmented outlet fitting is designed to allow sampling of the central region of the band. With this approach, significantly higher efficiencies are obtained because of the elimination of the wall effects (a virtually infinite diameter column) as well as concentrating the sample in the central zone. The sample from the central section is passed through a detector as a plug. Note that in this column technology, only the inlet and outlet ports have been altered. A traditional main body of the column (cylindrical tube) is utilized. It was shown that for a 5 µm C18 column (100x4.6 mm), which the reduced plate heights of butyl benzene decreased from 2.9 to 2.3, just by the curtain flow approach.

2.4 Conclusions and Perspectives.

Herein a unified approach toward the science of making high efficiency reproducible packed columns was presented. Theoretical considerations and non-Newtonian properties of suspensions were shown. The non-linear viscosity behavior of suspensions can govern the nature of the packed bed (e.g. jammed state, shear thickened state etc.). Therefore, column packing can be considered as an ultrahigh pressure filtration process of a non-Newtonian suspension. After gaining experience from a range of non-polar to polar stationary phases with modern SPP and FPP of narrow particle size distribution, a flow chart was developed to provide a logical progression of packing stationary phases of any chemistry. Illustrative examples were shown showing different packing phenomena and suspension properties. Results indicate that concentrated non-aggregating suspensions usually produce better packed analytical and narrow bore columns. The best packed capillaries usually require aggregating solvents. New directions in colloidal crystals, 3D printing are laid out and the use of non-conventional approaches such as 3D printing and active-flow management are highlighted. Future work on quantitative suspension rheology is needed to understand and model the dynamics of the column packing process – a technology which will continue to evolve for several decades to come.

Chapter 3

HYDROXYPROPYL BETA CYCLODEXTRIN BONDED SUPERFICIALLY POROUS PARTICLES BASED HILIC STATIONARY PHASES

3.1 Abstract

(R,S)-hydroxypropyl modified β-cyclodextrin (RSP-CD) is a well-known chiral stationary phase. In this work hydrophilic interaction liquid chromatographic (HILIC) selectivities of RSP-CD was demonstrated. Further, an evaluation of chromatographic performances of fully porous particles (FPPs) and superficially porous particles (SPPs) based of RSP-CD stationary phases was performed. The RSP-CD bonded SPP based stationary phase showed faster and more efficient HILIC separations compared to the FPP based stationary phases. In addition, the SPP based RSP-CD stationary phase showed excellent selectivities for many classes of small polar molecules. Since the SPP based stationary phase allowed for separations performed at high flow rates without significant loss of efficiency, ultrafast separations (analysis times under one minute) also was accomplished utilizing SPP based RSP-CD stationary phase.

3.2 Introduction

Hydrophilic interaction liquid chromatography (HILIC) is an increasingly popular chromatographic technique due to its ability to separate many classes of polar compounds (e.g., sugars, amino acids, peptides, proteins, neurotransmitters, salicylic acid derivatives, nucleic acid bases and nucleosides) which cannot be well separated/retained by reversed phase liquid chromatography[132-134]. HILIC utilizes a polar stationary phase and mobile

phases consisting of polar aprotic organic solvents, typically acetonitrile and small amounts (i.e.; ≤ 30%) of aqueous components[135,136]. One of the retention mechanisms of HILIC is the partitioning of analytes between bulk mobile phase and a water rich stagnant mobile phase layer[137]. Other reported mechanisms emphasize that polar-polar interactions such as hydrogen bonding and electrostatic interactions also play an important role in the retention mechanism[132].

A wide variety of HILIC stationary phases have been utilized for the separation of different classes of compounds[136-143]. Lucy et al. have employed a particular set of probe molecules to evaluate 29 commercial HILIC columns which were categorized as either bare silica gel, amino, amide, diol, or zwitterionic [138]. Columns within a similar category showed slight differences, but in general were fairly similar to one another [138]. One unique class of HILIC phases are based on cyclic oligosaccharides. Cyclofructans for example, have proven to produce excellent HILIC separations of small polar compounds such as nucleic acid bases and nucleosides, beta blockers etc.[18,143-145] .

Cyclodextrins (CD), another class of cyclic oligosaccharides, are composed of D-(+)-glucopyranose units linked by α-(1-4)-linkages [132]. CDs have toroid like structures where the mouth is hydrophilic and the cavity is hydrophobic [132]. CDs and their derivatives are commonly utilized in enantioselective chromatographic separations [2,132,146,147]. HILIC achiral separations of small polar molecules such as beta blockers, nucleic acid bases and nucleosides, xanthines, carboxylic acid derivatives analogues and maltooligosaccharides on the ASTEC Cyclobond I 2000 (native β-CD bonded to fully porous silica) have been reported[143-145]. (R,S)-hydroxypropyl modified β-CD (RSP-CD) possesses additional hydroxyl groups, which can be used in increasing the polarity of CD and perhaps enhancing its utility as a HILIC selector. All prior reports which use CDs as HILIC selectors were

performed on fully porous particle (FPP) based columns. The number of versatile applications of superficially porous particles (SPPs) is increasing rapidly since SPPs can be utilized to obtain fast separations without losing efficiency [148]. Compared to FPPs with similar dimensions, SPPs have less surface area, therefore, decreased analysis times have been observed [149].

Since better packing homogeneities are obtained for SPP based columns compared to FPP based columns, reduced contributions of Eddy dispersions to band broadening have been observed for the former [57,148,150]. Therefore, SPP based columns show reduced plate heights less than that of FPP based columns [148]. The presence of the shell leads to shorter trans-particle path lengths in SPPs [16-18]. Therefore, separation efficiencies of particularly large molecules with small diffusion coefficients and small molecules possessing slow adsorption-desorption kinetics can be improved when using SPP based columns [16-18].

3.3 Experimental

An Agilent 1200 series HPLC (Santa Clara, CA) with quaternary pump, degasser, auto- sampler, and temperature-controlled column chamber and diode array detector was used throughout this study. Agilent ChemStation Rev.B.01.03 was used under Microsoft XP operating system environment for data processing. Unless stated otherwise all the experiments were performed at ambient temperature. 2.7 µm superficially porous silica with a pore size of 120 Å was obtained from Agilent Technologies (Santa Clara, CA). 3 µm fully porous silica with a 100 Å pore size was purchased from Glantero (Cork, Ireland). A commercially available 5 µm RSP-CD based column (Cyclobond I 2000 HP-RSP, 150 mm X 4.6 mm i.d.) was obtained from Supelco (Bellefonte, PA). R,S-hydroxy propyl ether

(Sigma, St. Louis, MO) derivatized CD bonded silica (3 µm fully porous and 2.7 µm superficially porous) stationary phases were synthesized according to methods described in the literature [151]. Stationary phase material was slurry packed into 100 mm x 4.6 mm i.d. and 150 mm x 4.6 mm i.d. stainless steel columns for evaluation.

HPLC grade acetonitrile (ACN) was purchased from Sigma-Aldrich (St. Louis, MO). A Milli-Q water purification system (Millipore, Billerica, MA) was used to purify water. Reagent grade acetic acid (HOAc) and ammonium acetate (NH4OAc) were obtained from Sigma-Aldrich (St. Louis, MO). All the analytes (structures are shown in Figure 3.1) were obtained from Sigma-Aldrich (St. Louis, MO). Analytes were dissolved in acetonitrile or water or acetonitrile/methanol/water mixtures. Solvents were vacuum degassed for 5 minutes before running experiments. Chromatographic conditions are specified in the Results and Discussion section. The pH was adjusted for the aqueous mobile phase component before mixing with the organic modifier.

Related chromatographic parameters were calculated using the equations given below.

Efficiency (N) = $16(t_R / w_b)^2$, Retention factor (k) = $(t_R - t_0)/t_0$

Where, t_R = retention time of a particular analyte, t_0 = column dead time, and W_b = baseline peak width. To determine dead time a pure solvent, e.g. ACN, was injected under isocratic conditions. The observed peak from the change of the refractive index in distinction to the mobile phase versus the solvent was used in the determination of the column dead time.

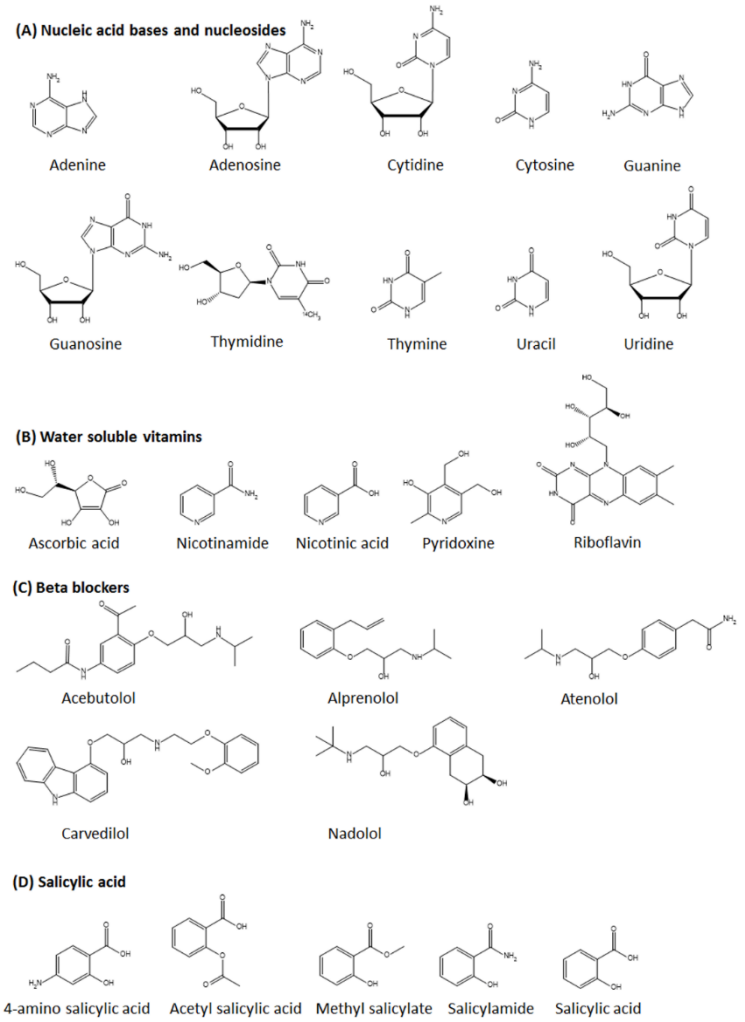

Figure 3.1 Classes of compounds separated on the RSP-CD stationary phases in HILIC mode. (A) nucleic acid bases and nucleosides (B) water soluble vitamins (C) beta blockers (D) salicylic acid derivatives

3.4 Results and Discussion

3.4.1. Comparison of FPP and SPP Based HILIC Phases.

HILIC separations of uracil, adenosine, and cytosine using the RSP-CD stationary phases based on three types of silica (5 and 3 µm FPPs and 2.7 µm SPPs) are illustrated in Figure 3.2. As illustrated in Figure 3.2, with decreasing particle size, efficiency is increasing. The 2.7 µm SPP based column showed higher efficiency for all three analytes when compared to FPP based columns.

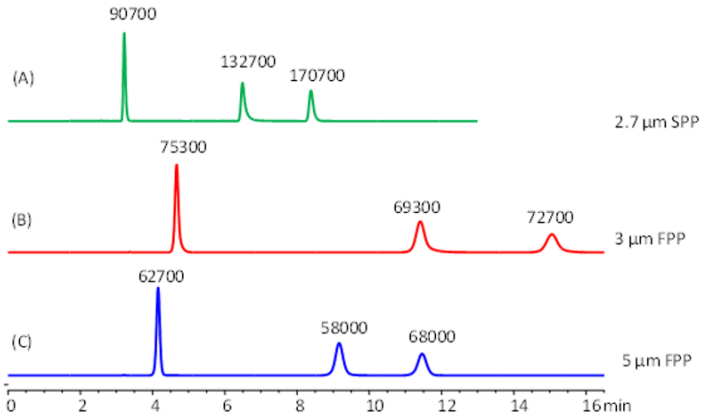

Figure 3.2 Comparison of efficiencies for RSP-CD 2.7 µm SPP, 3 µm FPP and 5 µm FPP based stationary phases. Chromatographic conditions: ACN: 25 mM NH_4OAc (90:10), 0.75 mL min^{-1}, 25 °C, and UV detection at 254 nm. Analytes: Uracil, Adenosine and Cytosine (in order of elution). Efficiencies are given in plates per meter corresponding to each peak in the chromatograms.

For the 5 µm FPP silica based stationary phase, decreased retention was observed compared to the 3 µm FPP silica based stationary phase. This is due to the total

CD loading on the silica which relates directly to the silica gel surface area [146]. Though the exact surface area of the commercial 5 µm material is not known, it is clear that it is lower than the in-house produced 3 µm media.

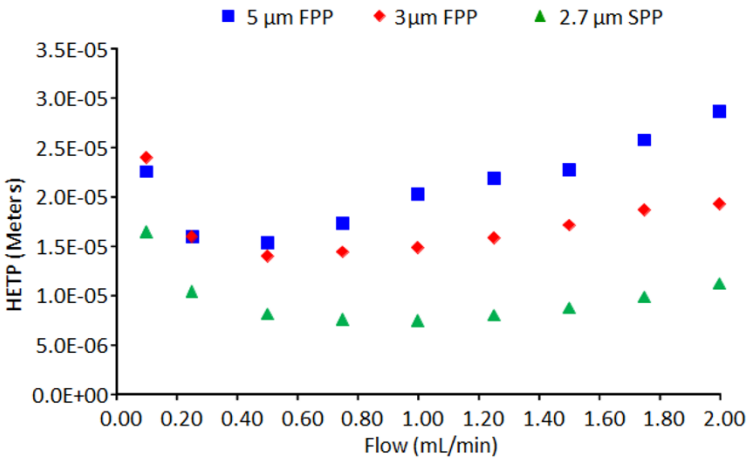

Figure 3.3. Kinetic plots for RSP-CD 2.7 µm SPP, 3 µm FPP and 5 µm FPP silica based stationary phases. ACN: 25 mM NH4OAc (90:10), 25 ◦C and UV detection at 254 nm. Analyte: Adenosine

Kinetic plots for RSP-CD SPP and FPP silica based stationary phases are shown in Figure 3.3. For the 5 µm and 3 µm FPP RSP-CD stationary phases, 0.25 mL/min and 0.5 mL/min optimum flow rates were observed respectively while for SPP stationary phase an optimum flow rate of 1.0 mL/min was observed. Height equivalent theoretical plates (H) at optimum flow rate (Hmin) of 2.9 x 10^{-5} m, 1.4 x 10^{-5} m, 7.5 x 10^{-6} m were observed for 5 µm FPP , 3 µm FPP and 2.7 µm SPP RSP-CD stationary phases respectively. Further the lowest reduced plate height (h = 2.8) was found for the 2.7 µm SPP based column. Also, H increased by a factor of 2.64, 1.35 and 1.33 for 5 µm FPP, 3 µm FPP and 2.7 µm SPP

RSP-CD stationary phases respectively when flow was increased from optimum flow rate to 2.0 mL/min. Therefore, the 2.7 SPP RSP-CD stationary phase is more beneficial than the FPP RSP-CD stationary phases when operating at high flow rates.

3.4.2. Evaluation of SPP Based HILIC Phase.

Lucy et al. constructed selectivity plots to evaluate the hydrogen bonding capabilities, hydrophilic nature, and ion exchange characteristics of wide variety of HILIC stationary phases [138]. Herein, the RSP-CD SPP stationary phase was evaluated to compare its retention factor ratio data with data presented by Lucy et al. under the same experimental conditions and the obtained values are given in Table 1. Compared to retention factor ratio data presented by Lucy et al., the RSP-CD SPP stationary phase is more hydrophilic than most available HILIC stationary phases including bare silica phases. Furthermore, the cation exchange behavior is less than that of bare silica HILIC phases and much greater than that of amine HILIC phases. The extent of hydrogen bonding capability exhibited by RSP-CD SPP is greater than bare silica HILIC phases but comparable with diol and zwitterionic HILIC phases. Therefore, the RSP-CD SPP phase demonstrates many unique hydrophilic characteristics in the HILIC mode.

Table 3.1. Retention factor ratios for selected probe molecule pairs.

Test pair	**Stationary phase characteristic**	**Retention factor ratio**
Cytosine/Uracil	Hydrophilic characteristics	3.50
BTMA/Cytosine	Ion exchange characteristics	2.80
Adenosine/Adenine	Hydrogen bonding capability	0.91

The effect of pH on the separation of small polar molecules using the RSP-CD SPP stationary phase has been tested with salicylic acid, uracil and BTMA at pH 3.0, 4.5 and 6.0 (Figure 3.4). Buffer concentration (30 mM) and pH of the aqueous component were adjusted before mixing with the organic modifier. The pKa of uracil is 9.45. Therefore, within the range of pH 3.0-6.0 uracil remains uncharged. As a consequence, the retention factor of uracil remains unchanged. BTMA (cationic at all pH values) showed consistent retention at pH 6.0 and 4.5, but decreased retention was observed at pH 3.0. This is an indication of decreased activity of free surface silanol groups leading to decrease retention of BTMA at low pH values. Interestingly, the retention of salicylic acid was little affected by the change in pH.

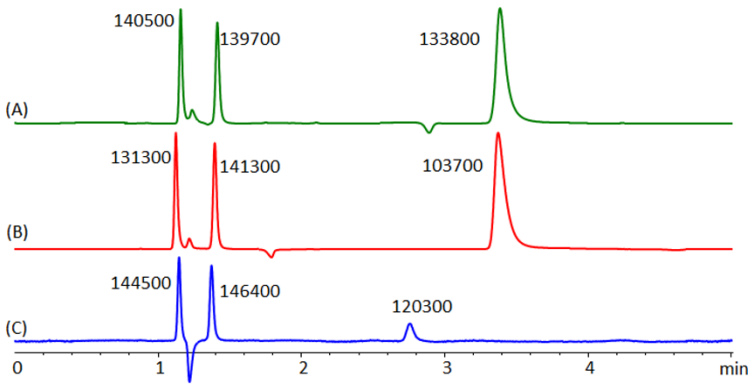

Figure 3.4 Effect of aqueous buffer pH on the separation of selected probe molecules using the RSP-CD SPP stationary phase. Analytes: salicylic acid, uracil, and benzyltrimethylammonium chloride (BTMA) (in order of elution). Chromatographic conditions: column - 100 mm x 4.6 mm i.d., flow rate: 1 mL min-1 and UV detection at 220 nm. (A) ACN: 30 mM NH4OAc, pH 6.0 (80:20), (B) ACN: 30 mM NH4OAc, pH 4.5 (80:20) and (C) ACN: 30 mM NH4OAc pH 3.0 (80:20).

Efficiencies are given in plates per meter corresponding to each peak in the chromatograms. 10 mM to 20 mM since ammonium ions compete with BTMA for interactions with free silanol groups. From 20 mM to 30 mM buffer concentration, retention time decrease was not very significant perhaps indicating that most active silanol groups had been saturated at buffer concentrations around 20 mM. Figure 3.5 shows effect of buffer concentration on the separation of salicylic acid, uracil, and BTMA. At pH 4.5, salicylic acid (pKa = 2.97) is negatively charged and free silanol groups are deprotonated. Therefore, salicylic acid is repelled electrostatically from the stationary phase. When the buffer concentration is increased, electrostatic repulsions can be minimized. Therefore, salicylic acid showed increasing retention time with increasing buffer concentration. On the other hand, uracil is uncharged at pH 4.5. Therefore, a pronounced effect on buffer concentration was not observed. BTMA showed a considerable decrease in retention time when buffer concentration was increased from from 10 mM to 20 mM since ammonium ions compete with BTMA for interactions with free silanol groups. From 20 mM to 30 mM buffer concentration, retention time decrease was not very significant perhaps indicating that most active silanol groups had been saturated at buffer concentrations around 20 mM.

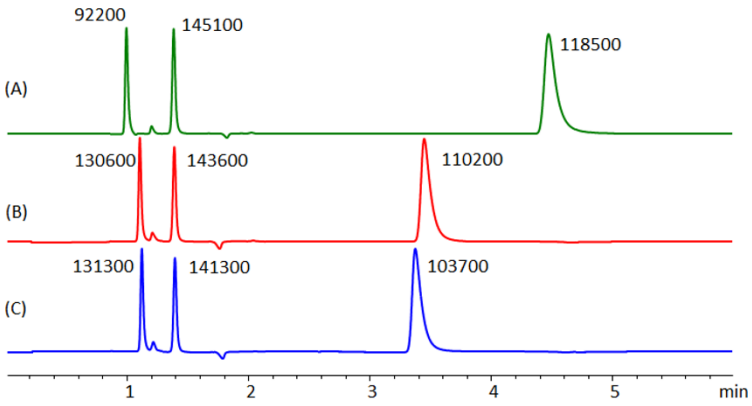

Figure 3.5. Effect of aqueous buffer concentration on separation of selected probe molecules on RSP-CD SPP stationary phase. Analytes: salicylic acid, uracil, and BTMA (in order of elution) Chromatographic conditions: column - 100 mm x 4.6 mm i.d., flow rate: 1 mL min-1 and UV detection at 220 nm. (A) ACN: 10 mM NH4OAc, pH 4.5 (80:20), (B) ACN: 20 mM NH4OAc, pH 4.5 (80:20) and (C) ACN: 30 mM NH4OAc, pH 4.5 (80:20). Efficiencies are given in plates per meter corresponding to each peak in the chromatograms.

Since SPP silica based columns can be operated at high flow rates with modest back pressure, ultra-fast separations can be obtained using these stationary phases [2,148]. Initially under mild conditions five beta blockers were separated within 4.5 minutes as shown in Figure 3.6A. Increasing the flow rate to its maximum of 3.0 mL/min due to pressure maximum of 400 bar at ambient temperature under the given chromatographic conditions (Figure 3.6B) allowed for a decrease in analysis time by 65% while efficiency loss was only about 20%. In order to obtain faster flow rates, the temperature was increased to 45 ^{o}C as to decrease the viscosity of the mobile phase. At 45 ^{o}C and a 4.3 mL/min flow rate ultra-fast separation (i.e. analysis time less than 60 s) of five beta blockers was obtained as

shown in Figure 3.5C. Therefore RSP-CD SPP stationary phase is beneficial in highly efficient, ultra-fast separations.

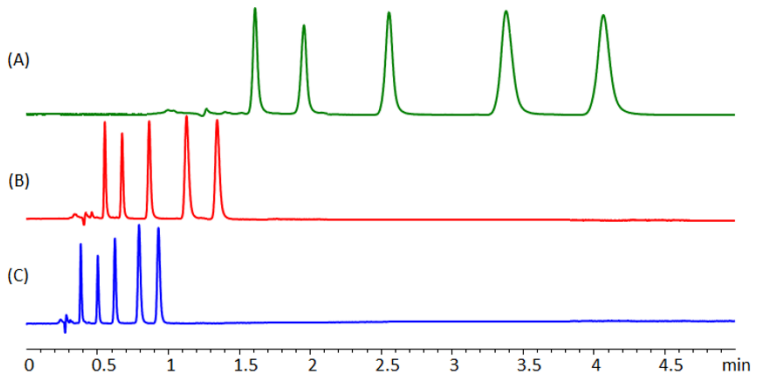

Figure 3.6 Ultrafast separation of five beta blockers using the RSP-CD SPP (100 mm x 4.6 mm i.d.) column. Chromatographic conditions: 80/20 ACN/ 20 mM NH4OAc, pH 4.5, UV detection at 254 nm. (A) Flow rate: 1.0 mL min-1, ambient temperature, (B) Flow rate: 3.0 mL min-1, ambient temperature, and (C) Flow rate: 4.3 mL min-1, 45 oC. Analytes: (1) carvedilol, (2) alprenolol, (3) acebutolol, (4) nadolol, (5) atenolol (in order of elution).

HILIC separations of other selected classes of compounds (nucleic acid bases and nucleosides, water soluble vitamins and salicylic acid derivatives) on the SPP based stationary phase are shown in Figure 3.7. Separation of five water soluble vitamins was obtained under 12 minutes and nucleic acid bases and nucleosides were separated under nine minutes as shown in Figure 3.7A – 3.7B. Five salicylic acid derivatives were separated within 2.5 minutes with considerably high efficiency as shown in Figure 3.7C.

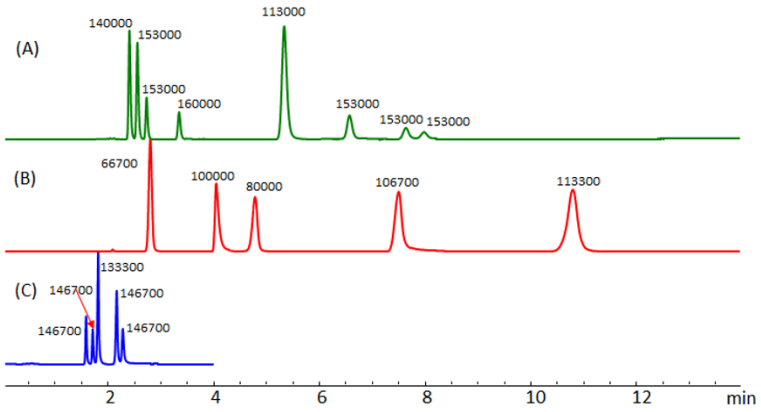

Figure 3.7 Separation of (A) nucleic acid bases and nucleosides, (B) water soluble vitamins and (C) salicylic acid derivatives using the RSP-CD 2.7 µm SPP silica (150 mm x 4.6 mm i.d.) column. Efficiencies are given in plates per meter corresponding to each peak in the chromatograms. Chromatographic conditions: (A) ACN: 20 mM NH4OAc pH 4.1 (90:10), 1.0 mL min-1, UV detection at 254 nm. Analytes (in order of elution): (1) uracil, (2) thymine, (3) thymidine, (4) uridine, (5) adenosine, (6) adenine, (7) cytosine, (8) cytidine, (9) guanine, (10) guanosine. (B) ACN: 20 mM NH4OAc pH 4.1 (90:10), 1.0 mL min-1, UV detection at 254 nm. Analytes (in order of elution) : (1) nicotinamide, (2) pyridoxine, (3) riboflavin, (4) ascorbic acid, (5) nicotinic acid. (C) ACN: 20 mM NH4OAc pH 4.1 (85:15), 1.0 mL min-1, UV detection at 228 nm. Analytes (in order of elution) : (1) methyl salicylate, (2) salicylamide, (3) salicylic acid, (4) acetyl salicylic acid, (5) 4-amino salicylic acid.

3.5 Conclusions

The new RSP-CD, 2.7 µm SPP stationary phase resulted in more efficient separations at all flow rates compared to fully porous particles-basedF columns. Also, the

SPP based phase allowed for fast separations without substantial loss of efficiency at higher flow rates in the HILIC mode compared to RSP-CD fully porous silica based stationary phases. The RSP-CD SPP stationary phase provided excellent fast separations of many classes of small polar compounds with considerably high efficiency (> 100,000 plates per meter in most of the cases). It can be also considered that changes in aqueous buffer concentration and pH on HILIC separations on RSP-CD SPP have an influence on many of the chromatographic parameters such as retention and efficiency in the separation of small charged polar molecules over uncharged small polar molecules. Ultra-fast separations are also possible with this RSP-CD SPP column since they allowed separations at high flow rates. An expanded use of RSP-CD SPP as a HILIC stationary phase for separation of small polar molecules is expected.

Chapter 4

SEPARATION OF PEPTIDES ON SUPERFICIALLY POROUS PARTICLES BASED MACROCYCLIC GLYCOPEPTIDE LIQUID CHROMATOGRAPHY STATIONARY PHASES: CONSIDERATION OF FAST SEPARATIONS

4.1 Abstract

Macrocyclic glycopeptide based liquid chromatography stationary phases are known for highly selective peptide separations. Fast and ultra-fast (tR < 1 minute) high efficiency separations were achieved using superficially porous particle (SPP) based stationary phases. Separations of pharmaceutically important classes of peptides such as enkephalins, bradykinins etc. have been achieved in less than 5 minutes in the isocratic elution mode. Selectivity for peptides structurally similar to one another was improved when using teicoplanin based stationary phases compared with commercial C18 stationary phases. Ultra-fast isocratic separations of structurally related peptides were obtained using teicoplanin and vancomycin based, short SPP columns. Acidic mobile phases produced better separations. Ammonium formate was the optimal mobile phase buffer additive. Use of an appropriate combination of macrocyclic glycopeptide stationary phase and mobile phase permits faster and more ESI-MS (Electrospray Ionization - Mass Spectrometry) compatible isocratic separations than previous gradient approaches. Tryptic peptide separation characteristics of the teicoplanin stationary phase is demonstrated. Additionally, teicoplanin showed tryptic peptide separations with different selectivities compared to C18 commercial stationary phases.

4.2 Introduction

Peptide-based therapeutics are emerging as potential high value, broadly applicable compounds in drug discovery pipelines [152]. Under traditional drug development protocols, peptides were considered marginal therapeutic drug candidates because of their facile deactivation by human peptidases and proteases [152,153]. However, it was known that peptides can be chemically modified to increase bioavailability and can be designated as artificial variants of naturally existing potent drug therapeutics [154]. For instance, increased bioavailability has been observed for chemically modified Met-Enkephalin and Leu-Enkephalin [155,156]. Most of these therapeutic peptides and their analogues are structurally related to each other. Some peptides differ from one another only by one amino acid in their sequence and this is known as a single amino acid polymorphism (SAAP) [157,158]. More specifically, some peptides are different from each other only by an inversion of chirality of a single stereogenic center (single amino acid chiral polymorphism (SAACP)/peptide epimers) [157-159]. Many naturally existing peptide epimers, such as deltrophins and dermorphins, are also available due to post translational modifications [160,161].

Highly selective separation techniques often are necessary to analyze closely related peptides. Liquid chromatography, especially reverse phase HPLC and LC-MS are popular techniques for such analyses due to their robustness and improving speed of analysis for biological molecules [162-164]. Radical directed dissociation mass spectrometry, NMR spectroscopy and stereoselective enzyme digestion also are used for distinguishing among SAACP peptides [159,165,166]. Proteomic strategies and electrophoresis are also employed in separation and identification of peptides [157,167,168].

A wide variety of stationary phases have been utilized in peptide separations. In most cases, C18 bonded silica has been used with gradient elution [162,169]. Macrocyclic

glycopeptide bonded silica are the most selective class of stationary phases for separating both SAAP and SAACP peptides [170,171]. The retention mechanism of peptides on macrocyclic glycopeptide stationary phases has been explained as a combination of electrostatic interactions, dipole-dipole interactions and hydrogen bonding [171]. Regardless of the nature of the stationary phase and in spite of using a variety of solvent gradients, it is not uncommon to see long analysis times for many peptide separations [158,169,172]. Also, severe solvent gradients can make ESI-MS detection and especially quantitation more difficult.

Superficially porous particles (SPPs, 2.7 µm diameter) based columns exhibit similar efficiencies as sub 2 µm fully porous particles (FPPs) based columns with considerably reduced back pressure allowing the former to operate at higher flowrates [13,148,173]. For small molecules improved efficiencies are exhibited by SPP columns due to the uniformity of packed bed and reduced eddy dispersions compared to FPP columns [13-15]. Larger molecules like peptides, proteins etc. with small diffusion coefficients and small molecules with slow adsorption-desorption kinetics exhibit lower band broadening even at higher flow rates [16-18]. Nonporous core of shell particles results lower packed bed volume. Therefore, reduced accessibility for longitudinal diffusion is granted. As a result, a smaller van-Deemter B term (longitudinal diffusion) is observed [19-21].

Peptides resulting from enzymatic digestion of a protein are different from each other by charge, chain length, hydrophobicity, etc. Therefore, they can be utilized as column performances evaluation standards [174]. Furthermore, LC-MS analysis of sequence dependent enzyme catalyzed protein digests is a versatile peptide mapping technique [175,176]. Here we report for the first time, tryptic peptides separations characteristics on teicoplanin bonded SPPs and compare the results with C18. The major goal of this work is

fast and effective separation of peptides under fast isocratic conditions using SPPs. The SPPs are bonded with teicoplanin (T) and vancomycin (V) selectors. Apart from tryptic peptide separations, we demonstrate fast and ultra-fast (tR < one minute) separations for different classes of peptides such as enkephalins, bradykinins, etc.

4.3 Material and Methods

4.3.1.Materials

HPLC grade solvents, acetonitrile (ACN), tetrahydrofuran (THF) and methanol (MeOH) were purchased from Sigma Aldrich (St. Louis, MO). All mobile phase additives, buffers and 5-methyl-5-phenylhydantoin were also obtained from Sigma Aldrich (St. Louis, MO). Sources and amino acid sequences of all the peptides utilized in this study are given in Table S1 (see Supplementary Information section). Milli-Q-water purification system (Millipore, Billerica, MA) was used to purify water. Mass spectrometric grade solvents, acetonitrile and water were purchased from Honeywell (Morris Plains, NJ). Since heme group cannot be digested enzymatically, in our study we utilize equine apomyoglobin (myoglobin without its heme group) tryptic digest in order to demonstrate column performances [36]. Apomyoglobin is considered as a stable model protein without disulfide bonds [37-39]. Trypsin cleaves proteins from c-terminus side of arginine and lysine when either is not followed by proline [35, 40]. Lyophilized tryptic digest (reduction – dithiothreitol and alkylation – iodoacetic acid) of equine apo-myoglobin was purchased from nanoLCMS Solutions (Ranco Cordova, CA). Amino acid sequences of expected equine apo-myoglobin tryptic peptides are given in Table 01.

4.3.2 HPLC and LC-MS Instrumentation

The Agilent 1200 series HPLC (Santa Clara, CA) equipped with degasser, quaternary pump, auto sampler temperature controlled column chamber and UV-visible diode array detector was used for all HPLC work. Instrument was controlled by Agilent ChemStation Rev.B.01.03 under Microsoft XP operating system environment. Surveyor HPLC system connected to Thermo Finnigan LXQ linear ion trap with ESI source (Lake Elsinore, CA) was utilized in LC-MS studies. The instrument was controlled by Thermo Fisher Scientific Xcalibra 2.0 data acquisition and processing software under Microsoft Windows environment. Only half of the HPLC effluent was directed into the MS using flow splitting technique (1: 1 ratio). All mobile phase compositions are given as volume: volume (v:v). pH is given for aqueous mobile phase component before mixing with organic modifier. All solvents were vacuumed degassed for 5 minutes before running experiments. Peptides were dissolved in mobile phase solvents or MeOH as concentration of 1 mg/mL. Experiments were performed at room temperature unless otherwise stated. UV detections were carried out at 220 nm and/or 280 nm.

4.3.3 Stationary Phases

Teicoplanin (T) and vancomycin (V) antibiotic macrocyclic glycopeptide chiral selectors were attached covalently to 2.7 µm SPPs surface (Poro shell - Agilent Technologies, Wilmington, DE) as described by Armstrong and co-workers 163,164. Core diameter and shell thickness of SPPs are 1.7 µm and 0.5 µm respectively. T and V stationary phases were slurry packed into 100 mm x 4.6 mm i.d. and 50 mm x 4.6 mm i.d. stainless steel columns. Pore size of particles is 120 Å and surface area is 120 m2/g. Agilent (Santa Clara, CA) Poroshell 120 EC-C18 (2.7 µm SPP) 100 mm x 4.6 mm i.d. column was utilized for LC-MS comparison purposes.

4.4 Results and discussion

4.4.1 Retention and Separation Characteristics of Peptides on Macrocyclic Glycopeptide Chiral Stationary Phases

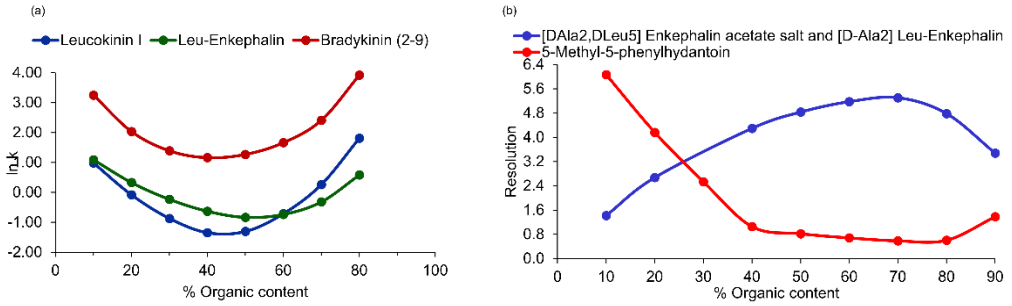

Figure 4.1 (a) Retention behavior characteristics of peptides with acidic, neutral and basic side chains on 2.7 µm SPP T. Chromatographic conditions: column – 50 mm x 4.6 mm i.d., flow rate – 2.0 mL/min, temperature - 40 ^{o}C and mobile phase composition – ACN: 50 mM NH_4HCO_2, pH 3.0. (b) Stereoisomeric resolution of epimeric peptides F versus regular chiral probe (5-Methyl-5-phenylhydantoin) on 2.7 µm SPP T. Chromatographic conditions : column – 50 mm x 4.6 mm i.d., , flow rate – 1.0 mL/min, detection - UV detection at 220 nm , temperature – room temperature and mobile phase composition – ACN : 2.5 mM NH_4HCO_2, pH 3.2.

It has been well known since the mid-1980s that the retention behavior of proteins and peptides on stationary phases is sensitive to the nature of the mobile phase and produce “U” shaped retention curves with changing organic modifier compositions [177]. The same is true for macrocyclic glycopeptide based stationary phases [178]. Figure 4.1a shows typical “U” shaped curves when the retention factors of Leucokinin I, Leu-Enkephalin and Bradykinin [153-160] are plotted against organic (or aqueous) modifier content (v:v).

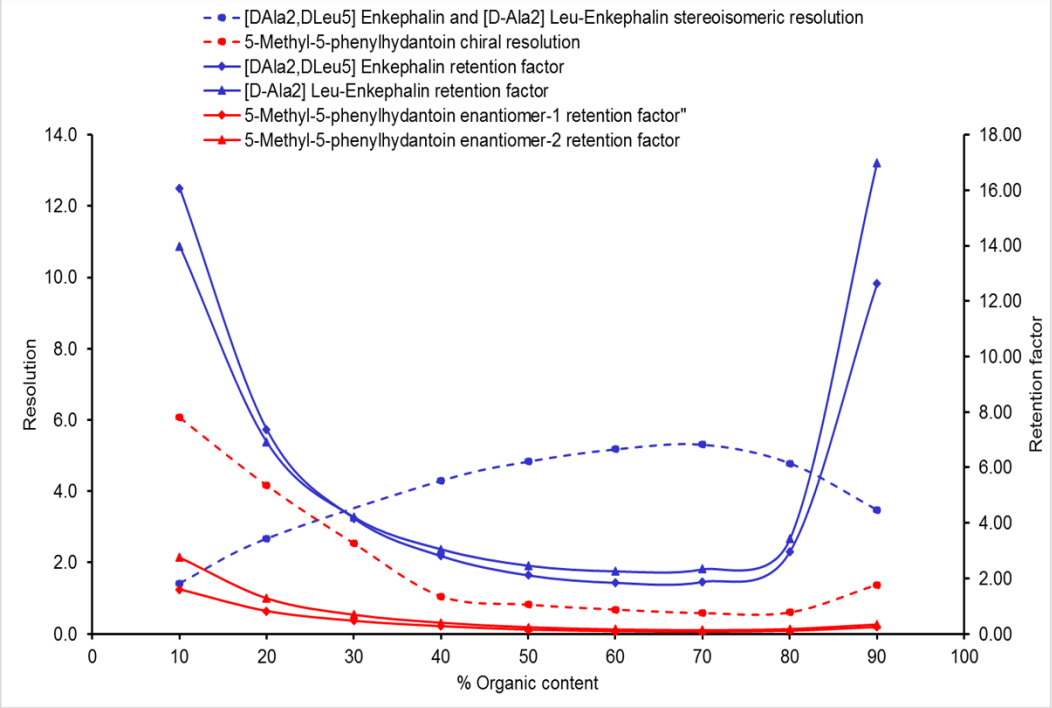

Figure 4.2 Stereoisomeric resolution and retention factors of epimeric peptides ([DAla2, DLeu5] Enkephalin and [D-Ala2] Leu-Enkephalin) versus regular chiral probe (5-Methyl-5-phenylhydantoin) on 2.7 µm superficially porous particles based teicoplanin stationary phase. Chromatographic conditions: column – 50 mm x 4.6 mm i.d., flow rate – 1.0 mL/min, detection - UV detection at 220 nm, temperature – room temperature and mobile phase composition – ACN : 2.5 mM ammonium formate, pH 3.2.

chosen probe peptides have acidic, neutral and basic side chains respectively. The “U” shape retention curve was observed regardless of charge of the peptide. Peptides show poor solubility at high concentrations of organic modifier and their retention is related to their solubility in organic rich mobile phase [177,179]. HILIC behavior of hydrophilic peptides

also can be considered in this particular case where the organic modifier is ACN. Therefore, with increasing ACN content, retention of peptides also can be observed as expected in typical HILIC separations. At higher aqueous concentrations, peptides exhibit typical reversed phase retention behavior. Lowest retention is typically observed in the vicinity of 1:1 (v:v) organic modifier: aqueous component mobile phase compositions. Thus, as for C18 stationary phases, reverse gradient separations are straight forward on macrocyclic glycopeptide chiral stationary phases.

Chromatographic resolution of separation of two peptide epimers ([DAla2,DLeu5] Enkephalin and [D-Ala2] Leu-Enkephalin) is plotted against mobile phase % organic modifier content on a teicoplanin column (Figure 4.1b) and compared to the behavior of a small molecule enantiomeric separation. 5-Methyl-5-phenylhydantoin showed high stereoisomeric resolution at high organic and high aqueous concentrations, whereas the peptide epimers showed the opposite trend. At high organic or aqueous concentrations peptides produced broad and less efficient peaks. In contrast at moderate organic or aqueous concentrations, sharper, and more efficient peaks were observed. Therefore, increased resolution is observed for peptides with decreasing organic or aqueous concentrations. In comparison, 5-Methyl-5-phenylhydantoin enantiomers show typical reversed phase retention behavior while SAACP peptide pair produce a “U” shape retention curve (Figure 4.2).

4.4.2 Effect of pH on Retention and Separation of Peptides

When peptides possess amino acid residues with acidic or basic side chains, their protonation and deprotonation contribute to their residual charge. Therefore, unlike C18 stationary phases, the charge of macrocyclic glycopeptide stationary phases is sensitive to pH. Therefore, pH further alters retention behavior of peptides on these stationary phases. Figure 4.3 shows the effect of pH on retention of some selected peptides using a teicoplanin stationary phase.

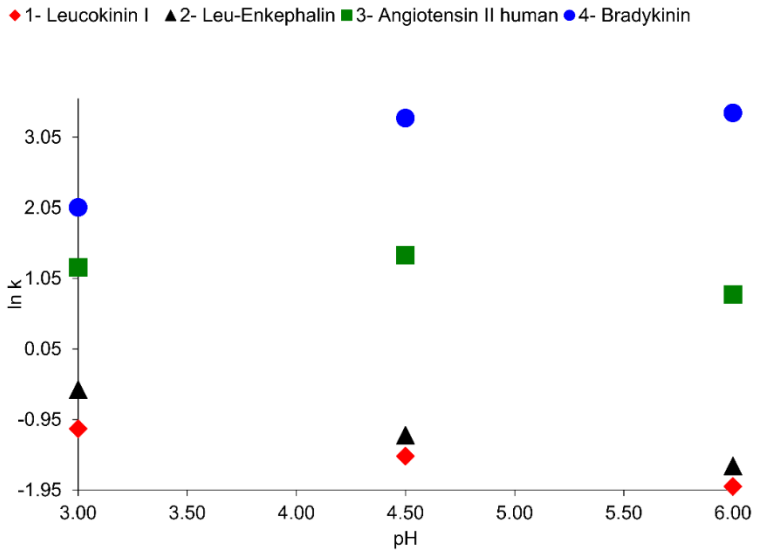

Figure 4.3 The pH effect on retention and separation of peptides containing acidic, basic, acidic and basic both and neutral side chains utilizing 2.7 µm SPP T. Analytes : 1-Leucokinin I, 2- Leu-Enkephalin, 3- Angiotensin II human, 4- Bradykinin (Amino acid sequences are given in Supplementary information: Table S1.) Chromatographic conditions : column – 100 mm x 4.6 mm i.d., flow rate – 2.0 mL/min, detection - UV detection at 220 nm , temperature - 40 ^{o}C and mobile phase composition – ACN : 50 mM ammonium formate (27:73).

At low pH, decreased retention was observed for peptides with basic side chains (bradykinin). Carboxylic acid groups of side chains (leucokinin I) tend to be deprotonated with increasing pH. Therefore, decreasing retention is observed as repulsive electrostatic interactions originating from deprotonated carboxylic acid groups of the stationary phase predominate. Peptides with neutral side chains also show the same trend since C-terminus carboxylic acid groups can become deprotonated. In addition, higher efficiencies were observed at low pH conditions. Therefore, low pH is often beneficial for fast and higher efficiency peptide separations.

4.4.3. Effect of Mobile Phase Buffer Type in Separation of Peptides

A study of the effect of five different mobile phase buffers/additives ($CF_3CO_2NH_4$, TFA, HCO_2NH_4, HCO_2H, and $CH_3CO_2NH_4$) was done. (The pH of the mobile phases containing $CF_3CO_2NH_4$, HCO_2NH_4, and $CH_3CO_2NH_4$ were adjusted to pH 3.0 by adding corresponding acids to the mobile phase aqueous component.) The experiments were performed in a constant mobile phase mode (Organic: aqueous ratio and buffer concentrations are kept constant.) and also in a constant retention time mode. Constant retention times were obtained utilizing two different strategies. In one approach, constant retention times were obtained by adjusting mobile phase organic: aqueous ratio without changing buffer concentrations. In the other approach, the aqueous buffer concentrations are adjusted while maintaining the organic: aqueous ratio constant. Experiments were performed utilizing four bradykinin family peptides as probe molecules as shown in Figure. 4.4. and Figure. 4.5. This type of comparison is essential in any method optimization, especially in LC-MS where the counter ion concentration affects signal intensity.HPLC methods developed in this work using 4.6 mm I.D. can be successfully transferred to LC-

MS by utilizing narrow bore columns or flow splitting technique that allows only a certain portion of effluent to enter into the MS.

4.4.3.1 Constant mobile phase conditions

When NH4CF3COO, NH4HCOO, and NH4CH3COO are used as mobile phase buffer additives, at a concentration of 35 mM, baseline separation of all four peptides was observed.

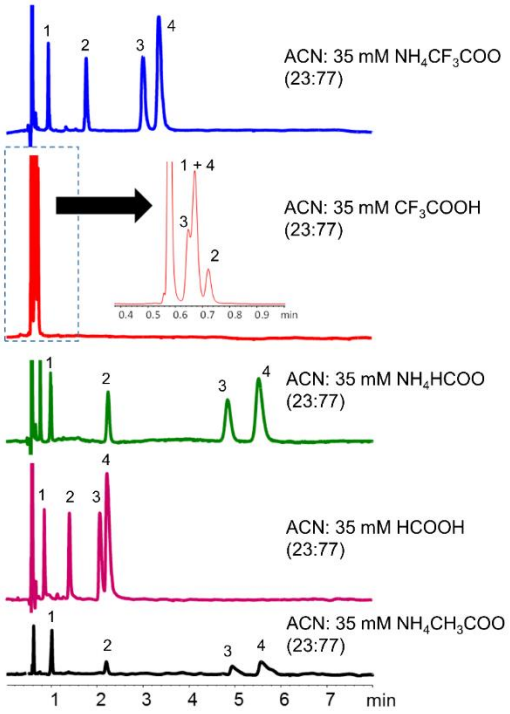

Figure 4.4 Effect of buffer additive type on retention and separation of bradykinin peptides on teicoplanin stationary phase. Organic to aqueous ratio and buffer concentrations are kept constant. Analytes: 1- Bradykinin (2-7), 2- Bradykinin (2-9), 3- Angiotensin I Converting Enzyme Inhibitor, 4- Bradykinin Chromatographic conditions: column – 100 mm x 4.6 mm i.d., 2.7 µm core shell silica, flow rate – 2.0 mL/min, temperature - 40 ^{0}C.

The best peak shapes, efficiencies, and selectivities were observed with NH_4HCOO and NH_4CF_3COO. Therefore, mobiles phase containing 35 mM CF_3COOH or HCOOH did not produce baseline separations of the bradykinin peptides under these experimental conditions. Elution strength (nearly per their acidity) of each buffer/additive can be ordered as CF_3COOH > HCOOH > NH_4CF_3COO > NH_4HCOO = NH_4CH_3COO.

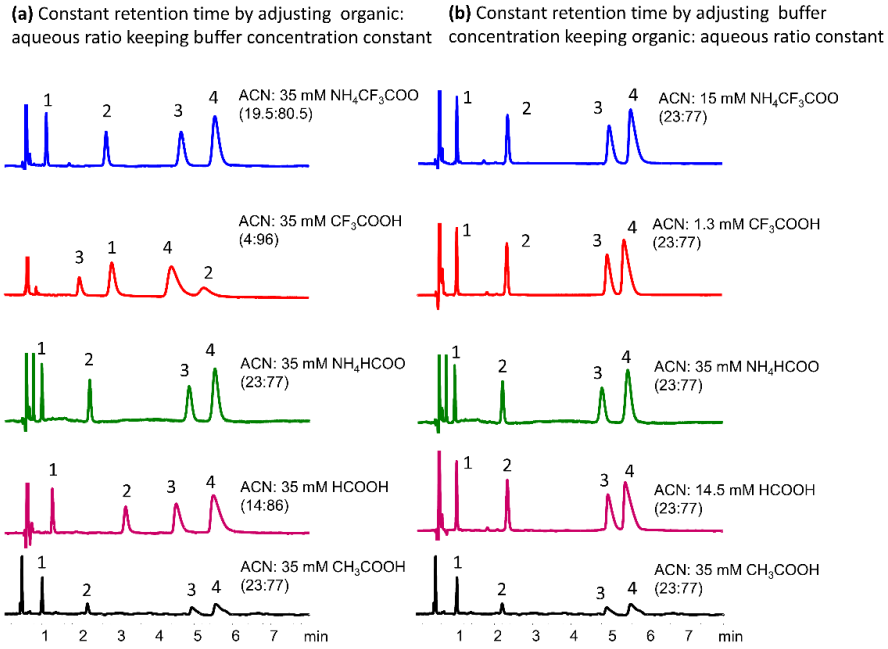

Figure 4.5 Effect of buffer additive type retention and separation of bradykinin peptides on teicoplanin stationary phase. Analytes: 1- Bradykinin (2-7), 2- Bradykinin (2-9), 3- Angiotensin I Converting Enzyme Inhibitor, 4- Bradykinin (Amino acid sequences are given in Table S1.) Chromatographic conditions: column – 100 mm x 4.6 mm i.d., 2.7 µm superficially porous particles, flow rate – 2.0 mL/min, detection - 220 nm UV-DAD detector, temperature - 40 ^{0}C.

4.4.3.1 Constant retention time mode

By adjusting the aqueous to organic modifier ratio, similar elutrophic strength was obtained for all mobile phases while keeping the buffer/additive concentration constant (35mM). Hence, baseline separation of probe peptides with constant retention was obtained with all five mobile phase conditions as shown in Figure 4.5. With $CF_3CO_2NH_4$ and HCO_2NH_4 as buffers, better peak shapes were obtained while other additives lead to mostly tailing peaks. In addition, when ammonium formate was used as the buffer, better efficiency and selectivity were obtained. Baseline separations at constant retention times shown in Figure 4.5 was obtained by adjusting the mobile phase buffer/additive concentration and maintaining aqueous to organic modifier ratio (23:77) constant. Except for HCO_2NH_4, all buffer/additives resulted in tailing peaks. Again both $CF_3CO_2NH_4$ and HCO_2NH_4 gave comparable efficiencies and selectivities. Better peak shapes and efficiencies were observed when using HCO_2NH_4 as the mobile phase additive compared to other mobile phase additives used in this experiment. In general, HCO_2NH_4 can be designated as the most effective buffer additive in peptide separations when using the teicoplanin stationary phase.

4.4.4 Effect of Mobile Phase Organic Modifier on Retention and Separation of Peptides

Methanol, ethanol, and acetonitrile are commonly utilized organic modifiers in peptides separations [171]. In this work, we report the effect of these organic modifiers on peptide separation efficiency and selectivity when using teicoplanin stationary phase. Figure 4.6 Shows the effect of MeOH, ACN, and THF on the separation of peptides (two vasopressin probe peptides) in the constant mobile phase mode (Figure 4.6.a) and constant retention time mode (Figure 4.6.b). The best selectivity is observed with MeOH in

the constant mobile phase mode and with THF in the constant retention mode. The highest efficiency was observed with ACN in both cases. Both ACN and THF produced more symmetric peak shapes in all cases, whereas Methanol produced tailing peaks in the constant mobile phase mode. It is apparent that aprotic organic modifiers are more effective for peptide separations when using the teicoplanin stationary phases.

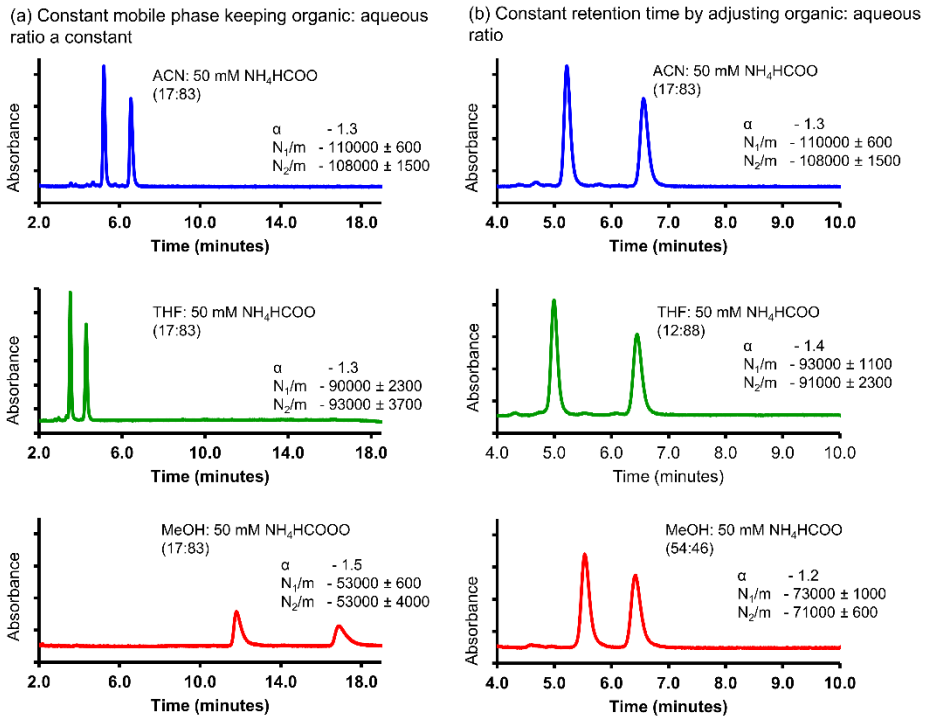

Figure 4.6 Effect of mobile phase organic modifier on retention and separation of peptides on teicoplanin stationary phase. Analytes: 1- [Arg8] Vasopressin /AVP, 2- [Lys8] Vasopressin, Chromatographic conditions: column – 100 mm x 4.6 mm i.d., 2.7 µm core shell silica, flow rate – 1.0 mL/min, , temperature 40 ^{0}C.

4.4.5. Comparison of Chromatographic Performances of Teicoplanin and Vancomycin 2.7 µm SPP Stationary Phases

Macrocyclic glycopeptide stationary phases have wide utility in separations of peptides as demonstrated previously [158,171]. Most of the reported peptides separations were performed using teicoplanin and ristocetin [158,171]. In addition, in this work utilization of vancomycin is examined as shown in Figure 4.7. The overall charge of the stationary phases play an important role in selectivity. Three common peptides classes (vasopressin, LHRH, and enkephalins) were separated on both stationary phases. The mobile phases with equal elutrophic strength were used.

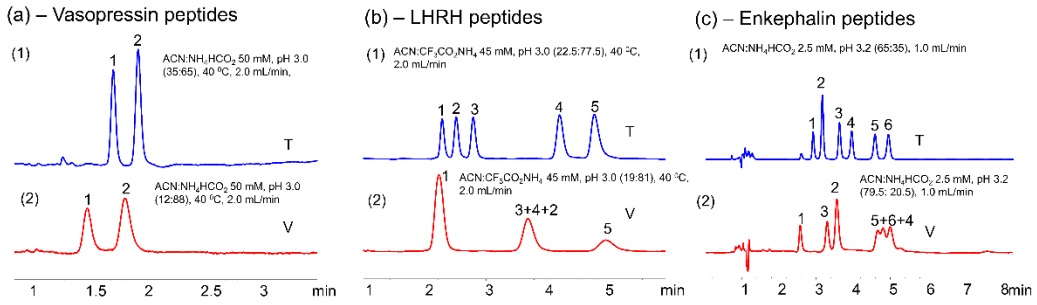

Figure 4.7 Comparison of chromatographic performances of teicoplanin and vancomycin-2 2.7 µm SPP stationary phases (100 mm x 4.6 mm i.d.). (a) Vasopressins: 1- [Arg8] Vasopressin /AVP, 2- [Lys8] Vasopressin (b) LHRH: 1- LHRH free acid, 2- [D-Phe2, D-Ala6]-LH-RH, 3. [D-Ala6]-LH-RH acetate salt hydrate, 4. [D-Lys6]-LH-RH, 5- [des-pGlu1]-LH-RH(c) Enkephalins: 1. [DAla2, DLeu5] Enkephalin acetate salt 2. [DAla2] Met-Enkephalin 3. [D-Ala2] Leu-Enkephalin 4. Met-Enkephalin 5. Leu-Enkephalin 6. [Ala2] Leu-Enkephalin

Vasopressin peptides can be baseline separated on both stationary phases while teicoplanin showed five times higher efficiencies than vancomycin (Figure 4.7). Teicoplanin provided baseline separation of five LHRH peptides with twice the efficiency compared to vancomycin where baseline separation was not observed. Baseline separation of six enkephalin peptides in the HILIC mode (based on retention behavior, see Figure 4.1 and Figure 4.2) were obtained using teicoplanin stationary phase with an efficiency of approximately 120,000 plates per meter whereas vancomycin did not give baseline separation of all six peptides. It is important to note that the last reported separations of LHRH, enkephalins and vasopressin peptides utilizing 5 µm FPPs based commercial teicoplanin stationary phases had analysis times of 30-50 minutes [158]. Separations reported in this work using SPPs based teicoplanin stationary phases are ≤ 5 minutes. In addition, all of the above reported separations are obtained in the isocratic mode. In contrast, most of these peptides have only been separated in the gradient mode using C18 stationary phases [172,180].

4.4.6 Ultrafast Peptide Separations

SPPs based stationary phases can provide fast separations without substantial loss of efficiency and they can be operated at high flow rates with moderate back pressure [2,181]. Both teicoplanin and vancomycin SPPs based short columns (5 cm x 4.6 mm i.d.) can be utilized in ultra-fast separations of both SAP and SAACP peptides as shown in Figure 4.8. Separation of [DAla2,DLeu5] Enkephalin and [D-Ala2] Leu-Enkephalin on a SPP based teicoplanin column is achieved within 30 seconds (Figure 4.8) [D-Ala2] Leu-Enkephalin and [Ala2] Leu-Enkephalin were separated within 30 seconds on vancomycin

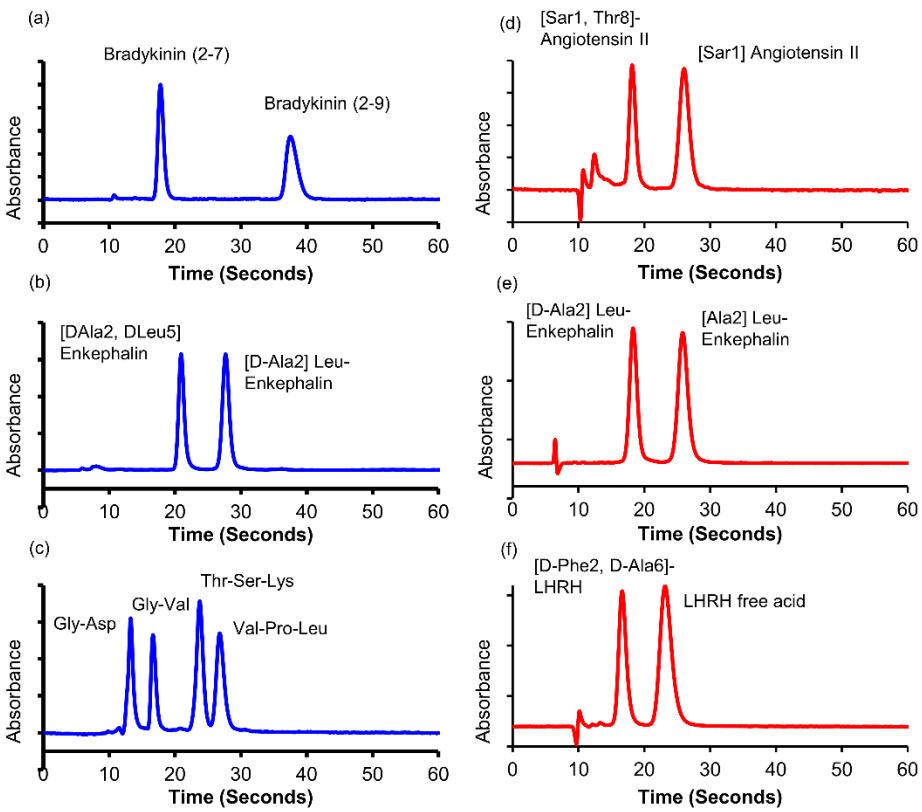

Figure 4.8 Ultra-fast enantiomeric (b and e) and non-enantiomeric (a, c, d, and f) peptide separations on teicoplanin and vacomycin-2. Chromatograms a, b and c were performed on Teicoplanin stationary phase whereas chromatograms d, e and f were performed on Vancomycin-2. Column : 2.7 µm SPP 50 mm x 4.6 mm i.d. (a) flow rate – 3.5 mL/min, temperature – 40 ^{0}C and mobile phase - ACN: NH_4HCO_2 50 mM, pH 3.0 (35:65). (b) flow rate – 4.0 mL/min, and mobile phase- ACN: NH_4HCO_2 5 mM, pH 3.2 (65:35). (c) flow rates – 3.0 mL/min, and mobile phase – ACN: NH_4HCO_2 20 mM, pH 3.0 (15:85), (d) flow rate – 3.0 mL/min, temperature - 40 ^{0}C and mobile phase – ACN : NH_4HCO_2 50 mM, pH 3.0 (30:70). (e) flow rate – 5.0 mL/min, and mobile phase – ACN: NH_4HCO_2 5 mM, pH 3.2 (79.5:20.5), (f) flow rate – 3.0 mL/min, mobile phase – ACN: NH_4HCO_2 50 mM, pH 3.0 (45:55)

(Figure 4.8). Bradykinin (2-7) and Bradykinin (2-9) are structurally related SAP peptides. that are separated in 45 seconds (Figure. 5a). All the peptides utilized in separations shown in Figure. 4.8, play important pharmaceutical roles as endorphins, inflammatory mediators, blood pressure regulators, etc. [182,183].

4.4.7 Comparison of Peptide Separations on Teicoplanin and C18 2.7 µm SPP Stationary Phases

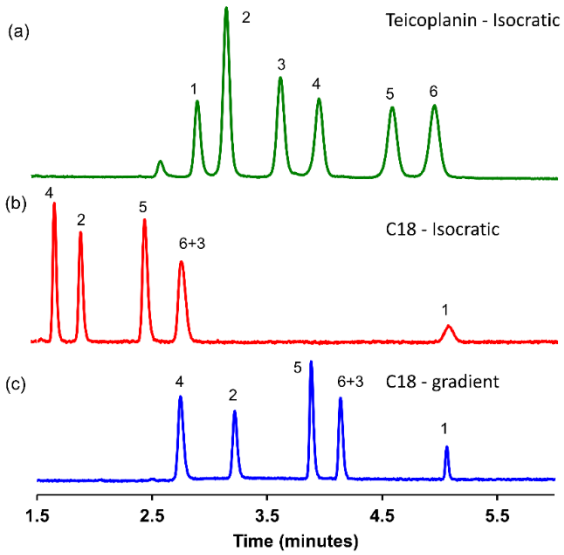

Figure 4.9. Comparison of enkephalin peptides separations on teicoplanin and C18 2.7 µm SPP stationary phases. Column dimensions: 100 mm x 4.6 mm i.d. Flow rate 1.0 mL/min, analytes: 1. [DAla2, DLeu5] Enkephalin acetate salt 2. [DAla2] Met-Enkephalin 3. [D-Ala2] Leu-Enkephalin 4. Met-Enkephalin 5. Leu-Enkephalin 6. [Ala2] Leu-Enkephalin. Mobile phase: A - ACN, B – 2.5 mM NH_4HCO_2, pH 3.2 (a) A: B (63:35) (b) A: B (23: 77) (c) A: B (20:80) to A: B (50:50) in 7 minutes

C18 is the most utilized stationary phase for the separation of peptides and proteins in the reversed phase mode. A performance comparison of C18 and teicoplanin stationary phases is given in Figure 4.9. All six peptides were baseline separated with efficiency of ≈ 150000 plates per meter on the teicoplanin column in the isocratic mode. Best separations of the same six enkephalin peptides on the C18 stationary phase in both isocratic and gradient modes are shown in Figure 4.9 a and Figure 4.9 b respectively. [Ala2] Leu-Enkephalin and [D-Ala2] Leu-Enkephalin (analytes 6 and 3) coeluted in both separation modes when the C18 stationary phase is utilized. Also, C18 showed lower efficiency (N ≈ 130000 plates per meter) in the isochratic isocratic mode than teicoplanin.

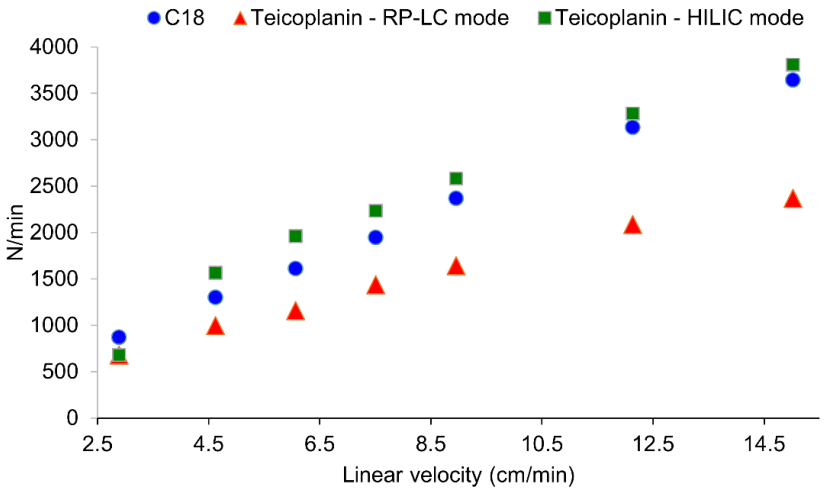

Figure 4.10 Kinetic performances of 2.7 µm superficially porous particles based C18 and teicoplanin stationary phases. Analyte: Leu-Enkephalin (Amino acid sequence are given in Table S1.) Chromatographic conditions: C18 and teicoplanin – RP-LC mode – ACN:2.5 mM, pH 3.2 ammonium formate (23:77), teicoplanin – HILIC mode –ACN:2.5 mM, ammonium formate, pH 3.2 (65:35).

The SAACP pair, [DAla2, DLeu5] Enkephalin and [D-Ala2] Leu-Enkephalin were baseline separated on both stationary phases. The [D-Ala2] Leu-Enkephalin and [Ala2] Leu-Enkephalin SAACP pair was baseline separated only on teicoplanin. All SAP pairs were baseline separated on both stationary phases.

Kinetic performances of SPPs based C18 and teicoplanin stationary phases were also compared (Figure 4.10). Leu-Enkephain was chosen as the probe peptide. Both stationary phases were evaluated the in reversed phase liquid chromatography mode. C18 shows better performances at higher linear velocities. Though reversed phase mode is the ideal operation mode for C18, it may not be the case for teicoplanin. When operated in the HILIC mode, at higher linear velocities teicoplanin showed better performances than C18. Comparatively similar performances were observed at slower linear velocities for both stationary phases regardless of the mode of operation. Therefore, more efficient separations can be obtained using teicoplanin stationary phase when it is operated its optimal mode.

4.4.8 Tryptic Peptide Separations on Teicoplanin- LCMS

Capability of separations of complex peptides mixtures using teicoplanin stationary phases was demonstrated. Both isocratic and gradient modes were examined. Tryptic peptide separations on teicoplanin stationary phase have not been reported previously. A comparison of C18 and teicoplanin columns is given in Figure 4.11 (constant retention mode). The selectivity of teicoplanin peptide separations in the gradient mode was significantly different than that obtained for C18 column. Also, the teicoplanin stationary phase separated more peptides than the commercial C18 stationary phase. In the isocratic mode, teicoplanin produced fast but less selective separations.

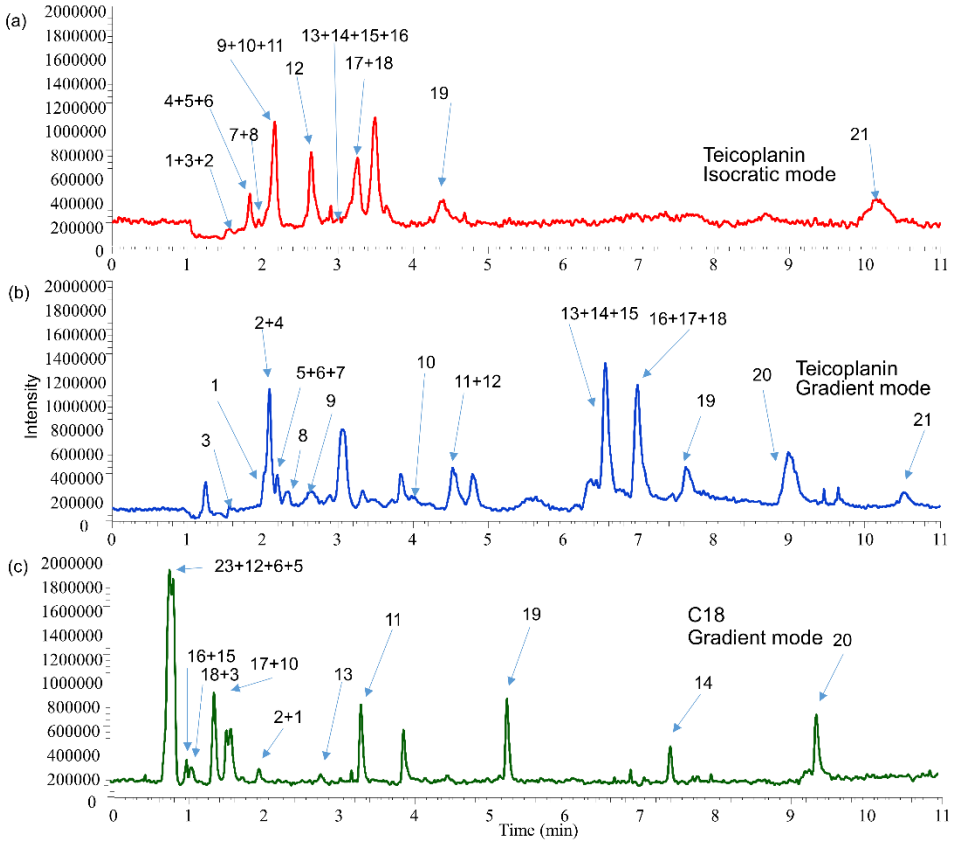

Figure 4.11 Comparison of equine apomyoglobin tryptic digest peptides separations (LCMS) on teicoplanin and C18 and 2.7 µm SPP stationary phases. Column dimensions: 100 mm x 4.6 mm i.d. Amino acid sequences of tryptic peptides are given in Table 1 .Mobile phase: solvent A - 0.1% HCO_2H in 30% water in ACN, solvent B - 0.1% HCO_2H in water (a) A: B (30:70) , (b) A: B (5:95) for 2 minutes and from A:B (5:95) to A:B (40:60) in next 13 minutes (c) A: B (5:95) to A: B (40:60) in 15 minutes. Flow rate 1.0 mL/min and only 50% of the flow was directed to ESI-MS detector

The teicoplanin column had peak capacity of 50 in the isocratic mode. However, it produced nearly three times higher peak capacities in the gradient elution mode.

Interestingly both C18 and teicoplanin produced comparative peak capacities in gradient elution mode (Isocratic peak capacities were calculated using the $n = 1 + \int_{t1}^{tn} \frac{\sqrt{N}}{4} \frac{dt}{t}$ where n is peak capacity, tn is retention time of last eluted peak, t1 is retention time of first eluted peak and N is number of theoretical plates [183].

Gradient peak capacity was calculated using the $n = 1 + \frac{tg}{w}$ where n is peak capacity, tg is gradient time and w is the average peak width [184,185]. Twenty peptides and lysine were identified using teicoplanin and 19 peptides and lysine were identified when C18 was used (For peptide identity and number of missed cleavages see Table 4.1. Each peptide was identified via ESI-MS extracted ion chromatogram. Some identified peptides do not show sharp peaks in the total ion chromatograms shown in Figure 4.11). HK and GHHEAELKPLAQSHATK were not identified in either case. The teicoplanin stationary phase is compatible in reversed phase mode with MS compatible mobile phases in peptide separations. Hence teicoplanin is a competitive stationary phase with C18, for analyzing tryptic peptides and for obtaining different selectivities. Note that Tryptic peptides 21, 22, 23, and 24 were not identified when the teicoplanin stationary phase was used. Tryptic peptides 21, 4, 9, 7, 8, and 24 were not identified when the C18 stationary phase was used.)

Table 4.1 Amino acid sequences, number of amino acid residues ($[M+H]^+$) and retention orders on teicoplanin and C18 stationary phase of predicted equine apomyoglobin tryptic digest peptides. (Tryptic digestion of equine apo-myoglobin was dissolved in ACN: 0.1 % HCOOH in water (5:95) as concentration of stock solution is 1 pmol of protein per µL. Highlig hted peptides were not detected.

Amino acid sequence	Range	Number of missed cleavages	$[M+H]^+$	Elution order
YNEFISDAIIHVLHSK	103-118	0	1885.98	20
GHHEAELKPLAQSHATK	**80-96**	**0**	**1853.96**	**21**
GLSDGEWQQVLNVWGK	42385	0	1815.90	14
VEADIAGHGQEVLIR	17-31	0	1606.86	17
HPGDFGADAQGAMTK	119-133	0	1502.67	15
HGTVVLTALGGILK	64-77	0	1378.84	19
LFTGHPETLEK	32-42	0	1271.66	18
ALELFR	134-139	0	748.44	11
TEAEMK	51-56	0	708.32	5
ASEDLK	57-62	0	662.34	4
ELGFQG	148-153	0	650.31	2

NDIAAK	140-145	0	631.34	6
IPIK	99-102	0	470.33	9
FDK	43-45	0	409.21	22
HLK	48-50	0	397.26	23
YK	146-147	0	310.18	7
FK	46-47	0	294.18	8
HK	**97-98**	**0**	**284.17**	**24**
K	63-63	0	147.11	3
K	78-78	0	147.11	3
K	79-79	0	147.11	3
YKELGFQG	146-153	1	941.47	10
ASEDLKK	57-63	1	790.43	12
HKIPIK	97-102	1	735.49	21
FDKFK	43-47	1	684.37	16
FKHLK	46-50	1	672.42	1
FKHLKTEAEMK	46-56	2	1361.72	13

4.5 Conclusions

SPP based macrocyclic glycopeptide stationary phases showed wide utility in peptide separations including tryptic peptide separations. High efficient fast and ultrafast peptide separations were achieved using SPP based columns in this work. Ultra-fast SAAP and SAACP peptide separations were obtained using both teicoplanin and vancomycin SPP based stationary phases. Separations were further improved by optimizing mobile phase organic modifier type, pH and mobile phase additive type. Shorter retention times were obtained when THF was used as the mobile phase organic modifier, but when ACN was used as a mobile phase organic modifier, it provided higher efficiency. Also by varying the organic modifier content SAACP peptide resolution can be optimized. Due to provided higher efficiency, ammonium formate can be designated as the most compatible mobile phase additive among the mobile phase additives used in this study when use teicoplanin stationary phase. The teicoplanin stationary phase resulted more efficient baseline separations of bradykinin peptides, vasopressin peptides and enkephalin peptides compared with vancomycin stationary phase. The teicoplanin stationary phase showed better selectivity in SAAP and SAACP peptides (enkephalins) baseline separations where C18 commercial stationary phases did not show baseline separations of all enkephalin peptides. Tryptic peptide separation characteristics of teicoplanin stationary phase were demonstrated comparatively to C18 commercial stationary phases using myoglobin tryptic digestion. Teicoplanin resolved 20 peptides and lysine where C18 resolved 18 peptides and lysine with different selectivities. Therefore, teicoplanin is a competitive stationary phase with commercial C18 stationary phases in tryptic peptide separations. Further, more MS compatible and isocratic separation methods have been developed in this work. Superficially porous particle based macrocyclic glycopeptide stationary phases can be successfully used to achieve more efficient, fast and ultra-fast separations of

pharmaceutically important peptides. Teicoplanin stationary phases should be considered as potential stationary phase for proteomics applications. Since these stationary phases provided fast and efficient separations, they can be potentially utilized as a good second dimension stationary phase in both heart cutting and comprehensive two-dimensional liquid chromatography.

Chapter 5

SALIENT SUB-SECOND SEPARATIONS

5.1 Abstract

Sub-second liquid chromatography in very short packed beds is demonstrated as a broad proof of concept for chiral, achiral, and HILIC separations of biologically important molecules. Superficially porous particles (SPP, 2.7 µm) of different surface chemistries namely, teicoplanin, cyclofructan, silica, and quinine were packed in 0.5 cm long columns for separating different classes of compounds. Several issues must be addressed to obtain the maximum performance of 0.5 cm columns with reduced plate heights of 2.6 to 3.0. Modified UHPLC hardware can be used to obtain sub-second separations provided extra-column dispersion is minimized and sufficient data acquisition rates are used. Further, hardware improvements will be needed to take full advantage of faster separations. The utility of power transform, which is already employed in certain chromatography detectors, is shown to be advantageous for sub-second chromatography. This approach could prove to be beneficial in fast screening and two dimensional liquid chromatography.

5.2 Introduction

One of the basic tenets of separation science is to achieve adequate resolution in the shortest possible time. Not surprisingly, the relative meaning of “shortest possible time” has evolved over five decades, where early separation of biological molecules in 30-60 min was once considered fast liquid chromatography.[186,187] By current standards, ultrafast liquid chromatography is usually considered as sub-minute separations although the lower limit will continue to decrease with developments in smaller particle synthesis, improved

packing technologies, design of the column hardware and peak detection methods.[2,11] Recently, researchers have shown unprecedented separation speeds of 4-5 seconds in packed beds by using high efficiency particles for both achiral and chiral separations in liquid chromatography as well as supercritical fluid chromatography.[3,54,188-191] It is not uncommon to obtain plate heights H<2dp (dp = particle diameter) with superficially porous particles (SPP) or fully porous sub 2 µm particles with exceptionally narrow size distribution.[192] The excellent performance of the former arises from lower contributions to eddy dispersion in the band broadening processes.[193] These efficiencies are providing an impetus to separation scientists to push the boundaries of analysis speed by utilizing very short columns. Ultrafast liquid chromatography is a very promising approach for high throughput screening methods[194] or in two dimensional chromatography of complex samples where it is necessary to have high speed separations in the second dimension .[195-198]

To date, ultrahigh speed separations of a few seconds or as low as milliseconds have been achieved in special electrophoretic microchip plates or in capillary zone electrophoresis.[5-8] Other approaches such as shear driven chromatography and wide bore hydrodynamic separations have also shown some promise in this regard.[9,10] Special detection technologies were employed such as on-column detection followed by image processing to extract the peak profile.[6,199] Handling of rapidly eluting peaks in the domain of conventional liquid chromatography is currently hindered by extra-column dispersion and even the data sampling rates on many commercial UHPLCs. The ideal chromatographic output from extremely high efficiency columns and fast eluting peaks is convoluted by several factors. The shape of the injector pulse, the cup-flow distribution pattern of the inlet and outlet frits, diffusion and mixing in plumbing unions, flow profiles in the tubings, data sampling rate and embedded noise suppressing algorithms in any

chromatographic set-up all affect the true peak shape in deleterious ways.[11,200] Secondly, in the majority of UHPLCs, the maximum flow rate is limited to 2 to 5 mL/min, which is another factor limiting separation speed.

The aim of this work is to analyze the conceptual and practical aspects of sub-second separations on state of the art ultrahigh performance instruments using 0.5 cm packed columns with 2.7 µm SPP particles. We discuss and propose simple instrumental modifications and simple mathematical approaches allowing chromatographers to circumvent the challenges in ultrafast LC (vide supra) and obtain sub-second separations. Shortest possible analytical column dimensions available commercially (0.5 x 0.46 cm i.d.) are used with four different chemistries (silica, cyclofructan-6, teicoplanin, and quinine bonded phases). These column chemistries are compatible with normal, reversed phase, HILIC, and polar organic/ionic modes and are used for a broad proof of concept. The polar organic mode uses ACN as a major component of the mobile phase while MeOH is used to adjust the retention time with small amounts of acid/base additives to modify the selectivity.

5.3 Experimental

5.3.1 Materials

All HPLC solvents, buffers, and analytes were obtained from Sigma-Aldrich (St. Louis, MO). The 2.7 µm superficially porous particles with 1.7 µm core diameter and 0.5 µm shell thickness were provided by Agilent Technologies (Wilmington, DE). Surface area of the particles is 120 m^2/g and pore diameter is 120 Å. Mobile phase compositions are given as volume/volume (v/v). The pH and mobile phase additive concentrations are given for the aqueous portion of the mobile phase before mixing with organic modifier and all experiments were conducted at room temperature.

5.3.2 Stationary Phases

The stationary phase materials were synthesized by AZYP LLC (Arlington, TX). Teicoplanin, cyclofructan-6 and quinine based stationary phases were prepared according to the reported methods.[151,178,201] The stationary phase material was either packed into 0.5 cm x 4.6 mm i.d. empty guard columns by Agilent Technologies, (Wilmington, DE) or packed in our laboratory using dispersed slurry techniques and pneumatic pumps. Superficially porous silica (2.7 µm) guard columns was purchased from Agilent Technologies. As reported earlier,[2] it was found that dispersed suspensions of core-shell particles produced optimum results with pressures of 10,000 psi. These pressures were necessary to stabilize the bed against high flow rates (5 mL/min max on the UHPLC) for sub-second chromatography. For further characterization of the column volume (and to estimate the dead times), pycnometry was performed using the density difference method with water and methanol (n=3).29 The dead volumes of the column were found to be 75, 69, and 75 µL for SPP silica, SPP teicoplanin and SPP quinine respectively. Therefore, at 5 mL/min the average dead time of SPP guard column (in Agilent's hardware) would be 0.83 to 0.89 s. These dead times are consistent with the elution time of acetone under HILIC mode conditions.

5.3.3 Instrumentation

The Agilent 1290 UHPLC is equipped with a degasser, quaternary pump, auto-sampler, temperature controlled column compartment, and diode array detector. The instrument was controlled by OpenLabs CDS ChemStation software (Rev. C.01.06 [61], Agilent Technologies 2001-2014) under Microsoft Windows 8.1. In order to operate the instrument at highest flow rate possible (5.0 mL/min, without pressure restriction); the in-line filter was removed. The pump outlet was directly connected to a pre-saturator column

(5 x 0.46 cm i.d.) filled with silica (M.S. Gel, D-50-120A, AGC SciTech Co., Ltd.). This column has two roles (a) to act as a filter (b) saturate the incoming mobile phase with dissolved silica before it hits the analytical column. This process ensures long life of a column without any back-pressure. The auto-sampler and the column oven were by-passed.

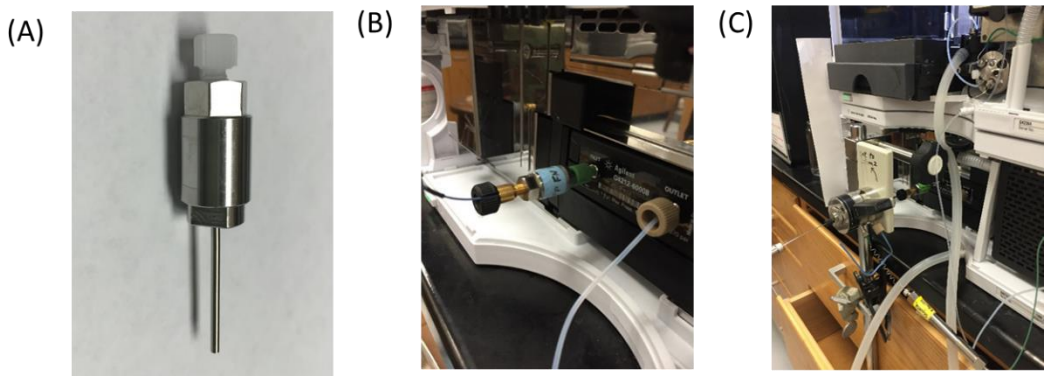

Figure 5.1. (A) Guard column design utilized in this work (Agilent Technologies, Wilmington, DE) (B) Direct connection of column to the UHPLC detector (C) Complete chromatographic set-up for sub-second chromatography. Rheodyne (7520) connected to 7 cm NanoViper, the NanoViper is joined to the 0.5 cm column and the permanent 3 cm extension from the guard column is coupled to the detector.

The pre-saturator column outlet was then connected to a Rheodyne 7520 manual injector (Rheodyne LLC, Rohnert Park, CA) with internal loop size of 1 µL. Full loop injections were made. The Rheodyne was connected to the column via 7 cm x 75 µm NanoViper tubing and the column outlet was directly inserted into the UHPLC detector flow cell. The final instrument setup after modifications is shown in Figure 6.1. The column consists of a 0.5 cm long barrel with a permanently sealed frit at one end followed by a 3 cm x120 µm stainless steel extension. The detector has a dispersion volume V(σ) of 1 µL (G4212-

60008). Although smaller flow cells are available (0.6 µL dispersion), there is a potential of bursting the flow cell with compressible mobile phases at high flow rates. The retention times were determined with respect to the pressure pulse generated by manual injection. Extra column volume dispersion of the system and retention time determination protocol are show in Table 6.1 and Figure 6.2.

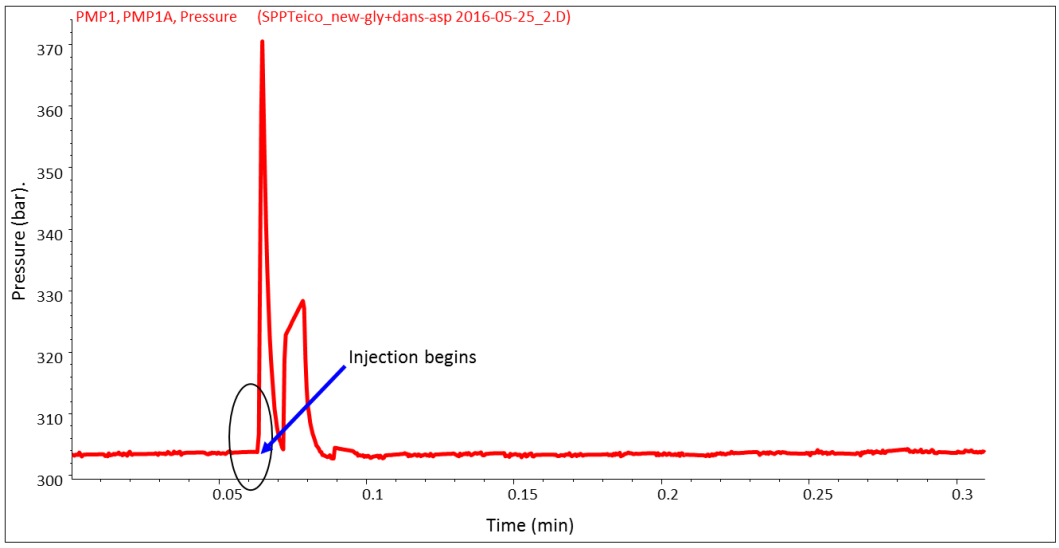

Figure 5.2 Determination of true starting point of injection from the respective pressure profile.

5.3.4 Data Processing.

Peak deconvolution and fitting of the peaks as exponentially modified Gaussians (EMG) and moment analysis were performed on PeakFit software v4.12.

Table 5.1 Instrument hardware parts and their contribution to extra column volume (represented by the means of their dimensions) after modifying the UHPLC

Instrument hardware part	**Dimensions**	**Volume μL**	**Perfect Mixer Variance/μL^2**
Rheodyne manual injector (model 7520)	-	1	1
nanoViper connection tubing from the injector to the column inlet	70 mm x 75 μm i.d.	0.31	0.096
Detector flow cell volume variance	Not disclosed	1 (stated as variance)	1
Guard column extension	30 mm x 120 μm i.d.	0.34	0.12
		SUM	2.2

5.4 Results and Discussion

5.4.1 Preparation and Characterization of Short 0.5 cm x 0.46 cm i.d. Columns.

In order to achieve sub-second liquid chromatography, short 0.5 cm columns were chosen. There is a question of which column diameter is best? Potentially, the narrow i.d. columns (0.21 or 0.30 cm i.d.) would provide very high superficial linear velocities at the maximum flow rates in the UHPLC, e.g. at 5 mL/min the superficial linear velocities in 0.46, 0.30 and 0.21 cm i.d. columns would be 0.501, 1.17, and 2.40 cm /s, respectively. It might appear that the 0.21 cm i.d. format would be the most suitable diameter for ultrafast separations. Unfortunately, the practical difficulties encountered in packing a 0.21 cm i.d.

column and minimizing the extra-column effects override the benefits of narrow bore columns currently. Even in the long column format for superficially porous particles, the 0.21 cm i.d. columns achieve about 60% of the plates of the 0.46 cm i.d. format. For further work, 0.5 cm x 0.46 cm i.d. columns were chosen for slurry packing; since the wall effects are virtually negligible in 0.46 cm i.d. columns.

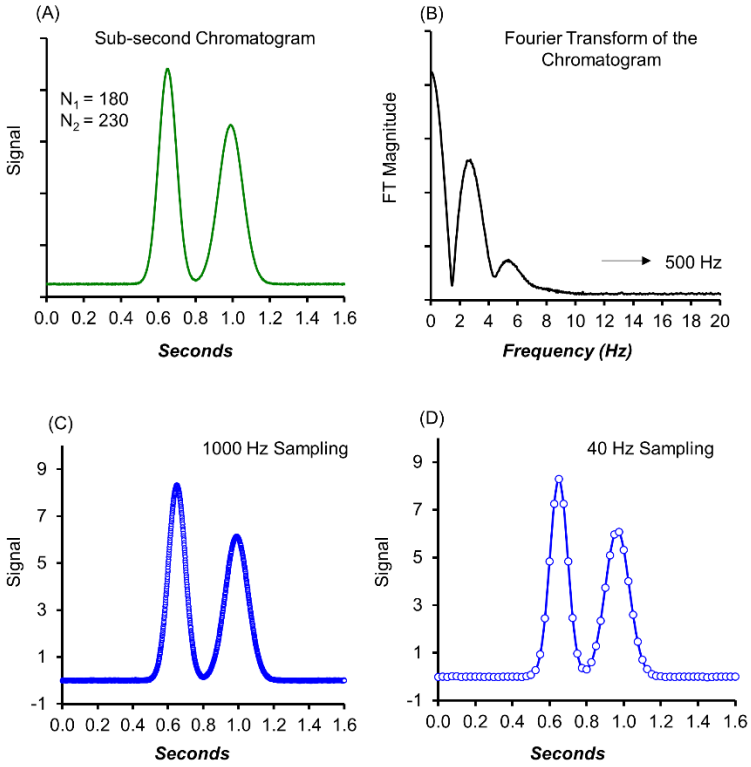

Figure 5.3 Computer simulation of a sub-second separation with rms noise of ±0.06 under a second in (A) time domain, (B) frequency domain via Fourier analysis, (C) time domain signal at 1000 Hz of sampling frequency, and (D) time domain signal at 40 Hz of sampling frequency. Computer simulations are done with OriginPro 2015 (Origin Lab Corporation, MA).

5.4.2 Is the Sampling Frequency Available for Sub-Second Chromatography?

For sub-second chromatography, it was necessary to simulate the separation and assess the required sampling frequency based on the efficiencies observed in the 0.5 cm columns. Shannon's theorem dictates that in order to accurately capture the analytical signal, the minimum sampling frequency must be equal to twice the maximum frequency components in the signal being acquired.[23] In Figure 6.3(A), we simulate two sub-second Gaussian peaks in the presence of root mean square noise of ±0.06 units.

This is the typical noise expected in a modern UV UHPLC detector. The plates counts of 0.5 cm column (150 -200 per second) were set on basis of realistic numbers obtained under very high flow rates (~ 5 mL/min). In order to extract the frequency components of such signals, Fourier transform (FT) of this simulated chromatogram was done. As the FT shows > 95 % of the useful chromatographic information is under 15 Hz. Shannon's theorem guides us to sample the data at a minimum of 2x15 Hz, therefore 40 Hz and 1000 Hz should be sufficient as shown in Figure 6.3C and 6.3D. Note the number of points is less than 20 points per peak in the 40 Hz chromatogram. Two modern UHPLCs can sample the data up to 160 to 250 Hz respectively.

In the near future, ever higher efficiencies are likely in very short columns, and then even these sampling frequencies and response times may be insufficient in sub-second chromatography. The Agilent's UHPLC employed here couples the sampling frequency with a rather sophisticated undisclosed digital filter which behaves very closely like a centered moving average with Gaussian weights.[11] The effect of this coupling is shown in the Figure 6.4.

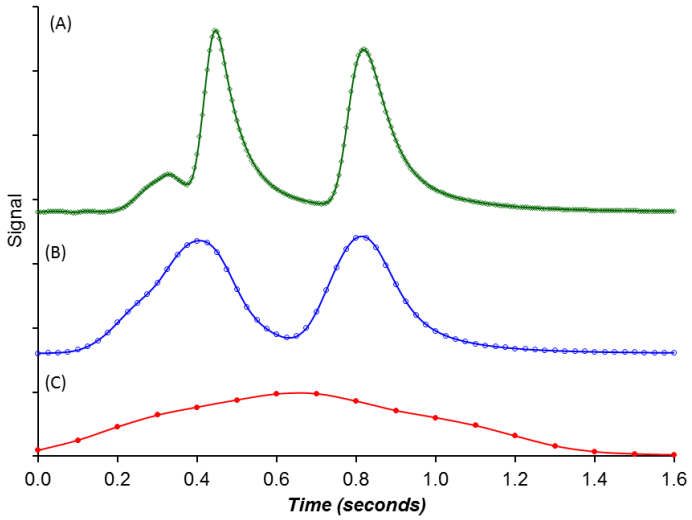

Figure 5.4 Effect of sampling frequency with coupled noise removing Gaussian kernel embedded in the data acquisition software of Agilent's UHPLC. A real sub-second separation of dansyl-L-aspartic acid and glycine (in order of elution) under one second at (A) 160 Hz, 0.016 s, (B) 40 Hz, 0.13 s, and (C) 10Hz, 0.5 s. Column - 0.5 cm x 4.6 mm i.d. SPP Teicoplanin, ACN: water (30:70), 5 mL/min, detection – UV at 220 nm.

5.4.3 Hardware Considerations in Sub-Second Chromatography.

To achieve ultrafast separations in packed 0.5x0.46 cm i.d. columns, packing approaches, and extra-column dispersion of UHPLC needed extensive optimization. The most convenient approach to make very short columns is to pack the superficially porous particles in available (empty) guard columns using dispersed slurry techniques.[106] Based on the previously optimized hardware[2] (low dispersion UHPLC auto-sampler, 25 cm x75 µm tubing, and 1µL detector), 600-700 plates at optimum flow rates (0.8 mL/min) were considered as well-packed columns as shown in Table 6.2.

Table 5.2 The column efficiencies of 0.5 cm long columns (0.46 cm i.d.)

Stationary phase	Efficiency (plates per column length)	
	Uracil	Cytosine
Silica	535 ± 5	643 ± 7
Cyclofructan-6	575 ± 8	697 ± 12
Teicoplanin	569 ± 2	614 ± 5
Quinine	539 ± 4	678 ± 9

This efficiency (N) corresponds to H~ $2.3d_p$ to $3.0d_p$ without subtracting any source of dispersion. For column lengths of 0.5 cm, the extra-column dispersions on any state of the art UHPLC cannot be ignored.[11] Assuming all the extra-column volumes behaved as a perfect mixer,[11] the extra-column variances were estimated to be 2.2 μL^2. The second moment analysis also confirmed that the extra-column variance was only ~ 11% of the chromatographic peak variance at low flow rates. Despite this ultra-low dispersion, there is an additional fundamental challenge with very short connection tubings (3 and 7 cm) employed in this work. Indeed, the Aris-Taylor Gaussian dispersion breaks down because of short residence time of the analyte in the tubings.[202] The eluting peaks (in the absence of column) were observed to produce non-Gaussian tailing profiles, as predicted by Golay along with a “foot” at the tailing end.[202] The “foot” or the hump is marked with an arrow in Figure 6.5C.

It is interesting that this peak shapes neither fits and exponentially modified Gaussian (EMG) nor other empirical versions of peak fitting software (PeakFit v 4.12) such as the “Half Gaussian Modified Gaussian (GMG)” models or their hybrids (EMG-GMG). Obviously, even those relatively poor fit models (R2 ~ 0.98) show that the second moment is higher in terms of μL^2 than the second moment at low flow rates (0.8 mL/min). Similar

peak shapes with “foot” in the tailing region without columns were reported by Gritti et al.[203] The tailing envelope may be superimposed on the band profile eluting from very short columns. A simple but elegant approach for overcoming such fundamental challenges in sub-second chromatography is outlined in the last section of this monograph.

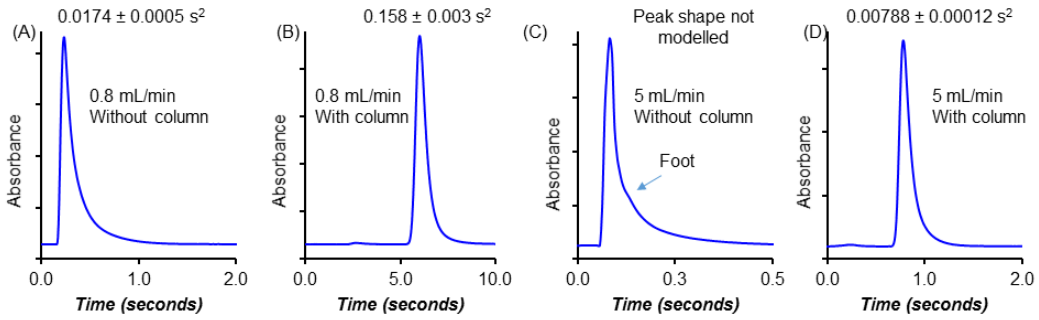

Figure 5.5 Demonstration of effect of extra column effect originating from short connection tubing. Chromatographic conditions - Column: 0.5 cm x 4.6 mm i.d. 2.7 µm core shell silica guard column (Agilent Technologies), mobile phase: ACN: water (80:20), analyte : thymine, connection tubing: 70 mm x 75 µm i.d. NanoViper (A) at 0.8 mL/min without column, (B) at 0.8 mL/min with the column, (C) at 5.0 mL/min without the column, and (D) 5.0 mL/min with the column (second moments are given with the corresponding peak)

5.4.4 Illustrative Examples of Sub-Second Chromatography.

Examples of several different chiral and non-chiral sub-second separations in various chromatographic modes are given in Figure 6.6 and Table 6.3.

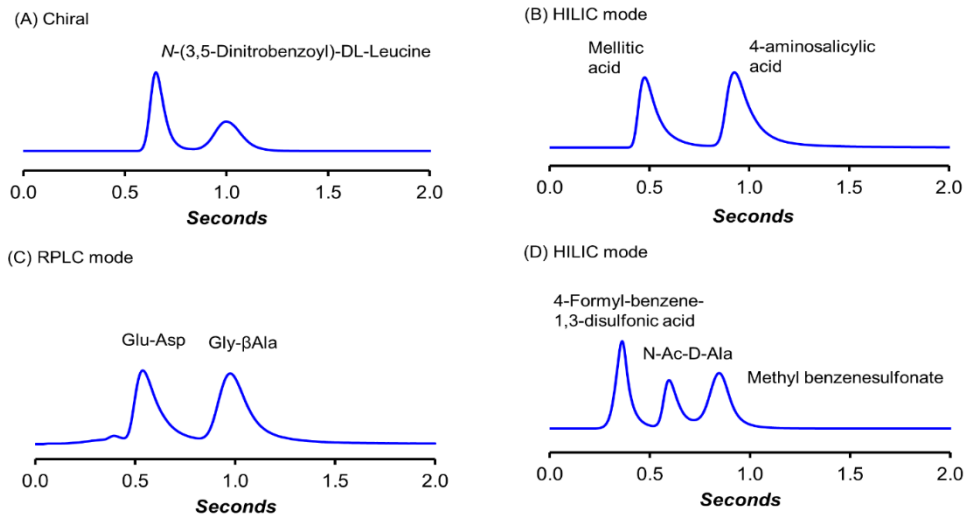

Figure 5.6 Sub-second chromatography on various stationary phases using 0.5 x 0.46 cm i.d. columns: (A) SPP Quinine, 70:30 (ACN:20 mM NH4CO2H), 5 mL/min (B) SPP silica, 94:6 (ACN:15 mM NH4CH3CO2), 5 mL/min (C) SPP Teicoplanin, 42:58 (ACN:20 mM NH4CO2H), 5 mL/min, (D) SPP Teicoplanin, 70:30 (ACN:Water), 5 mL/min. Data sampling rate 160 Hz. For Figure (A) and (D) see next section on power transforms

Table 5.3 Sub-second screening for achiral, chiral in various chromatographic modes

Analyte	**Chromatographic conditions (stationary phase, mobile phase, and flow rate)**	**t_{R1} (s)**	**t_{R2} (s)**	**Rs***	**Rs****
Chiral separations					

1.	DNPyr-DL-Leucine	Teicoplanin, 60:40 (MeOH:20 mM NH_4CO_2H), 5 mL/min	0.56	0.91	1.2	1.6
2.	DNPyr-DL-Norvaline	Teicoplanin, 70:30 (MeOH:20 mM NH_4CO_2H), 5 mL/min	0.66	1.00	1.4	1.9
3.	(±)-4-Methyl-5-phenyl-2-oxazolidinone	Teicoplanin, 100% MeOH, 5 mL/min	0.60	0.98	1.5	2.1
4.	N-Acetyl-Alanine	Teicoplanin, 40:20:40 (MeOH: ACN: 5 mM NH_4CO_2H), 4 mL/min	0.56	0.99	1.5	2.2
5.	*N*-(3,5-Dinitrobenzoyl)-DL-Leucine	Quinine, 70:30 (ACN:20 mM NH_4CO_2H), 5 mL/min	0.66	0.98	1.3	1.6
Achiral separations - HILIC mode						
6.	Mellitic acid + Benzamide	Cyclofructan, 95:5 (ACN:15 mM $NH_4CH_3CO_2$), 5 mL/min	0.49	0.90	2.5	4.5
7.	Mellitic acid + Benzamide	Silica, 95:5 (ACN:15 mM $NH_4CH_3CO_2$), 5 mL/min	0.48	0.91	2.4	3.5

8.	Mellitic acid + 4-Amino salicylicacid	Silica, 94:6 (ACN:15 mM $NH_4CH_3CO_2$), 5 mL/min	0.48	0.93	1.8	3.9
9.	Mellitic acid + 2,3-dihydroxybenzoic acid + 4-Amino salicylicacid	Silica, 94:6 (ACN:15 mM $NH_4CH_3CO_2$), 5 mL/min	0.48	0.66 (t_{R3} = 0.93)	1.2 1.1	2.6 2.8
10.	4-Formyl-benzene-1,3-disulfonic acid + N-Ac-D-Alanine + Methyl benzenesulfonate	Teicoplanin, 70:30 (ACN: Water), 5 mL/min	0.40	0.61 (t_{R3} = 0.87)	1.2 1.1	1.9 1.7
Achiral separations - Reversed phase mode						
11.	Acetylsalicylic acid + Salicylamide	Teicoplanin, 35:65 (ACN:20 mM NH_4CO_2H), 5 mL/min	0.60	0.94	1.8	2.5

12.	Salicylicacid + Methylsalicylate	Teicoplanin, 40:60 (ACN:20 mM NH_4CO_2H), 5 mL/min	0.61	0.93	1.5	2.3
13.	4-Formyl-benzene-1,3-disulfonic acid + Methyl benzenesulfonate	Teicoplanin,40:60 (ACN:20 mM NH_4CO_2H), 5 mL/min	0.55	0.87	1.8	28
14.	Dansyl-Asp + Gly	Teicoplanin, 30:70 (ACN:Water), 5 mL/min	0.44	0.81	2.0	3.1
15.	Asp-Asp-Asp-Asp + Gly-Gly	Teicoplanin, 33:67 (ACN:20 mM NH_4CO_2H), 5 mL/min	0.47	0.88	1.9	3.0
16.	Asp + β-Ala	Teicoplanin, 35:65 (ACN:Water), 5 mL/min	0.44	0.78	1.8	2.7
17.	Gly-Asp + Gly-Val	Teicoplanin, 26:74 (ACN:20 mM NH_4CO_2H), 5 mL/min	0.59	0.84	1.3	2.0
18.	Asp-Asp + Gly-Trp	Teicoplanin, 42:58 (ACN:20 mM NH_4CO_2H), 5 mL/min	0.56	0.98	1.8	2.9

19. Glu-Glu + Gly-Leu	Teicoplanin, 40:60 (ACN:20 mM NH_4CO_2H), 5 mL/min	0.52	0.90	1.7	2.8
20. Glu-Asp + Gly-βAla	Teicoplanin, 42:58 (ACN:20 mM NH_4CO_2H), 5 mL/min	0.54	0.99	1.9	2.9

Baseline sub-second separations are more easily achieved when the first analyte elutes before the dead time e.g. due Donnan exclusion. The separation window becomes small between the dead time and 1 s. However, this upper 1s limit is arbitrary in this work and ultrafast separations can be readily achieved in a few seconds. 4,9 Using a flow rate of 5 mL/min, the dead time is estimated to be ~ 0.8 s from pycnometric measurements on the silica column. Figure 5.6A shows the enantiomeric separation of N-(3,5-dinitrobenzoyl)-DL leucine on a SPP quinine phase. In Figure 5.6B, a HILIC mode separation of mellitic acid from benzamide is shown. Note that mellitic acid is repelled from the stationary phase. Similarly two dipeptides Glu-Asp and Gly-βAla are baseline separated on the teicoplanin bonded SPP column (Figure 5.6C). Examples of four additional pairs of dipeptides are shown in Table 1. In Figure 5.6D we show that it is possible to perform ultrafast screening by resolving 3 peaks (two sulfonic acids and a derivatized amino acid) under a second using the methods outlined in the next section. A doubly charged sulfonic acid is repelled from the stationary phase like mellitic acid. It is also important to have retention time reproducibility for sub-second separations. Using the HILIC the mode, six injections were made and retention times calculated for mellitic acid and 4-aminosalicylic acid. The % RSD for the retention time of both peaks was found to be < 2% (See Figure 7).

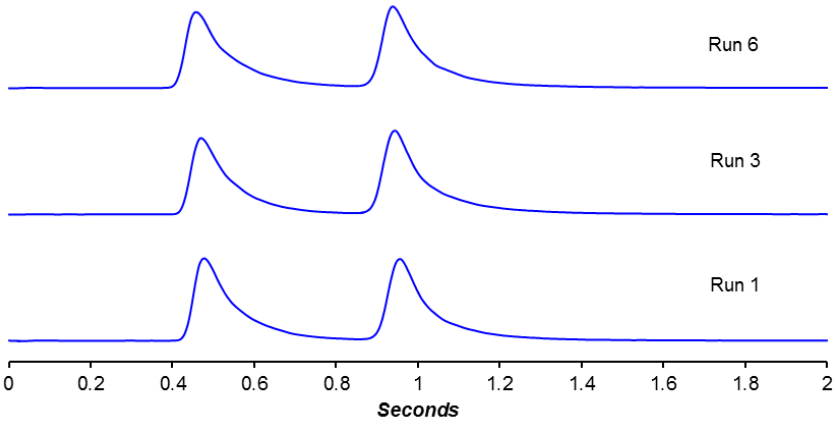

Figure 5.7 Reproducibility of sub-second separations. SPP silica, 94:6 (ACN:15 mM $NH_4CH_3CO_2$), 5 mL/min.

5.4.5 The Power of "Power Transform" in Sub-Second Chromatography.

It can be noted that under ultrafast separations and short columns, the peaks are non-Gaussian (tailed) due to trans-velocity biases in the tubings, frits as well as the particulate bed (vide supra). Additionally, if the peaks are eluting before the dead time (due to Donnan exclusion) the efficiencies of such peaks can be compromised. In Table 6.3, the efficiency of dansyl aspartic acid and glycine are 90 and 240 respectively. The former analyte elutes at 0.44 s which is much before the dead time (0.8 s). . Under the highest flow rates available on the UHPLC (5 mL/min), the 0.5 cm SPP columns provided about 150 to 200 plates. Using the simplest expression for peak capacity in the isocratic mode, and where there is a possibility of a peak eluting before the dead time, we can write the peak capacity (P) for a sub-second separation in a time span of 0.4 to 1.0 s (see Table 6.3), with a chromatographic resolution of 1 as[204]

$$P = 1 + \int_{0.4}^{1.0} \frac{\sqrt{200}}{4t}\,dt = 1 + (\frac{\sqrt{200}}{4})(\ln 1.0 - \ln 0.4) \qquad \approx \mathbf{4}$$

Using the same approach for the peak capacity for analogous higher efficiency separations, it is determined that for N= 500, P = 6, and for N = 1200, the P =9). In Figure 4, we demonstrate the full potential of fitting 3 peaks under a second in the HILIC mode. The resolution (~ 0.6) is a result of the extra-column tailing effect alluded to above. The chromatographic profile of peaks can be deconvoluted into three exponentially modified Gaussians at (0.48 s, 0.68 s and 0.93 s) as shown in Figure 5.8B. It is clear from the peak fitting model that tailing is causing this lowered resolution. It is known that raising Gaussian functions to any power (n> 0), still maintains them as Gaussian functions with an effect of reducing their standard deviations. Thus, squaring or cubing the output signal yields a peak at the identical retention time but with a narrower width (See Rs values in Table 5.3 and Figure 8). It can be shown mathematically that for Gaussian peaks, the efficiency directly scales as the power n and the resolution scales as $\sqrt{n}$.[205] Such an approach is already embedded in some commercial detectors such as the evaporative light scattering detector without the user's control.[204] Recently Thermo launched an UHPLC that allows the chromatographer to choose the power "n" to transform the chromatograms.

Figure 8C shows that if the same chromatographic data (y-ordinate) is raised to power of 3, the same separation can now be baseline resolved into 3 components. This approach is a very powerful method for extracting information for ultrafast screening purposes from a low resolution chromatogram, which is indeed the main purpose of sub-second chromatography. There is a caveat, however, in that the peak areas change in this power transformation as $A_{pt} = Y_{max}[\sigma\sqrt{(\pi/n)}]$, where A_{pt} is the peak area after applying the

power n, Y_{max} is the maximum amplitude, and σ is the standard deviation of the peak.[205] Calibration curves constructed can be non-linear if quantitation is desired.

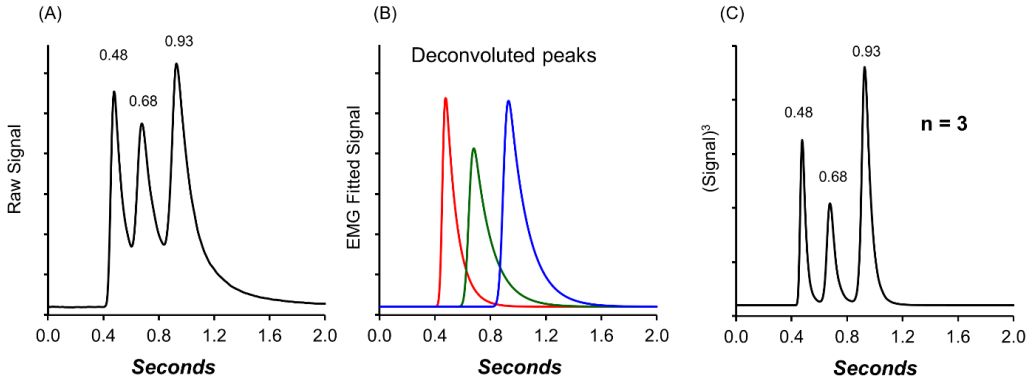

Figure 5.8 Application of power transforms in sub-second chromatography of 3 components (mellitic acid, 2,3-dihydroxybenzoic acid, and 4-aminosalicylic acid). (A) The original sub-second chromatogram,(B) shows the deconvoluted chromatogram into three exponentially modified Gaussian peaks and (C) power transform with cubic of the original data. Column - 0.5 cm x 4.6 mm i.d. 2.7 µm SPP silica, Mobile phase- ACN:15 mM ammonium acetate 94:6 (v/v), 5 mL/min at 220 nm.

5.5 Conclusions

The foundations of performing sub-second chromatography in small packed beds using superficially porous particles are outlined. Various modes of chromatography were demonstrated including reversed phase, HILIC, and chiral separations as a proof of concept. Detection and hardware challenges need to be further addressed. Although the sampling frequencies are adequate for the current efficiencies achievable in ultrafast chromatography, they may not be for future improved columns. The bigger challenge so

far is the peak shapes due to non-Gaussian dispersion in short tubings, which can be circumvented by on-column injection and on column detection technologies as is done in electrophoretic methods. Modern UHPLCs are limited to 2-5 mL/min flow rates at higher pressures (>500 bar) and this is less than desirable for these separations. Using power transforms on exponential functions (as those used for modelling peak shapes) are a very simple way to improve peak shapes, reduce variances and decrease noise in sub-second screening.

Chapter 6

GEOPOLYMERS AS A NEW CLASS OF HIGH PH STABLE SUPPORTS WITH DIFFERENT CHROMATOGRAPHIC SELECTIVITY

6.1 Abstract

Geopolymers belong to an interesting class of X-ray amorphous polycondensed alumino-silicate ceramic solids. The high mechanical strength, chemical stability in basic conditions and water insolubility make geopolymers a unique solid support in separation science. This work describes a new straight forward synthetic procedure for making spherical porous geopolymer particles with high surface area which are amenable for chromatographic purposes. In-depth physicochemical evaluation of geopolymers is conducted via particle size distribution, porosity measurements, X-ray diffraction, pH titration, energy dispersive spectroscopy and compared with silica, titania, and zirconia. Chromatographic selectivity shows that the surface chemistry of geopolymers has strong hydrophilic and electrostatic character, which makes it different from 36 chromatographic columns. Hydrophilic interaction liquid chromatography in columns packed with geopolymer particles shows different selectivity than silica with excellent peak shapes. Phosphate or fluoride additives are not required as they are for zirconia or titania phase.

6.2 Introduction

The reaction of solid aluminosilicates with highly concentrated alkali solutions yields an interesting class of inorganic polymeric ceramic materials referred to as

geopolymers[25]. The resulting solids are essentially X-ray amorphous polycondensed solids consisting of a polymeric network of Si-O-Al bonds (Figure 5.1) with varying Si:Al ratios. Geopolymers and zeolites both consist of a polymeric Si–O–Al frameworks,[28] but the fundamental difference between the two is the long-range order, i.e., zeolites are X-ray crystalline materials.[206-208] The geopolymer three-dimensional polymer network mainly comprises of tetrahedrally coordinated Si^{4+} and Al^{3+}.[26,30,31]. The overall negative charge results from the bridging oxygens in the aluminate tetrahedron and is balanced by alkali metal counter ions, more commonly K^+ or Na^+, but other multivalent cations can be present[31]. Nanometer-scale porous aluminosilicate clusters have been observed in transmission electron micrographs of geopolymer gels.[209,210] However, the size and micro-arrangement of these clusters are responsible for the long-range ordering of the final geopolymer composite.[28] Geopolymers have received significant attention in construction and environ-mental engineering as they exhibit excellent mechanical properties such as high compression strength, heat resistance, and chemical resistance.[25,27,28]

The promising physicochemical features of geopolymers (vide supra) fulfill all the primary criteria for a new stationary phase for liquid chromatography.[34] Additionally, a new chemically stable, geopolymer stationary phase should offer:(a) unique/different selectivity compared to existing phases (b) superior chromatographic properties such as stability at elevated pHs and figures of merit such as efficiency and (c) reproducible synthesis. Silica based supports are broadly accessible and practical for most traditional separation modes including hydrophilic interaction liquid chromatography (HILIC), despite its very well-known narrow pH working window of 3 to 7. A recent study showed that bare silica, which is a popular HILIC phase, has very high bleed even with mild mobile phases consisting of acetonitrile and buffers.[211] The hydrolytic stability of HILIC phases has been extensively investigated by several groups.[105,211-213] As a result, alternative chromatographic materials

have been proposed such as zirconia, carbon clad zirconia, titania and porous graphitic carbon, along with polymeric materials coated onto silica.[106] These materials that have met with partial success, e.g., zirconia and titania have very strong Lewis acid sites, requiring fluoride or phosphate containing mobile phases to quench these sites.[36] Similarly, chemically modified porous graphitic carbon or polymer coated supports for HILIC offers lower efficiency than silica despite their very different selectivity features.[105]

In this work, we synthesize and propose an aluminosilicate geopolymer as a new material for chromatography and evaluate its chromatographic properties in HILIC, normal phase, and ion chromatography. Given the hydrophilic nature of geopolymers, these materials are very promising for HILIC applications as HILIC is one of the fastest growing techniques for the separation of highly to moderately polar compounds that cannot be easily separated in the reversed phase chromatography mode.[4,22,132,212,214-216] Usually, in HILIC mode, polar stationary phase, and organic-rich aqueous mobile phase is an essential requirement.[137] Polar surfaces are also beneficial in multi-modal chromatography. The geopolymer stationary phase is attractive as a stationary phase due to its excellent hydrolytic stability and hydrophilic/polar character. Effective applications of alkaline pH stable geopolymers in HPLC have not been reported to the best of our knowledge. In this work, we report the first efficient and simple synthetic route to obtain porous spherical geopolymer particles with a high surface area and reproducible surface chemistry. Its hydrolytic stability and selectivity are evaluated and compared to silica gel.

6.3 Experimental

6.3.1. Materials

Metakaolin was purchased from Advanced Cement Technologies, Blaine, WA, USA and used without further treatment. Submicron-sized (0.007 μm) fumed silica (fused and

branched) was obtained from Sigma-Aldrich, St. Louis, MO, USA. Canola oil was obtained from J.M. Smucker Company, Orrville, Ohio, USA. Porous polystyrene/divinylbenzene polymer resins (PolyRP 10/300) were purchased from Sepax Technologies (Newark, DE). All reagents and solvents for synthesis were purchased from Sigma-Aldrich, St. Louise, MO, USA. Ultra-purified water (Millipore, Billerica, MA, USA) was utilized throughout the synthesis and chromatography experiments. All analytes and solvents used in chromatography experiments were obtained from Sig-ma-Aldrich, St. Louis, MO, USA.

6.3.2. Synthesis of Metakaolin Geopolymer Stationary Phases

6.3.2.1 Synthesis of Porous Geopolymer Particles

The activator solution was prepared in high-density polyethylene (HDEP) beaker by dissolving KOH and fumed silica in water. The required amount of metakaolin was then added to the activator solution to obtain initial geopolymer composition where Si: Al: K molar ratio is 2:1:2. Three approaches were tested for the synthesis of geopolymer material. The details of monolithic structures and alternative approaches for particle synthesis such as particle templating is also outlined.

Water in oil emulsion (reverse emulsion) templating technique.

Water in oil emulsion was prepared by mixing appropriate volumes of canola oil and aqueous geopolymer mixture to maintain oil to aqueous volume ratio 25:1 in an HDEP beaker. Overhead stirrer with a three-blade propeller (Talboys 101, Troemner, Thorofare, NJ) was utilized in emulsion preparation. The shear rate of 4000 rpm was provided at ambient temperature for 8-72 hours to complete the geopolymerization process. The particles were then extracted into the water via hexane and water solvent extraction.

Particles were washed with MeOH, hexane, EtOH, and required amount of water (until the filtrate was neutral pH). The particles were cured in an incubator (I2400 incubator shaker, New Brunswick Scientific, Edison, NJ) at 60 °C for 48 hours. Particles were sintered in a muffle furnace (Sentry 2.0, Oriton Ceramic Foundation, Westerville, OH) at different temperatures (400 - 800 °C) in an air atmosphere.

6.3.2.2. Alternative Geopolymer Particle Synthesis Approach

Polymer resin templating technique – Polymer resins were dispersed in hexane and wetted with Span 80 by stirring (Corning PC 420-D, Corning, NY, USA) and ultra-sonication (Aquasonic 250 Hz, VWR, Radnor, PA, USA) for 30 minutes. Then wetted resins were filtered and extracted. Wetted resins were suspended in geopolymer reaction mixture and stirred (Corning PC 420-D, Corning, NY, USA) followed by sonication (Aquasonic 250 Hz, VWR, Radnor, PA, USA) for 30 minutes to fill pores with geopolymer reaction mixture. Resins were then isolated by centrifugation followed by filtration. Then curing was carried out at 60 °C in an incubator (I2400 incubator shaker, New Brunswick Scientific, Edison, NJ). Finally, the resin was burnt out at 800 °C in Sentry 2.0 furnace (Oriton Ceramic Foundation, Westerville, OH) and particles were isolated

6.3.2.3. Geopolymer Monolith Synthesis

The geopolymer monolith was synthesized using an unconventional route of the “sticky period” during “suspension polymerization.”1 The sticky period is defined as the period in which partially polymerized droplets cannot re-divide, but coalescence can still occur. This coagulation of particles has been deliberately brought about by bringing the particles in

proximity using centrifugation. Eventually, the curing leads to the formation of connecting necks between particles, fabricating the monolithic structure.

A potassium silicate solution was prepared by dissolving 3.30 g of potassium hydroxide and 3.00 g of fumed silica in 7.59 mL deionized water. The mixture was stirred for 30 minutes at room temperature. Then, 6.25 g of metakaolin was added and stirred for five minutes. The resulting homogeneous slurry was then added to 700 mL of soybean oil (Crisco® Pure Vegetable Oil) with stirring at 5000 rpm (Talboys overhead mixer was used). The fractions were taken out from the reaction mixture during the sticky period (between 3rd and 4th hour, in these synthetic conditions) and put in a polycarbonate tube. The filled tube was then centrifuged for 2 minutes to settle the solid particles at the bottom, and the oil was decanted. This process was repeated until the mold was filled. The curing of geopolymer was done at 60 °C for 24 hours during which time the particles fused forming a monolith. The monolith was removed from the mold and sintered at 500 °C in an air atmosphere for 4 hours at 2 °C/min ramp to burn off all the organics. The monolith was cladded inside 200 mm x 4.6 mm ID stainless steel column using epoxy resin. The chromatography was performed after equilibrating the column with mobile phase. The optimization of synthetic conditions for monolith continued to be a subject of future studies in our laboratory.

6.3.2.4. Characterization of Geopolymer Particles and Monoliths

Particles and monolith morphology were characterized using scanning electron microscopy (Hitachi S-3000N Variable Pressure SEM, Hitachi High-Technologies Science America, Inc., Northridge, CA, USA). Shimadzu SALD-7101 laser diffraction particle size analyzer (Shimadzu Scientific Instruments, Columbia, MD, USA) was used to determine average

particle size and particle size distribution. BET specific surface area and pore size were measured using Tristar II 3020 (Micromeritics, Norcross, GA, USA). Elemental composition of the geopolymer particles was analyzed using X-ray energy dispersion spectroscopy (Shimadzu EDX-7000, Shimadzu Scientific Instruments, Columbia, MD, USA.) The amorphous nature of the geopolymer material was examined using powder X-ray diffraction method (Shimadzu MAXima X XRD-7000 X-ray diffractometer, Shimadzu Scientific Instruments, Columbia, MD, USA).

6.3.2.5. Chromatographic Setup for Stationary Phase Evaluation

Geopolymer particles were slurry packed into empty stainless-steel columns using an air-driven high-pressure pump (Haskel International Inc., Burbank, CA, USA). Dispersed slurries produced the best results as stated in the literature.[22] All chromatography experiments were run using an Agilent 1200 series HPLC instrument (Agilent Technologies, Santa Clara, CA, USA). The instrument was equipped with an UV-visible diode array detector, temperature-controlled column compartment, auto-sampler, quaternary pump, and a degasser. The Agilent ChemStation version B.01.03 under the Microsoft Windows XP operating system environment was utilized to control the instrument

6.4 Results and Discussion

6.4.1. Synthetic Aspects of Geopolymer Particles

The geopolymerization reaction is a polycondensation process. Reverse emulsion polymerization is the principal technique used in this work to synthesize geopolymer particles as shown schematically in Figure 6.1a-g. Aqueous alkaline (with KOH) aluminosilicate solution droplets are dispersed in a continuous oil phase to obtain a reverse emulsion. The partial hydrolysis of oil produces potassium salts of fatty acids, resulting in

a surfactant system. The surfactant stabilizes the water-in-oil emulsion (see Experimental and Figure 6.1g) The synthesis protocol resulted in reproducible particle morphologies and surface chemistries. More than 20 batches were prepared as replicates, and the chromatographic parameters were reproducible (Figure 6.2)

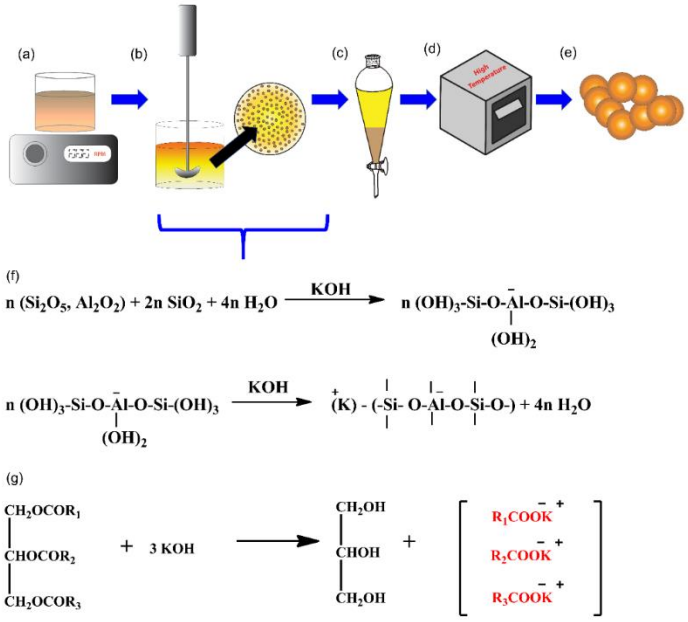

Figure 6.1 Schematic representation of geopolymer particle synthesis protocol (a) Geopolymer reaction mixture preparation (b) High speed stirring of geopolymer reaction mixture and canola oil to obtain water in oil emulsion (c) Isolation of particles - Hexane-water solvent extraction (d) Particles sintering at elevated temperatures in a furnace (e) Sintered geopolymer particles. Reaction schemes for geopolymer particle synthesis (f) Geopolymerization reaction (g) Production of ionic surfactant by saponification reaction

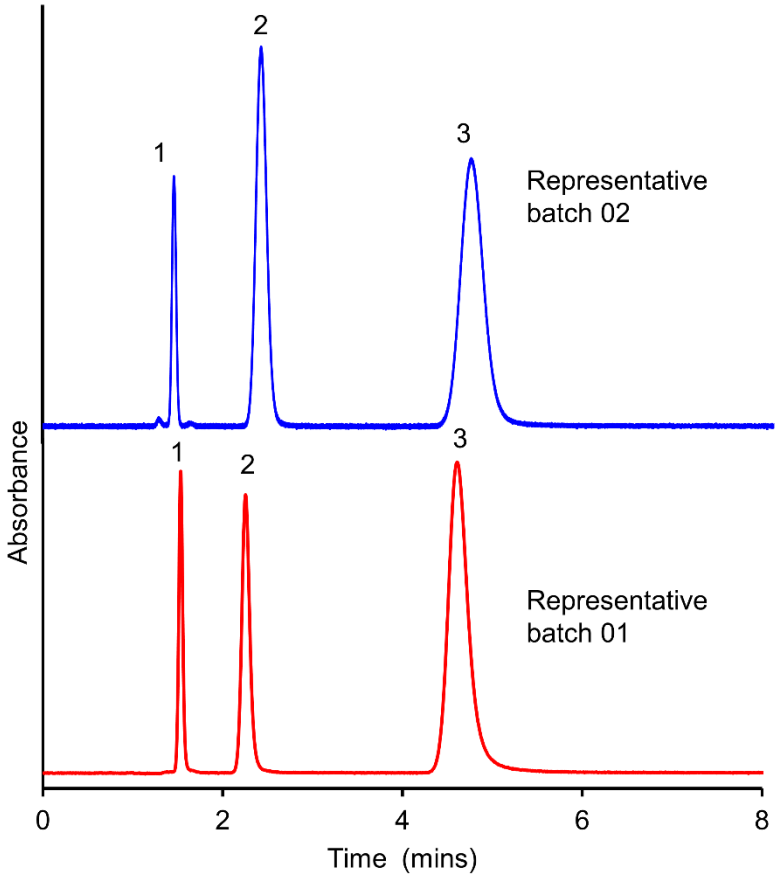

Figure 6.2 Batch to batch chromatographic reproducibility of geopolymer stationary phase. Analytes – 1. Acetone (dead time marker) 2. Uracil 3. Cytosine, mobile phase – ACN/25 mM NH_4OAC (80/20), 0.425 mL per min, column – 3 mm ID x 150 mm, detection at 254 nm

As noted in the experimental, shear rate and the experiment setup were intentionally chosen to generate turbulence in the reaction mixture and control particle size. After the desired reaction time, particles are extracted into water, and the fatty acid carboxylates and glycerol were readily removed from the system as they are water soluble. The amount

of base in the geopolymer reaction mixture is crucial since the rate of saponification in the system is controlled by the amount of free base. Excess or inadequate amounts of the base resulted in irregularly shaped particles and broad particle size distributions (results not shown). Curing of particles was carried out at 60 °C to obtain optimum physical and mechanical properties.[33,217] Curing at elevated temperatures other than ambient temperature accelerates the geopolymerization reaction while improving the compressive strength and surface area by increasing the mesoporosity.[217] Based on our own observations and the literature sintering at high temperatures (400 °C – 800 °C) sometimes results in microcracks (size ranging the few microns) [32], a small degree of compressive strength loss,[218,219] and reduction of particle size. The formation of micro cracks was not observed when slow temperature ramps (e.g., 2 °C/min) are utilized (Data not shown). Further heating can result in crystalline material such as leucite and kalsilite.[220] Reduction of particle size due to thermal shrinkage is advantageous in chromatography as theoretical plates are inversely proportional to the particle diameter at the van Deemter minimum. Additionally, potassium geopolymer was chosen over sodium geopolymer because potassium geopolymer shows less mechanical strength degradation after exposing to high temperatures.[32]

6.4.2. Characterization of Synthetic Geopolymer Particles and Monolithic Materials

The synthesis, curing and sintering temperature should ensure that the material remains X-ray amorphous (compared to zeolites). Secondly, particle shape and size distribution are critical parameters for any chromatographic support. Scanning electron micrographs (Figure 6.3) showed that particles are spherical. Irregular particles do not pack as well in slurry packing procedures. Hence spherical particles are preferred.[22] The surface

roughness of the particles also was observed in scanning electron micrographs as shown in Figure 6.4

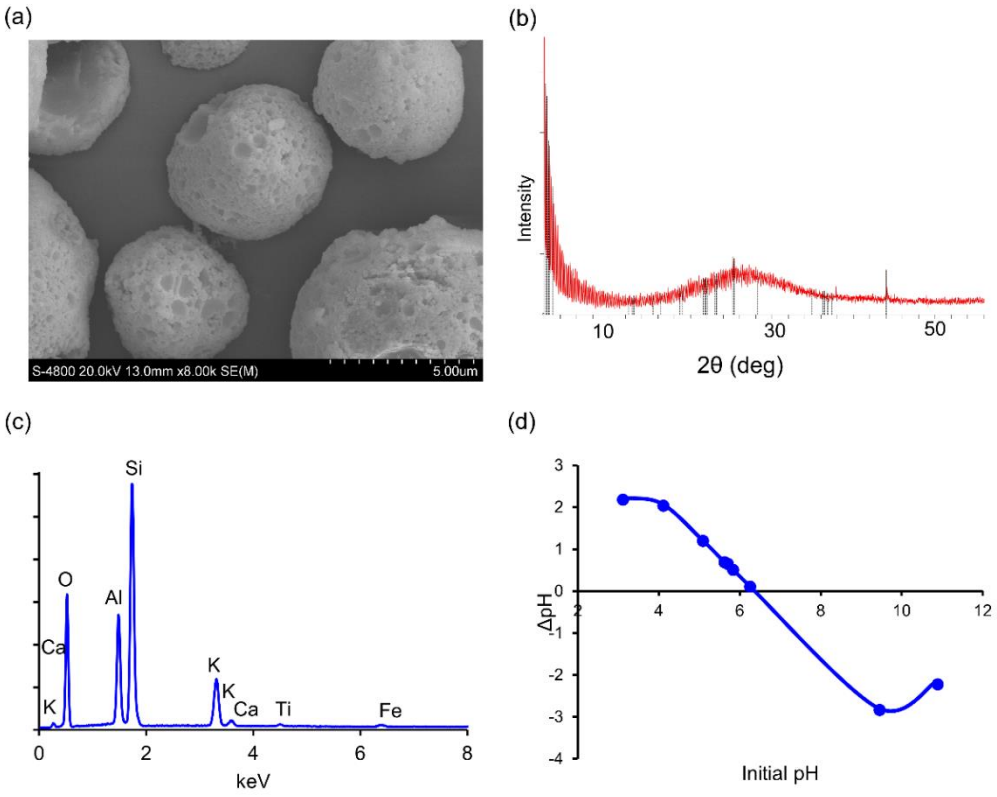

Figure 6.3 Characterization of geopolymer particles (a) Scanning electron microscopy (b) Powder X-ray diffraction patterns (c) Energy dispersive spectroscopy (Peak identity (element) is mentioned next to the peak) (d) Surface charge of the geopolymer stationary phase (pHpzc by pH drift method in waterLaser diffraction particle size distribution (PSD) data (Figure 6.5) showed average particle size of 6.1 µm and D90/D10 of 2.9 after a de-fining procedure in water.

.

The relationship between particle size distribution and column efficiency is still subject to debate.[221] Nevertheless, it appears that narrower the particle size distribution, better the efficiency.[221] The RSD of geopolymer PSD was calculated to be 7.6% resulting acceptable packing material. Comparatively, RSD as high as ≈ 20% has been reported for state of the art fully porous regular silica particles.[222]

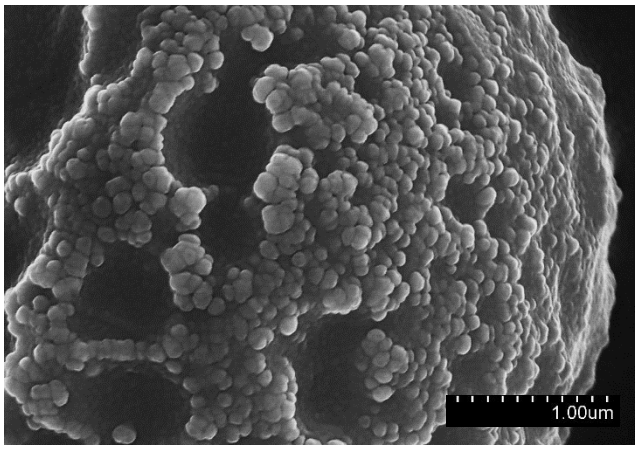

Figure 6.4 Surface structure of a metakaolin geopolymer particle

Geopolymerization was confirmed by powder X-ray diffraction analysis (Figure 6.3b). The broad 2θ peak around 28° is a characteristic feature of metakaolin based geopolymers indicating amorphous nature.[223-225] Note the absence of any other crystalline peaks in the XRD. It is very common that the crystalline form of the metal oxides (e.g., ZrO_2, TiO_2) are employed when they are utilized as chromatographic stationary phases.[36,225] In contrast, one of the unique features of geopolymer stationary phase is that it can be recognized as a non-silica, completely amorphous HPLC stationary phase. Many commercial silica

phases are often partially crystalline.[35] A detailed X-ray diffraction study showed that the degree of crystallinity positively correlated with pore-size in many cases such as titania and zirconia.[35] How-ever, this statement should not be over-generalized since hydrothermal treatment history and calcination temperature are not disclosed for commercial phases. The dispersive energy spectrum (Figure 6.3c) indicates that potassium has been successfully incorporated into the geopolymer matrix (Kα 3.3 eV). Trace metal impurities were observed in final geopolymers which also were found in the starting material (For quantitative results, see Table 5.1). Figure 6.3.d shows the pH of the point of zero charge. It will be discussed in detail in later sections.

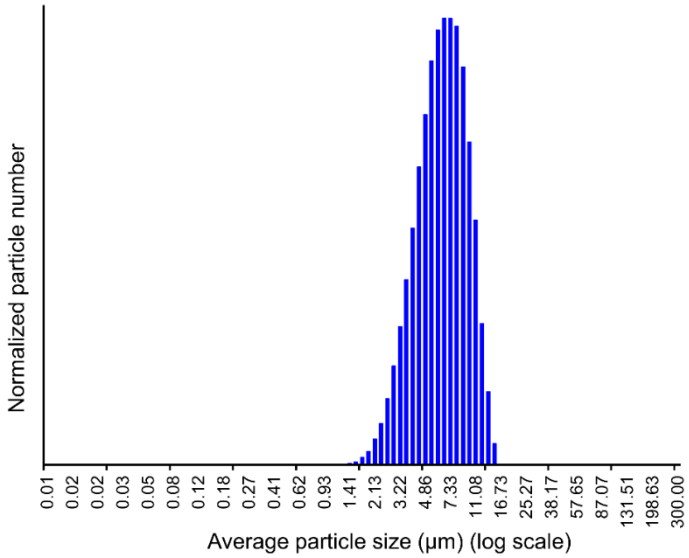

Figure 6.5 Laser diffraction particle size distribution

Table 6.1 Elemental composition comparison of geopolymer particles and metakaolin (starting material) as weight percentage by EDS

Element	Weight %	
	Metakaolin	Geopolymer
O	54.95	52.43
Al	20.42	10.74
Si	22.42	28.06
K	0.16	7.52
Ca	0.06	0.12
Ti	0.89	0.46
Fe	1.10	0.68
Total	**100.00**	**100.00**

Compared to the surface area of commercially available or laboratory synthesized metal oxide HPLC stationary phases, the specific surface area of geopolymers is very promising. For titania and alumina phases, ≈ 50 - 150 m^2/g specific area have been reported.[226,227] For zirconia even less, specific surface area (≈ 30 m^2/g) has been reported by manufacturers. Despite the excellent chemical stability, these metal oxide stationary phases were unable to produce satisfactory chromatographic retention due to the limited specific surface area. Geopolymer particles produced 385 m^2/g BET specific surface area, the highest among the existing metal oxide containing HPLC stationary phases. BJH

(Barrett-Joyner-Halenda) average pore size was measured to be 35 Å. On the other hand, the geopolymer specific surface area is comparable with a specific surface area of commercially available fully porous silica (200 – 450 m^2/g). A new support/stationary phase should be able to withstand high pressures encountered in modern liquid chromatography instruments (400 bar above). Systematic studies on column packing[22] showed geopolymer particles as a mechanically stable material. Multiple columns lengths (5, 10, 15 cm) were packed at 10,000-11,000 psi, and no peak shape distortion due to column settling or extensive pressure build-up was observed throughout the entire process and subsequent usage. Using toluene as the probe molecule and pure ACN as the mobile phase, 53000 plates per meter column efficiency and reduced plate height of 3.1 were observed. Comparatively, optimally packed 10 µm fully porous silica resulted in similar efficiencies. For some acidic compounds, i.e., ketoprofen 20% increased efficiency was observed with geopolymer stationary phase compared to 10 µm fully porous silica stationary phase. These studies show that geopolymers can sustain the pressures encountered in HPLC. To make prototype monolithic structures of geopolymers, the so called sticky period phenomenon was employed. During the initial phase of geopolymerization when emulsions lack stabilizers and are exposed to extreme shear stress, the cohesion forces cause droplets to coagulate and form polymer aggregates. This phenomenon is informally known as the “sticky state”.[228] The growth of the water-in-oil emulsion prepared as described in the Experimental section was monitored carefully (scanning electron microscopy) to trace the experimental “sticky state.”[228] Centrifugation of the emulsion brought the sticky particles close enough to promote self-assembly of the monolithic structure of the geopolymer. The “necks” formed in between the neighboring sticky particles resulted in the rigid monolithic

skeleton as shown in Figure 6.6. A prototype geopolymer monolith was made by connecting two 2 cm x 0.46 cm i.d. columns in HILIC mode.

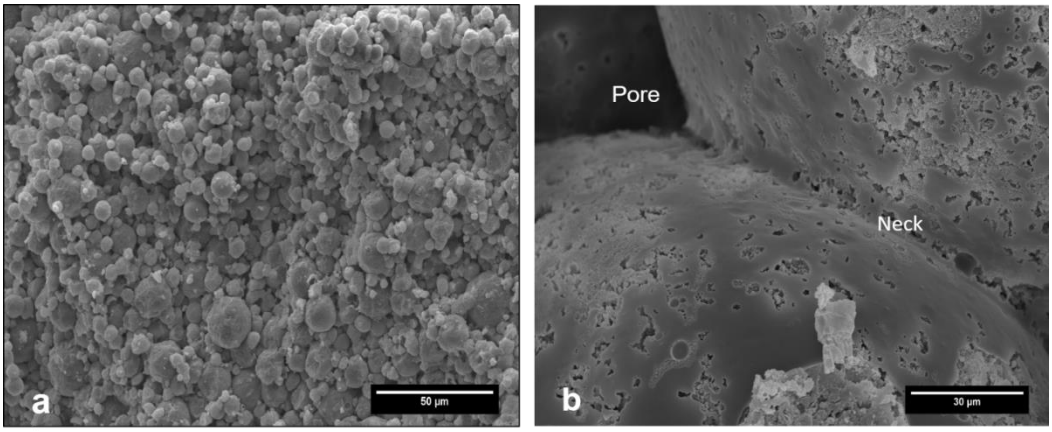

Figure 6.6 (a) Cross-sectional image of geopolymer monolith (b) SEM image showing the neck and pore formation between 2 particles

6.4.3. High pH Stability of Geopolymer Stationary Phase in HILIC Mode

Hydrolytic stability is the Achilles heel of a majority of HILIC phases, especially at high pH. Extensive studies have highlighted this issue with different HILIC chemistries.[105,139,212,229] Retention time drift is one of the significant problems in HILIC because of continuous leaching of silica and /or ligands. The leaching of bonded phases on HILIC is postulated as follows: The polar surface of HILIC stationary phase promotes the adsorption of the water layer. Silica has a propensity to dissolve in pure water (0.01 to 0.012%), and the siloxane linkage (Si-O-Si) is prone to hydrolysis and form silanols.[212] Basic conditions can be harmful to silica owing to the formation of water-soluble silicates. The presence of silicates has been observed via a silicomolybdate test in silica columns with various pH buffers.[230] With state of the art silica SPP, we reported a % retention time

drift in 30 hours with a “mild” mobile phase consisting of 75% ACN and 25% buffer at (aqueous) pH of 6.8.15 One of the unique features of the geopolymer stationary phase is excellent pH and hydrolytic stability as shown in Figure 6.7.

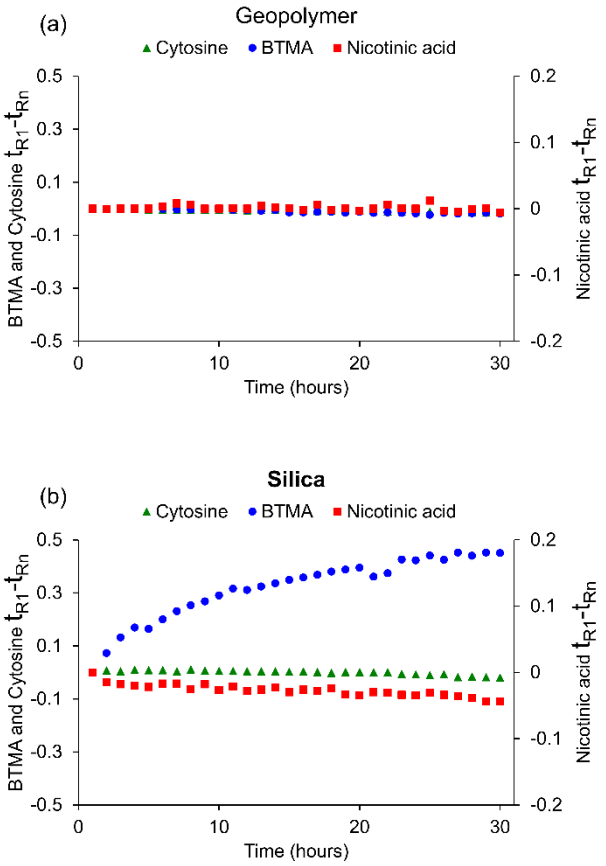

Figure 6.7 Ultra-high stability of the geopolymer stationary phase at extreme high pH compared to silica, (a) Geopolymer (b) Silica, mobile phase – ACN/25 mM NH4OAc pH 10 (80/20), 0.425 mL/min, column – 3 mm ID x 100 mm. The pH was adjusted with aqueous ammonia. Detection at 220 nm

The hydrolytic and pH stability test was conducted at pH 10 for 30 hours with three probes. The capability of a stationary phase to operate in a broad range of pH is highly desirable as it ultimately allows one to optimize separations freely using mobile phase pH. Probes

were chosen in such way that it allowed examining the retention behavior of neutral, negative, and positive charge analytes on the geopolymer stationary phase.[212] Nicotinic acid is negatively charged at this operating pH and the cationic species, BTMA is positively charged at all pHs. Cytosine is the hydrophilic neutral probe. Figure 6.7 plots the value of retention -original retention time vs. time (hours). Over the designated time span, the geopolymer stationary phase did not show in any significant drift in retention times for the test analytes (Figure 6.7a). According to both Davidovits and Barbosa geopolymer network model, the oxygen atoms are mainly bonded to other non-hydrogen atoms, thus limiting the number of free surface silanol groups.[28,230-233] Furthermore, geopolymers are known to have exceedingly low water solubility.[234,235]

The hydrolytic stability of silica and geopolymer stationary phases can be further quantitatively represented and compared when retention time drift (retention time of n^{th} injection – retention time of the first injection) is plotted against time or column volumes passed through the column (Figure 6.7 and Figure 6.8). The slopes of the retention time curves can indicate the stability. Ideally, a stationary phase should show a slope of zero (perfectly horizontal). For geopolymer stationary phase, the slope values are nearly zero (Table 5.2) indicating negligible drift. , The opposite behavior of nicotinic acid and BTMA is observed universally on modified and unmodified silica.[212] This trend is attributable on silica to the formation of Si-OH groups, which increase the cation exchange behavior of silica with time. The neutral (uncharged) analyte, cytosine showed negligible retention time drift both on the silica stationary phase and the geopolymer stationary phase (See TableS4).

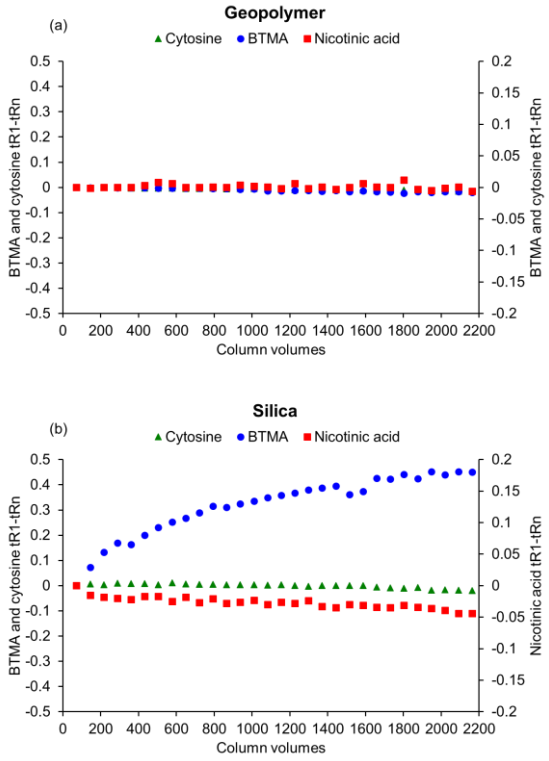

Figure 6.8 Comparison of hydrolytic stability of (a) geopolymer stationary phase and (b) 10 µm fully porous silica stationary phase based on column volumes. (tR1 is the retention time of the first injection, and tRn is any n^{th} injection after the first injection.)

However, the retention time drift is more significant for charged analytes as expected if the retention is being affected by the charged state of the surface. Note that retention time drift of nicotinic acid is not significant compared to BTMA as nicotinic acid has a smaller retention factor. The retention time drift per hour for BTMA on fully porous silica stationary phase is significantly high compared to the geopolymer stationary phase (See Figure 6.7). Nicotinic acid also exhibits nearly 14 times greater retention time drift per hour, under these

conditions, compared to geopolymer. At pH 10, the silica stationary phase shows sequential deterioration within the experimental period as expected. The effect is most noticeable with positively charged species, BTMA (Figure 6.7b).

Table 6.2 Slopes of the stability data sets and quantitative comparison of slopes.

Analyte	**Geopolymer**		**Silica**		**|mSi/mGP|**
	Slope - (mGP)	**Standard error of slope**	**Slope - (mSi)**	**Standard error of slope**	
Nicotinic acid	-7.5E-05	8.0E-05	-9.5E-04	8.6E-05	1.3E+01
Cytosine	-4.7E-04	2.3E-05	-8.3E-04	9.5E-05	1.8E+00
BTMA	-7.6E-04	4.9E-05	1.3E-02	8.8E-04	1.7E+01

6.4.4 Selectivity Comparison *and Surface Charge Properties of Geopolymers*

For any new stationary phase, it is essential to explore the nature of the stationary phase com-pared to other existing stationary phases to understand selectivity, stability and method optimization. To date, a large number of HILIC stationary phases are available with a wide range of hydrophilicity and ion exchange capabilities. Based on the data of Irgum, Lucy, and our own studies, a simple selectivity chart has been constructed to examine

hydrophilicity and ion ex-change capabilities of available stationary phases (Figure 6.9).[105,138,212,236] The compiled data allowed us to compare geopolymer particles with 36 commercial (and published) stationary phases. The diagram shows clustering of different classes of stationary phases. The traditional reverse phase media appears on the left, and more polar phases on the right. This data is visualized graphically in the “selectivity chart.”

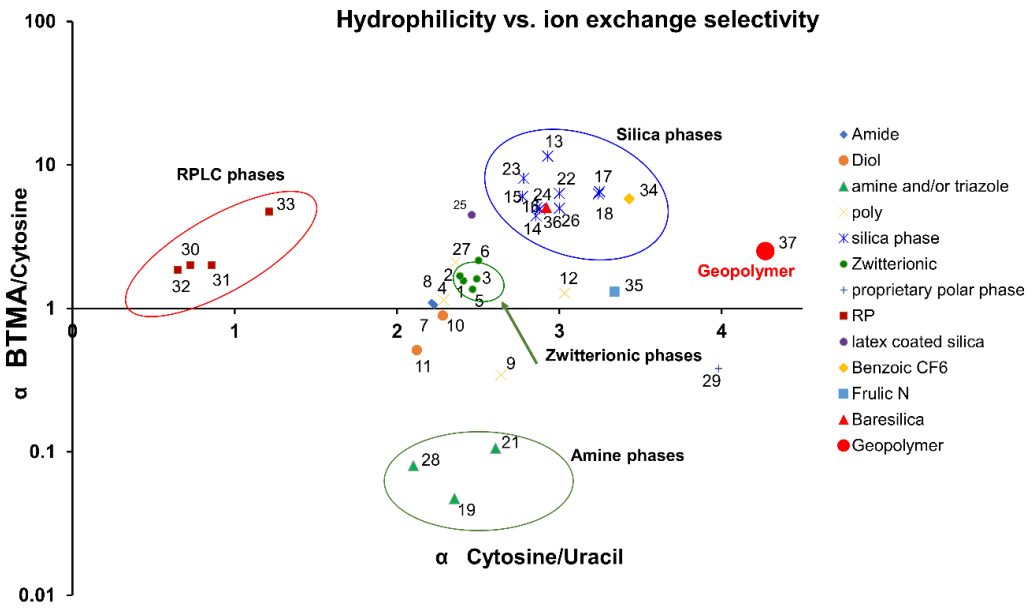

Figure 6.9. Hydrophilicity and ion exchange selectivity of geopolymer stationary phase com-pared to other stationary phase chemistries. Mobile phase Acetonitrile/25 mM NH4OAc (80/20), Flow rate 0.50 mL/min, detection at 254 nm. The key to actual points is provided in Table 5.3.

The x-axis plots the selectivity of cytosine /uracil indicating hydrophilicity of the stationary phase. The y-axis consists of selectivity of BTMA/cytosine, which is taken as a measure of the ion exchange characteristics of the stationary phase. The choice of BTMA/cytosine pair

has been made on the basis of previous data for more than 30 columns used for selectivity comparison.[138,212,236] Geopolymer phases showed less propensity as cation exchange media, than silica phases, but more than that of zwitterionic phases (Figure 6.9). The geopolymer stationary phase occupies in a unique position of this selectivity chart showing that geopolymer stationary phase is the most hydrophilic HILIC stationary phase among all those in the selectivity plot.

To further understand the retention mechanism of (an) analyte/s of interest on the geopolymer stationary phase, it is essential to understand the fundamental interactions of the stationary phase with the analyte. The selectivity chart (Figure 6.9) employed an ACN buffer mixture. How-ever, the concept of surface charge is more meaningful in purely aqueous media. This type of understanding is helpful for rationalizing the behavior of ionizable analytes (acids and bases) and simple ions. The pH of the surface where the net charge of the solid surface of interest is zero is known as pH of the point of zero charge (pH_{PZC}).[237] The pH_{PZC} is a good indicator of the charge of the surface of the stationary phase. The salt addition method was used to determine pH_{PZC} of geopolymer stationary phase following the experimental procedures reported in the literature.[237] The pH_{PZC} of geopolymer stationary phase was found to be 6.4 (Figure 6.3d) implying that when pH < 6.4, the stationary phase is positively charged and when pH > 6.4, the stationary phase is negatively charged. The pH_{PZC} of silica is reported as ~ 3 in the literature.[238,239]

Table 6.3 Selectivity chart data interpretation (The selectivity plot was constructed based on information provided in literature and our experimental data.)[138,212,236]

Stationary phase type	Column ID	Description
Zwitterionic	1	ZIC-HILIC 100x4.6, 5µm, 200Å
Zwitterionic	2	ZIC-HILIC 150x4.6, 3.5µm, 200Å

Zwitterionic	3	ZIC-HILIC 150x4.6, 3.5µm, 100Å
Poly	4	ZIC-pHILIC 50x4.6, 5µm, ??Å
Zwitterionic	5	Nucleodur 100x4.6, 5µm, 100Å
Zwitterionic	6	Shiseido 100x4.6, 5µm, 100Å
Amide	7	Tosoh Amide 80 100x4.6, 5µm
Amide	8	Tosoh Amide 80 50x4.6, 3µm
poly	9	PolyHYDROXYETHYL A 100x4.6, 5µm, 100Å
Diol	10	LiChrospher Diol 100x4, 5µm, 100Å
Diol	11	Luna 5u HILIC 100x4.6, 5µm (514356-6)
Poly	12	PolySULFOETHYL A 100x4.6, 5µm, 100Å
Si	13	Chromolith SI 100x4.6, 5µm, 200Å
Si	14	Atlantis HILIC SILICA 100x4.6, 5µm, 200Å
Si	15	Purospher SI 100x4, 5µm, ??
Si	16	LiChrospher SI 100x4, 5µm, 100Å
Si	17	LiChrospher SI 100x4, 5µm, 60Å
Si-C	18	Cogent Silica-C 100x4.6, 4µm
NH2	19	LiChrospher NH2 100x4, 5µm, 100Å
NH2	20	Purospher NH2 100x4, 5µm, 100Å
NH2	21	Tosoh NH2 50x4.6, 3µm
Si	22	Atlantis HILIC Silica 50×1.0mm, 3µm, 100Å
Si	23	Onyx monolithic Si 100×4.6mm, 2µm, 130Å
Si	24	Agilent ZORBAX HILIC plus 100×4.6mm, 3.5µm 95Å
Si	25	AS9-sc Si monolith 80*
Si	26	Agilent ZORBAX RRHD HILIC PLUS 100×3mm, 1.8µm, 95Å
Poly-Si	27	Acclaim Trinity P1, 150×3mm, 3µm
NH2	28	Cosmosil 150×4.6mm, 5µm, 120Å
Proprietary polar phase	29	Acclaim HILIC-10 150×4.6mm, 3µm, 120Å
RP	30	Agilent Eclipse XDB-C18 150×4.6mm, 5µm, 80Å
RP	31	Waters Xbridge C18 150×4.6mm, 5µm,
RP	32	YMC Pro C18 150×2.0mm, 3µm,120Å
RP	33	ZORBAX SB-C18 150×4.6mm, 3.5µm
	34	Benzoic CF6
	35	Frulic N
	36	baresilica
	37	**Geopolymer**

6.4.5 Chromatographic Assessment of the Geopolymer Phases

6.4.5.1 Geopolymer as a HILIC Stationary Phase.

With the promising selectivity and surface charge properties observed in the selectivity chart and surface charge studies, geopolymers have appeared to have promise when utilized as a HILC phase. To be useful as a HILIC phase, the geopolymer surface must be "wettable" by water to form a surface water layer.[105] HILIC has always been recognized as mass spectrometry friendly chromatography mode. This is not necessarily the case with alternative high pH stable metal oxides (TiO_2, ZrO_2,) based stationary phases which are operated in HILIC. These phases invariably require fluoride or phosphate buffer additives in the mobile phase due to the presence of active Lewis acid sites. This is especially true for carboxylic acids which can adsorb strongly on titania surfaces.[240] Carboxylic acids are known to show extremely long retention times, and poor plate counts on zirconia and titania with acetate buffers.[240] Many drug molecules and their synthetic precursors have a carboxylic acid group. Ketoprofen, acetylmandelic acid and indoprofen are small acidic molecules of pharmaceutical interest are used as synthetic precursors. All three were baseline separated (Figure 6.10a) on a geopolymer stationary phase with no significant tailing or fronting at pH 8.0. The USP tailing factor for ketoprofen, acetylmandelic acid and indoprofen were found to be 1.16, 1.09, 1.15 respectively. On the other hand, indoprofen eluted before acetylmandelic acid on silica stationary phase but not the geopolymer (Figure 6.10a). Also, note that ketoprofen and indoprofen have only partial separations on silica under optimized mobile phase conditions. Thymidine, adenine, and uridine belong to the class of nucleosides. As shown in Figure 6.10b, adenine elutes before uridine on the geopolymer stationary phase with the resolution of 2.35 where on silica stationary phase retention order is switched and resolution is lowered (resolution – 1.35) under similar

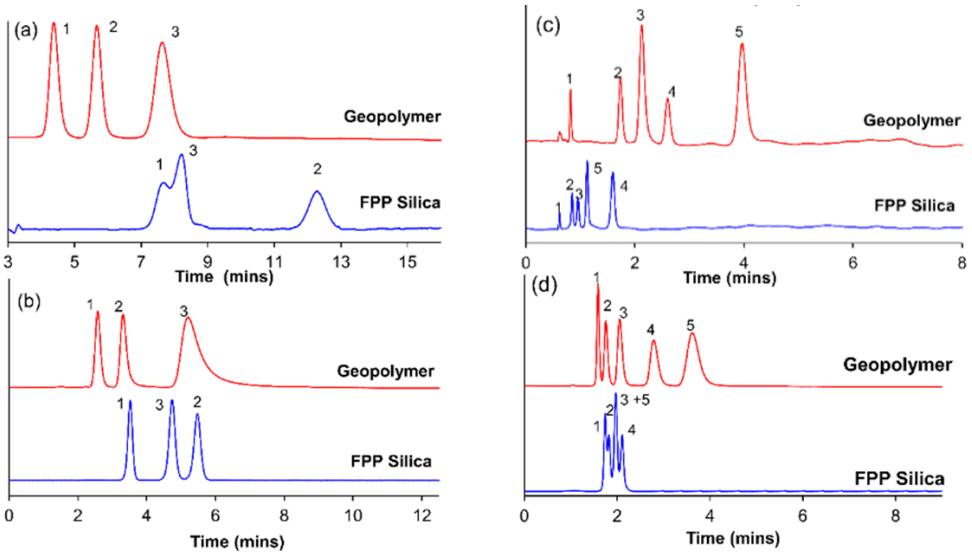

Figure 6.10 HILIC selectivity comparison of geopolymer stationary phase and silica (a) separation of aromatic acids and derivatives, analytes – 1. ketoprofen 2. acetylmandelic acid 3. indoprofen, mobile phase – ACN/25 mM NH_4COOH pH 8.0 (92/8), 0.425 mL/min, on geopolymer, ACN/100 mM NH_4OAc (92/8) on silica columns – 3 mm ID x 150 mm. detection at 220 nm (b) Separation of nucleic acid bases and nucleosides, analytes – 1. thymidine 2. adenine 3. uridine, mobile phase – ACN/100 mM NH_4OAc (87/13), 0.425 mL/min, columns – 3 mm ID x 150 mm. detection at 254 nm (c) Inorganic anion separation, analytes – 1. iodide 2. nitrate 3. azide 4. bromide 5. nitrite, mobile phase - ACN/50 mM NH_4COOH pH 4.0 (91/9), 1.00 mL/min, columns – 3 mm ID x 150 mm. detection at 200 nm (d) analytes – 1. methyl-3-Boc-2,2-dimethyl-4-oxazolidine-carboxylate 2. 4-isopropyl-5,5-diphenyl-2-oxazolidinone 3. 4-(diphenylmethyl)-2-oxazolidinone 4. 4-isopropyl-2-oxazoli-dinone 5. (1H-Indol-3-ylmethyl)-2-oxazolidinone, mobile phase – ACN/100 mM NH_4OAc (90/10), 0.425 mL/min, column – 3 mm ID x 150 mm, detection at 220 nm

mobile phase composition. On both stationary phases adenine, thymine and uridine were separated. Having inverse retention order is beneficial especially in quantitation when the first peak is tailing. As a general trend, the silica gel stationary phase showed lower retention times compared to the geopolymer stationary phase under identical mobile phase conditions. One of the reasons for this observation could be the higher hydrophilicity of the geopolymer stationary phase. Therefore, geopolymer stationary phase can be recognized as a promising new material for the separation of very hydrophilic compounds that cannot be easily separated on commonly existing HILIC phases. The selectivity of geopolymers clearly indicates that retention/ partitioning is not solely due to an adsorbed water layer (otherwise all HILIC separations would have similar selectivity on silica and geopolymer phases).19 The nature of the stationary phase chemistry also is vital since HILIC is essentially a multi-mode retention mechanism which also involves hydrogen bonding, dipole-dipole interactions, and ionic interactions.[132,212,215]

Analysis of inorganic ions is generally accomplished using ion-exchange and ion chromatography. HILIC has offered an alternative by using acetonitrile and buffers to separate simple in-organic ions. Based on the surface charge properties, it is expected that geopolymers, like zeolites, should display interactions with ionic analytes. A mixture of five UV detectable anions, iodide, nitrate, azide, bromide, and nitrite were baseline separated using a geopolymer stationary phase and isocratic conditions within 4 minutes (Figure 6.10c). Comparatively, on silica stationary phase the same mixture was separated within 2 minutes under the same conditions, but with different selectivity and low resolution. Recently, it was demonstrated that anions (e.g., iodide and bromide) could be separated using a multi-step gradient on 2.7 µm bare silica superficially porous particles.[241] However, these authors did not test azide ion and nitrite-nitrate pair. Additionally, the anion selectivity of geopolymers is different from the majority of commercial ion chromatography phases

(latex coated sulfonated anion exchangers), where the iodide invariably has large retention factors and broad peak shapes. This observation (Figure 6.10c) implies different retention modes on geopolymers vs. latex coated polymers.[106] Most likely the separation of the halides is based on different hydration levels. Indeed this is the case with iodide ion which is least hydrated among the halogens.[242] On the geopolymer stationary phase, bromide showed higher retention than azide anion. However, on silica, the opposite selectivity was observed. A unique selectivity for inorganic anions is observed on geopolymers compared to commercially available divinylbenzene particle based strong cation or anion exchange ion chromatography phases and other metal oxide based stationary phases such as alumina. [243-245]

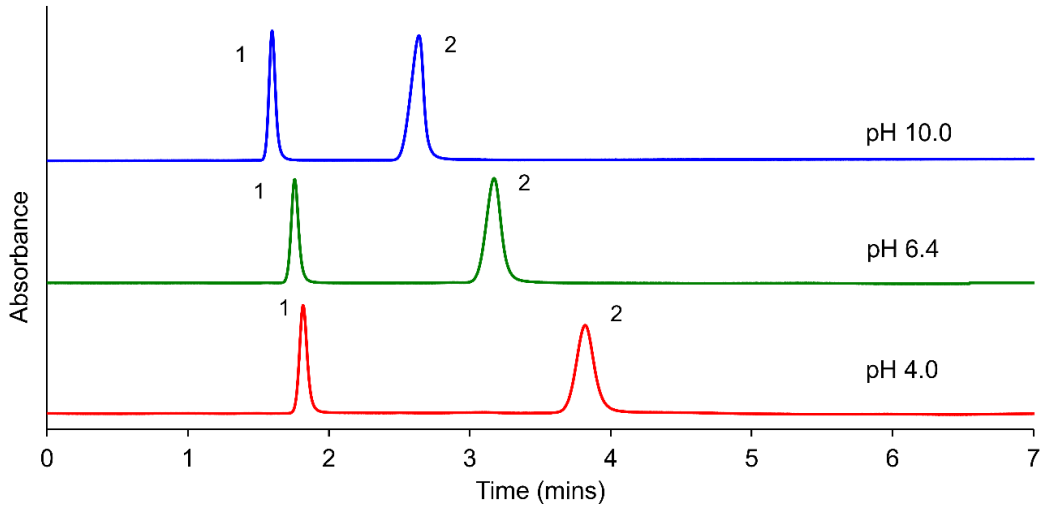

Figure 6.11 The effect of the stationary phase surface charge on electrostatic interactions in HILIC mode, analytes - 1. iodide 2. nitrate, mobile phase - ACN/100 mM NH_4COOH (91/9), 0.425 mL/min , column – 3 mm ID x 150 mm

To further understand the retention behavior of ions Figure 6.11 shows the chromatographic behavior of two UV absorbing inorganic anions, namely iodide and nitrate on a geopolymer stationary phase at different pHs in the HILIC mode. The retention of iodide and nitrate were evaluated at three pre-adjusted pH values (4.0, 6.4, 10.0) of the aqueous ammonium acetate portion of the mobile phase. The highest retention time and selectivity were observed at pH of 4 which is below the "pure aqueous" pH_{PZC}, as expected (given the surface should be positively charged. So the pH of the aqueous portion of the mobile phase increases to 10, retention times decreased, indicating that high pH can be used to decrease analysis times and optimize many separations, provided the stationary phase is stable.

Oxazolidinones are an essential class of antibacterial compounds against gram-positive organisms.[246] They are neutral and structurally very closely related. Since oxazolidinones are very polar, HILIC is an excellent tool to separate them with reasonable retention and selectivity. Five oxazolidinones, methyl-3-Boc-2,2-dimethyl-4-oxazolidinecarboxylate,4-isopropyl-5,5-diphenyl-2-oxazolidinone, 4-(diphenylmethyl)-2-oxazolidinone, 4-isopropyl-2-oxazolidinone, and (1H-Indol-3-ylmethyl)-2-oxazolidinone have been baseline separated on geopolymer stationary phase where none of them was completely separated on 10 µm FPP silica phase (Figure 6.10d). The optimized separation of oxazolidinones on 10 µm FPP is shown in the Figure 6.10d Also (1H-Indol-3-ylmethyl)-2-oxazolidinone and 4-isopropyl-2-oxazolidinone show elution order inversion on silica stationary phase. 4-(diphenylmethyl)-2-oxazolidinone and (1H-Indol-3-ylmethyl)-2-oxazolidinone are baseline resolved on geopolymer stationary phase with $\alpha = 3.8$. In contrast, they coelute on the silica stationary phase. Representative HILIC separations on

geopolymer monolith is shown in Figure 6.12. Further studies are currently going on in our laboratory.

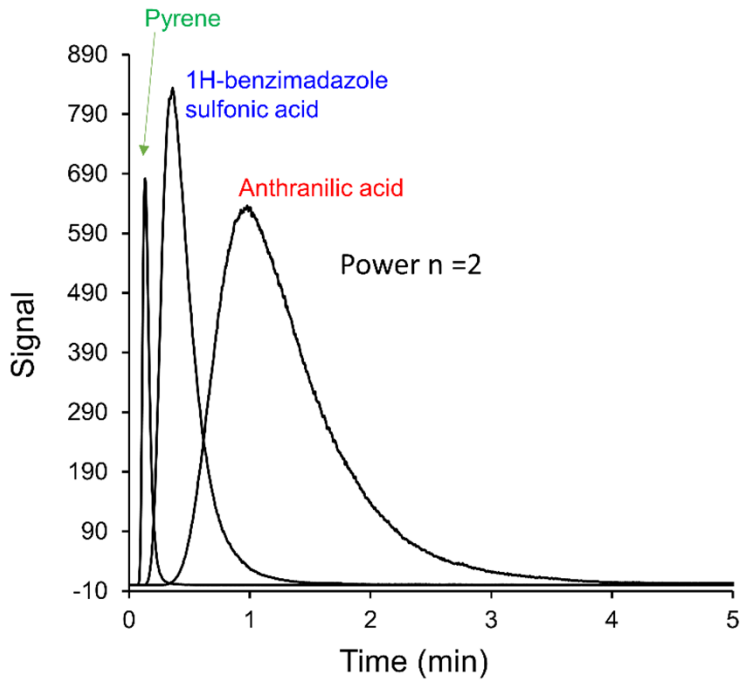

Figure 6.12 Chromatograms of 1) Pyrene 2) 1-H Benzimidazole-2-sulfonic acid 3) Anthranilic acid at a flow rate of 1mL min-1. Mobile Phase: 95 % Acetonitrile 5% 5 mM Ammonium formate adjusted to pH 10.50. Column: 2 x (20 x 4.6 mm ID) monolith coupled. Injection volume= 0.1 µL, UV detection at 220 nm. Overlaid individual chromatogram plotted after applying power law (n =2) on individual chromatograms.[205]

6.4.5.2 Geopolymers as a Normal Phase Stationary Phase

Normal phase and HILIC share a common property in terms of requiring a polar adsorbent. The advantage of normal phase over RPLC is its power to separate structural isomers since the ad-sorption mechanism in normal phase is sensitive to structural changes.[247] As

a result, normal phase chromatography holds its potential in petroleum analysis and shape selective separations. As shown in Figure 6.13 excellent selectivity for structural isomers has been obtained. Nitrobenzene, 2-nitroaniline, 3-nitroaniline, and 4-nitroaniline can be baseline separated on geopolymer stationary phase within 2 minutes.

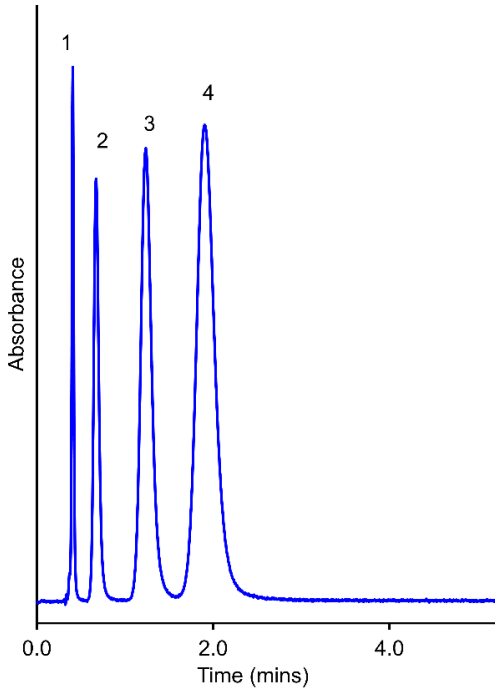

Figure 6.12 Structural isomers separation on geopolymer stationary phase in normal phase chromatography mode, analytes – 1. nitrobenzene 2. o-nitroaniline 3. m-nitroaniline 4. p-nitroaniline, mobile phase - Hexane/Ethanol (84/16), 1.425 mL/ min, column – 3 mm ID x 100 mm, detection at 254 nm

6.5 Conclusions

Geopolymers were shown to be promising new materials for liquid chromatography. The aluminosilicate geopolymer is a high-pH stable stationary phase with negligible retention time drift even at pH 10 in the HILIC mode. Reverse emulsion

polymerization and resin templating techniques were successfully utilized to synthesize metakaolin geopolymer particles with reproducible surface chemistry. Geopolymer stationary phases are effective HILIC phases for the separation of remarkably hydrophilic analytes. Geopolymer stationary phase can be designated as the most hydrophilic HILIC stationary phase existing to date. Ultrahigh hydrolytic and pH stability of the stationary phase is another attractive feature of the geopolymer stationary phase. This exceptional pH stability and excellent hydrophilicity ultimately facilitate method optimization flexibility allowing one to obtain best separations possible. Unique selectivities for a broad range of analytes was observed on geopolymer stationary phases compared to the most common chromatographic stationary phase, silica. A unique selectivity for inorganic ions was produced by geopolymer stationary phase compared to most of the existing ion chromatography stationary phases. Also, geopolymer stationary phase can be successfully utilized in the separation of structural isomers in normal phase chromatography mode.

Chapter 7

GENERAL SUMMARY

Ultrafast chromatography is a feasible and emerging technology in the field of the separation science. The second chapter reveals the potential of novel column packing technology and the future of the packing technology. Therefore, the influence of column packing in ultrafast chromatography. The effect of microscopic properties and non-Newtonian properties of suspensions on reproducible column packing have been discussed. After careful examination of a broad range of stationary phase chemistries, a general column packing guidelines/protocol was developed. Successful utilization of SPPs bases stationary phases in ultrafast high throughput separations demonstrated. The new RSP-CD, 2.7 µm SPP stationary phase provided significantly high efficiency, (> 100,000 plates/m in most of the cases) separations compared to FPPs based stationary phases analogs. Excellent ultrafast separation of pharmaceutically important small molecules was obtained on this these stationary phases without substantial loss of the efficiency. Chapter 4 discusses the utilization of SPP based macrocyclic glycopeptide stationary phases in ultrafast and high throughput separations of simple and complex mixtures of small biomolecules. Ultra-fast separations of structurally closely related peptide (peptide epimers) were obtained using both vancomycin and teicoplanin SPP based stationary phases. Peptide separation method development guidelines have been developed by evaluating mobile phase organic modifier type, pH and mobile phase additive type. Peptide epimers and tryptic peptide separation characteristics of SPPs based macrocyclic glycopeptide stationary phases and SPPs based C18 phases have been evaluated using LC-MS methods and kinetic plots. Superficially porous particles based teicoplanin stationary phase has been recognized as a potential candidate in proteomics and also a

potential second dimension stationary phase in 2D-LC in the analysis of complex biological samples. In Chapter 5, the first salient sub-second separations have been demonstrated using small beds packed with superficially porous particles. This work is presented as the proof of concept. Both achiral and chiral Sub-second separations were obtained in various chromatographic modes. Limitations of instrument hardware and current detector technology have been addressed. It is predicted that further improvement of instrumentation will expand the further investigation of potentials of sub-second chromatography. Utilization of resolution enhancement and peak detection techniques such as power law and peak deconvolution (Currently known as iterative curve fitting) discussed briefly.

In Chapter 6, the development of new geopolymer based stationary phase media has been discussed. Geopolymers was recognized as a promising material for liquid chromatography. It was identified as the first amorphous ceramic type liquid chromatography stationary phase with excellent base stability even at pH 10. Chromatographic performances of geopolymers were compared with other commercially available or reported stationary phase in HILIC mode. Geopolymers was recognized as the most hydrophilic HILIC phase among 37 known HILIC phases. A wide variety of analytes such as nucleobases, oxazolidinones, and inorganic ions were separated on geopolymers with unique selectivity compared to silica phase. Further geopolymer stationary phase offered excellent normal phase separations for analytes such as structural isomers. A simple but effective synthetic scheme was devised to synthesis geopolymer particles. Revers emulsion templating technique was utilized as the basis of the synthesis protocol. Due to its pH stability and unique selectivity geopolymers based stationary phases offers more flexibility in chromatographic method development.

Appendix A

NAMES OF CO-CONTRIBUTING AUTHORS

Chapter 2: M Farooq Wahab, Darshan C Patel, Daniel W Armstrong

Chapter 3: Choyce A Weatherly, Zachary S Breitbach, Daniel W Armstrong

Chapter 4: Zachary S Breitbach, Jauh T Lee, Daniel W Armstrong

Chapter 5: M Farooq Wahab, Yadi Wang, Chandan L Barhate, Darshan C Patel, Daniel W Armstrong

Chapter 6: Choyce A Weatherly, M Farooq Wahab, Nimisha Thakur, Daniel W Armstrong

Appendix B

RIGHTS AND PERMISSIONS

Title: Hydroxypropyl beta cyclodextrin bonded superficially porous particle-based HILIC stationary phases

Author: Rasangi M. Wimalasinghe, Choyce A. Weatherly, Zachary S. Breitbach, et al

Publication: Journal of Liquid Chromatography and Related Technologies

Publisher: Taylor & Francis

Date: May 27, 2016

Rights managed by Taylor & Francis

Thesis/Dissertation Reuse Request

Taylor & Francis is pleased to offer reuses of its content for a thesis or dissertation free of charge contingent on resubmission of permission request if work is published.

BACK CLOSE WINDOW

SPRINGER NATURE LICENSE TERMS AND CONDITIONS

Oct 20, 2018

This Agreement between The University of Texas at Arlington -- Rasangi M Wimalasinghe Kulugammana K D Gedara ("You") and Springer Nature ("Springer Nature") consists of your license details and the terms and conditions provided by Springer Nature and Copyright Clearance Center.

License Number	4453270978565
License date	Oct 20, 2018
Licensed Content Publisher	Springer Nature
Licensed Content Publication	Analytical and Bioanalytical Chemistry
Licensed Content Title	Separation of peptides on superficially porous particle based macrocyclic glycopeptide liquid chromatography stationary phases: consideration of fast separations
Licensed Content Author	Rasangi M. Wimalasinghe, Zachary S. Breitbach, Jauh T. Lee et al
Licensed Content Date	Jan 1, 2017
Licensed Content Volume	409
Licensed Content Issue	9
Type of Use	Thesis/Dissertation
Requestor type	academic/university or research institute
Format	electronic
Portion	full article/chapter
Will you be translating?	no
Circulation/distribution	<501
Author of this Springer Nature content	yes
Title	Student
Institution name	The University of Texas at Arlington
Expected presentation date	Nov 2018
Order reference number	1618-2650
Requestor Location	The University of Texas at Arlington Department of chemistry and biochemistry University of Texas at Arlington ARLINGTON, TX 76019 United States Attn: Rasangi Madhumali Wimalasinghe Kulugammana Kande Dadahoma Gedara
Billing Type	Invoice
Billing Address	The University of Texas at Arlington Department of chemistry and biochemistry University of Texas at Arlington ARLINGTON, TX 76019 United States

	Dadahoma Gedara
Total	0.00 USD

Terms and Conditions

Springer Nature Terms and Conditions for RightsLink Permissions Springer Nature Customer Service Centre GmbH (the Licensor) hereby grants you a non-exclusive, world-wide licence to reproduce the material and for the purpose and requirements specified in the attached copy of your order form, and for no other use, subject to the conditions below:

1. The Licensor warrants that it has, to the best of its knowledge, the rights to license reuse of this material. However, you should ensure that the material you are requesting is original to the Licensor and does not carry the copyright of another entity (as credited in the published version).

   If the credit line on any part of the material you have requested indicates that it was reprinted or adapted with permission from another source, then you should also seek permission from that source to reuse the material.

2. Where **print only** permission has been granted for a fee, separate permission must be obtained for any additional electronic re-use.

3. Permission granted **free of charge** for material in print is also usually granted for any electronic version of that work, provided that the material is incidental to your work as a whole and that the electronic version is essentially equivalent to, or substitutes for, the print version.

4. A licence for 'post on a website' is valid for 12 months from the licence date. This licence does not cover use of full text articles on websites.

5. Where **'reuse in a dissertation/thesis'** has been selected the following terms apply: Print rights of the final author's accepted manuscript (for clarity, NOT the published version) for up to 100 copies, electronic rights for use only on a personal website or institutional repository as defined by the Sherpa guideline (www.sherpa.ac.uk/romeo/).

6. Permission granted for books and journals is granted for the lifetime of the first edition and does not apply to second and subsequent editions (except where the first edition permission was granted free of charge or for signatories to the STM Permissions Guidelines http://www.stm-assoc.org/copyright-legal-affairs/permissions/permissions-guidelines/), and does not apply for editions in other languages unless additional translation rights have been granted separately in the licence.

7. Rights for additional components such as custom editions and derivatives require additional permission and may be subject to an additional fee. Please apply to Journalpermissions@springernature.com/bookpermissions@springernature.com for these rights.

8. The Licensor's permission must be acknowledged next to the licensed material in print. In electronic form, this acknowledgement must be visible at the same time as the figures/tables/illustrations or abstract, and must be hyperlinked to the journal/book's homepage. Our required acknowledgement format is in the Appendix below.

9. Use of the material for incidental promotional use, minor editing privileges (this does not include cropping, adapting, omitting material or any other changes that affect the meaning, intention or moral rights of the author) and copies for the disabled are permitted under this licence.

1. Minor adaptations of single figures (changes of format, colour and style) do not require the Licensor's approval. However, the adaptation should be credited as shown in Appendix below.

Appendix — Acknowledgements:

For Journal Content:
Reprinted by permission from [**the Licensor**]: [**Journal Publisher** (e.g. Nature/Springer/Palgrave)] [**JOURNAL NAME**] [**REFERENCE CITATION** (Article name, Author(s) Name), [**COPYRIGHT**] (year of publication)

For **Advance Online Publication papers:**
Reprinted by permission from [**the Licensor**]: [**Journal Publisher** (e.g. Nature/Springer/Palgrave)] [**JOURNAL NAME**] [**REFERENCE CITATION** (Article name, Author(s) Name), [**COPYRIGHT**] (year of publication), advance online publication, day month year (doi: 10.1038/sj.[JOURNAL ACRONYM].)

For Adaptations/Translations:
Adapted/Translated by permission from [**the Licensor**]: [**Journal Publisher** (e.g. Nature/Springer/Palgrave)] [**JOURNAL NAME**] [**REFERENCE CITATION** (Article name, Author(s) Name), [**COPYRIGHT**] (year of publication)

Note: For any republication from the British Journal of Cancer, the following credit line style applies:

Reprinted/adapted/translated by permission from [**the Licensor**]: on behalf of Cancer Research UK: : [**Journal Publisher** (e.g. Nature/Springer/Palgrave)] [**JOURNAL NAME**] [**REFERENCE CITATION** (Article name, Author(s) Name), [**COPYRIGHT]** (year of publication)

For **Advance Online Publication** papers:
Reprinted by permission from The [**the Licensor**]: on behalf of Cancer Research UK: [**Journal Publisher** (e.g. Nature/Springer/Palgrave)] [**JOURNAL NAME**] [**REFERENCE CITATION** (Article name, Author(s) Name), [**COPYRIGHT**] (year of publication), advance online publication, day month year (doi: 10.1038/sj.[JOURNAL ACRONYM])

For Book content:
Reprinted/adapted by permission from [**the Licensor**]: [**Book Publisher** (e.g. Palgrave Macmillan, Springer etc) [**Book Title**] by [**Book author**(s)] [**COPYRIGHT**] (year of publication)

Other Conditions:

Version 1.1

References

(1) Fekete, S.; Oláh, E.; Fekete, J. *Journal of chromatography A* **2012**, *1228*, 57-71.

(2) Patel, D. C.; Breitbach, Z. S.; Wahab, M. F.; Barhate, C. L.; Armstrong, D. W. *Analytical Chemistry* **2015**, *87*, 9137-9148.

(3) Regalado, E. L.; Welch, C. J. *Journal of Separation Science* **2015**, *38*, 2826-2832.

(4) Wimalasinghe, R. M.; Breitbach, Z. S.; Lee, J. T.; Armstrong, D. W. *Analytical and bioanalytical chemistry* **2017**, *409*, 2437-2447.

(5) Jacobson, S. C.; Culbertson, C. T.; Daler, J. E.; Ramsey, J. M. *Analytical Chemistry* **1998**, *70*, 3476-3480.

(6) Moore, A. W.; Jorgenson, J. W. *Analytical Chemistry* **1995**, *67*, 3448-3455.

(7) Piehl, N.; Ludwig, M.; Belder, D. *Electrophoresis* **2004**, *25*, 3848-3852.

(8) Guetschow, E. D.; Steyer, D. J.; Kennedy, R. T. *Analytical Chemistry* **2014**, *86*, 10373-10379.

(9) Clicq, D.; Vervoort, N.; Vounckx, R.; Ottevaere, H.; Buijs, J.; Gooijer, C.; Ariese, F.; Baron, G. V.; Desmet, G. *Journal of Chromatography A* **2002**, *979*, 33-42.

(10) Umehara, R.; Harada, M.; Okada, T. *Journal of Separation Science* **2009**, *32*, 472-478.

(11) Wahab, M. F.; Dasgupta, P. K.; Kadjo, A. F.; Armstrong, D. W. *Analytica chimica acta* **2016**, *907*, 31-44.

(12) Gritti, F.; Leonardis, I.; Shock, D.; Stevenson, P.; Shalliker, A.; Guiochon, G. *Journal of Chromatography A* **2010**, *1217*, 1589-1603.

(13) Cunliffe, J. M.; Maloney, T. D. *Journal of separation science* **2007**, *30*, 3104-3109.

(14) Schuster, S. A.; Boyes, B. E.; Wagner, B. M.; Kirkland, J. J. *Journal of Chromatography A* **2012**, *1228*, 232-241.

(15) Gritti, F.; Cavazzini, A.; Marchetti, N.; Guiochon, G. *Journal of Chromatography A* **2007**, *1157*, 289-303.

(16) Gritti, F.; Guiochon, G. *LC GC North America* **2012**, *30*.

(17) Spudeit, D. A.; Dolzan, M. D.; Breitbach, Z. S.; Barber, W. E.; Micke, G. A.; Armstrong, D. W. *Journal of Chromatography A* **2014**, *1363*, 89-95.

(18) Dolzan, M. D.; Spudeit, D. A.; Breitbach, Z. S.; Barber, W. E.; Micke, G. A.; Armstrong, D. W. *Journal of Chromatography A* **2014**, *1365*, 124-130.

(19) Gritti, F.; Guiochon, G. *Journal of Chromatography A* **2010**, *1217*, 8167-8180.

(20) Gritti, F.; Guiochon, G. *Journal of chromatography A* **2012**, *1221*, 2-40.

(21) Tanaka, N.; McCalley, D. V. *Analytical chemistry* **2015**, *88*, 279-298.

(22) Wahab, M. F.; Patel, D. C.; Wimalasinghe, R. M.; Armstrong, D. W. *Analytical chemistry* **2017**, *89*, 8177-8191.

(23) Shannon, C. E. *Proceedings of the Institute of Radio Engineers* **1949**, *37*, 10-21.

(24) Kivilompolo, M.; Hyötyläinen, T. *Journal of Chromatography A* **2007**, *1145*, 155-164.

(25) Davidovits, J. *Journal of Thermal Analysis and calorimetry* **1991**, *37*, 1633-1656.

(26) Davidovits, J. *Journal of Thermal Analysis and Calorimetry* **1989**, *35*, 429-441.

(27) Kriven, W. M. *American Ceramics Society Bulletin* **2010**, *89*, 31-34.

(28) Duxson, P.; Fernández-Jiménez, A.; Provis, J. L.; Lukey, G. C.; Palomo, A.; Van Deventer, J. *Journal of Materials Science* **2007**, *42*, 2917-2933.

(29) Duxson, P.; Mallicoat, S. W.; Lukey, G. C.; Kriven, W. M.; van Deventer, J. S. *Colloids and Surfaces A: Physicochemical and Engineering Aspects* **2007**, *292*, 8-20.

(30) Biscan, G.; Hojaji, H.; Melmeth, D. L.; Pham, T.; Zhang, H.; Google Patents, 2013.

(31) Medpelli, D.; Seo, J. M.; Seo, D. K. *Journal of the American Ceramic Society* **2014**, *97*, 70-73.

(32) Kong, D. L.; Sanjayan, J. G.; Sagoe-Crentsil, K. *Journal of Materials Science* **2008**, *43*, 824-831.

(33) Alonso, S.; Palomo, A. *Mater. Lett.* **2001**, *47*, 55-62.

(34) Alzeer, M.; Keyzers, R. A.; MacKenzie, K. J. *Ceramics International* **2014**, *40*, 3553-3560.

(35) Kurganov, A.; Trüdinger, U.; Isaeva, T.; Unger, K. *Chromatographia* **1996**, *42*, 217-222.

(36) Nawrocki, J.; Dunlap, C.; McCormick, A.; Carr, P. W. *Journal of Chromatography A* **2004**, *1028*, 1-30.

(37) Weber, T. P.; Jackson, P. T.; Carr, P. W. *Analytical Chemistry* **1995**, *67*, 3042-3050.

(38) Paek, C.; Huang, Y.; Filgueira, M. R.; McCormick, A. V.; Carr, P. W. *Journal of Chromatography A* **2012**, *1229*, 129-139.

(39) Paek, C.; McCormick, A. V.; Carr, P. W. *Journal of Chromatography A* **2011**, *1218*, 1359-1366.

(40) Muna, G. W.; Swope, V. M.; Swain, G. M.; Porter, M. D. *Journal of Chromatography A* **2008**, *1210*, 154-159.

(41) West, C.; Elfakir, C.; Lafosse, M. *Journal of Chromatography A* **2010**, *1217*, 3201-3216.

(42) Knox, J. H.; Kaur, B.; Millward, G. R. *Journal of Chromatography A* **1986**, *352*, 3-25.

(43) Wahab, M. F.; Pohl, C. A.; Lucy, C. A. *Journal of Chromatography A* **2012**, *1270*, 139-146.

(44) Shalliker, R. A.; Broyles, B. S.; Guiochon, G. *Journal of Chromatography A* **2000**, *878*, 153-163.

(45) Koh, J.-H.; Broyles, B. S.; Guan-Sajonz, H.; Hu, M. Z.-C.; Guiochon, G. *Journal of Chromatography A* **1998**, *813*, 223-238.

(46) Verzele M., D. *LC-GC* **1986**, *4(7)*, 616-618.

(47) Wu, Y.; Ching, C. *Chromatographia* **2003**, *57*, 329-337.

(48) Godinho, J. M.; Reising, A. E.; Tallarek, U.; Jorgenson, J. W. *Journal of Chromatography A* **2016**, *1462*, 165-169.

(49) James Jorgenson, C. P., Fabrice Gritti, Wahab, M. Farooq, . *Personal Communication* **2017**.

(50) Cheong, W. J. *Journal of separation science* **2014**, *37*, 603-617.

(51) Spain, I. L.; Paauwe, J. *High pressure technology Volume I,* ; Dekker: New York, N.Y., 1977.

(52) Gritti, F.; Bell, D. S.; Guiochon, G. *Journal of Chromatography A* **2014**, *1355*, 179-192.

(53) Catani, M.; Ismail, O. H.; Cavazzini, A.; Ciogli, A.; Villani, C.; Pasti, L.; Bergantin, C.; Cabooter, D.; Desmet, G.; Gasparrini, F.; Bell, D. S. *Journal of Chromatography A* **2016**, *1454*, 78-85.

(54) Barhate, C. L.; Wahab, M. F.; Breitbach, Z. S.; Bell, D. S.; Armstrong, D. W. *Analytica Chimica Acta* **2015**, *898*, 128-137.

(55) Billen, J.; Guillarme, D.; Rudaz, S.; Veuthey, J.-L.; Ritchie, H.; Grady, B.; Desmet, G. *Journal of Chromatography A* **2007**, *1161*, 224-233.

(56) Cabooter, D.; Billen, J.; Terryn, H.; Lynen, F.; Sandra, P.; Desmet, G. *Journal of Chromatography A* **2008**, *1204*, 1-10.

(57) Gritti, F.; Farkas, T.; Heng, J.; Guiochon, G. *Journal of Chromatography A* **2011**, *1218*, 8209-8221.

(58) Zats, J. L. *Journal of the Society of Cosmetic Chemists* **1985**, *36*, 393-411.

(59) Bristow, P. A.; Brittain, P. N.; Riley, C. M.; Williamson, B. F. *Journal of Chromatography A* **1977**, *131*, 57-64.

(60) Blue, L. E.; Jorgenson, J. W. *Journal of Chromatography A* **2015**, *1380*, 71-80.

(61) Kromasil. *https://www.kromasil.com/support/dac_packing.php (Jan 19, 2017)*.

(62) Broquaire, M. *Journal of Chromatography A* **1979**, *170*, 43-52.

(63) Domagalska, D. E.; Loscombe, C. R. *Chromatographia* **1982**, *15*, 657-659.

(64) Karapetyan, S. A.; Yakushina, L. M.; Vasiyarov, G. G.; Brazhnikov, V. V. *Journal of High Resolution Chromatography* **1983**, *6*, 440-441.

(65) Szumski, M.; Buszewski, B. *Critical Reviews in Analytical Chemistry* **2002**, *32*, 1-46.

(66) Zimina, T.; Smith, R. M.; Highfield, J. C.; Myers, P.; King, B. W. *Journal of Chromatography A* **1996**, *728*, 33-45.

(67) Zimina, T. M.; Smith, R. M.; Myers, P.; King, B. W. *Chromatographia* **1995**, *40*, 662-668.

(68) Reed, G. D.; Loscombe, C. R. *Chromatographia* **1984**, *18*, 695-697.

(69) Roumeliotis, P.; Chatziathanassiou, M.; Unger, K. K. *Chromatographia* **1984**, *19*, 145-150.

(70) Giesche, H.; Unger, K. K.; Esser, U.; Eray, B.; Trüdinger, U.; Kinkel, J. N. *Journal of Chromatography A* **1989**, *465*, 39-57.

(71) Avery, N. C.; Light, N. *Journal of Chromatography A* **1985**, *328*, 347-352.

(72) *Knauer Wissenschaftliche Geräte GmbH, High Pressure Column Packing Device Manual* **2007**, 19.

(73) Karapetyan, S. A.; Yakushina, L. M.; Vasijarov, G. G.; Brazhnikov, V. V. *Journal of High Resolution Chromatography* **1985**, *8*, 148-149.

(74) Wong, V.; Shalliker, R. A.; Guiochon, G. *Analytical Chemistry* **2004**, *76*, 2601-2608.

(75) Vissers, J. P. C.; Hoeben, M. A.; Laven, J.; Claessens, H. A.; Cramers, C. A. *Journal of Chromatography A* **2000**, *883*, 11-25.

(76) MacNair, J. E.; Patel, K. D.; Jorgenson, J. W. *Analytical Chemistry* **1999**, *71*, 700-708.

(77) Bocian, S.; Nowaczyk, A.; Buszewski, B. *Anal. Bioanal. Chem.* **2012**, *404*, 731-740.

(78) Corradini, C.; Corradini, D.; Huber, C. G.; Bonn, G. K. *Chromatographia* **1995**, *41*, 511-515.

(79) Jewett, D.; Lawless, J. G. *Journal of High Resolution Chromatography* **1980**, *3*, 647-648.

(80) Tyrrell, É.; Hilder, E. F.; Shalliker, R. A.; Dicinoski, G. W.; Shellie, R. A.; Breadmore, M. C.; Pohl, C. A.; Haddad, P. R. *Journal of Chromatography A* **2008**, *1208*, 95-100.

(81) Hou, Y.; Zhang, F.; Liang, X.; Yang, B.; Liu, X.; Dasgupta, P. K. *Analytical Chemistry* **2016**, *88*, 4676-4681.

(82) Gilbert, M. T.; Knox, J. H.; Kaur, B. *Chromatographia* **1982**, *16*, 138-146.

(83) Harkins, W. D.; Feldman, A. *Journal of the American Chemical Society* **1922**, *44*, 2665-2685.

(84) Binks, B. P.; Clint, J. H. *Langmuir* **2002**, *18*, 1270-1273.

(85) Kinloch, A. J. *Adhesion and Adhesives: Science and Technology*; Chapman and Hall, pg. 26-34.: New York, 1987.

(86) Kirkland, J.; DeStefano, J. *Journal of Chromatography A* **2006**, *1126*, 50-57.

(87) Vissers, J. P. C.; Claessens, H. A.; Laven, J.; Cramers, C. A. *Analytical Chemistry* **1995**, *67*, 2103-2109.

(88) Dong, L.; Johnson, D. *Langmuir* **2003**, *19*, 10205-10209.

(89) Mewis, J.; Wagner, N. J. *Colloidal Suspension Rheology*, 1 ed.; Cambridge University Press, 2012, p 416.

(90) Shelly, D. C.; Edkins, T. J. *Journal of Chromatography A* **1987**, *411*, 185-199.

(91) Wagner, N. J.; Brady, J. F. *Physics Today* **2009**, *62*, 27-32.

(92) Barnes, H. *Journal of Rheology* **1989**, *33*, 329-366.

(93) Gritti, F.; Guiochon, G. *Analytical chemistry* **2013**, *85*, 3017-3035.

(94) Knox, J. H.; Parcher, J. F. *Analytical Chemistry* **1969**, *41*, 1599-1606.

(95) Benenati, R. F.; Brosilow, C. B. *AIChE Journal* **1962**, *8*, 359-361.

(96) Shalliker, R. A.; Broyles, B. S.; Guiochon, G. *Journal of Chromatography A* **2000**, *888*, 1-12.

(97) Reising, A. E.; Godinho, J. M.; Hormann, K.; Jorgenson, J. W.; Tallarek, U. *Journal of Chromatography A* **2016**, *1436*, 118-132.

(98) Reising, A. E.; Godinho, J. M.; Jorgenson, J. W.; Tallarek, U. *Journal of Chromatography A* **2017**, *1504*, 71-82.

(99) Bröckel, U.; Löffler, F. *Powder Technology* **1991**, *66*, 53-58.

(100) Wahab, M. F.; Patel, D. C.; Armstrong, D. W. *Journal of Chromatography A* **2017**, *In Press. https://doi.org/10.1016/j.chroma.2017.06.031*.

(101) Brown, E.; Forman, N. A.; Orellana, C. S.; Zhang, H.; Maynor, B. W.; Betts, D. E.; DeSimone, J. M.; Jaeger, H. M. *Nat Mater* **2010**, *9*, 220-224.

(102) Gonzalez, B.; Calvar, N.; Gomez, E.; Dominguez, A. *Journal of Chemical Thermodynamics* **2007**, *39*, 1578-1588.

(103) Sovilj, M. N. *Journal of Chemical and Engineering Data* **1995**, *40*, 1058-1061.

(104) Wei, I. C.; Rowley, R. L. *Journal of Chemical & Engineering Data* **1984**, *29*, 332-335.

(105) Wahab, M. F.; Ibrahim, M. E.; Lucy, C. A. *Analytical chemistry* **2013**, *85*, 5684-5691.

(106) Wahab, M. F.; Pohl, C. A.; Lucy, C. A. *Analyst* **2011**, *136*, 3113-3120.

(107) Patel, D. C.; Breitbach, Z. S.; Yu, J.; Nguyen, K. A.; Armstrong, D. W. *Analytica Chimica Acta* **2017**, *963*, 164-174.

(108) Verzele, M. *Journal of Chromatography A* **1984**, *295*, 81-87.

(109) Soliven, A.; Dennis, G. R.; Hilder, E. F.; Andrew Shalliker, R.; Stevenson, P. G. *Chromatographia* **2014**, *77*, 663-671.

(110) MacNair, J. E.; Lewis, K. C.; Jorgenson, J. W. *Analytical Chemistry* **1997**, *69*, 983-989.

(111) Treadway, J. W.; Wyndham, K. D.; Jorgenson, J. W. *Journal of Chromatography A* **2015**, *1422*, 345-349.

(112) Bruns, S.; Franklin, E. G.; Grinias, J. P.; Godinho, J. M.; Jorgenson, J. W.; Tallarek, U. *Journal of Chromatography A* **2013**, *1318*, 189-197.

(113) Patel, K. D.; Jerkovich, A. D.; Link, J. C.; Jorgenson, J. W. *Analytical Chemistry* **2004**, *76*, 5777-5786.

(114) Colón, L. A.; Maloney, T. D.; Fermier, A. M. *Journal of Chromatography A* **2000**, *887*, 43-53.

(115) Shalliker, R. A.; Broyles, B. S.; Guiochon, G. *Analytical Chemistry* **2000**, *72*, 323-332.

(116) Khirevich, S.; Höltzel, A.; Hlushkou, D.; Tallarek, U. *Analytical Chemistry* **2007**, *79*, 9340-9349.

(117) Andreolini, F.; Borra, C.; Novotny, M. *Analytical Chemistry* **1987**, *59*, 2428-2432.

(118) Malik, A.; Li, W.; Lee, M. L. *Journal of Microcolumn Separations* **1993**, *5*, 361-369.

(119) Pieranski, P. *Comptes Rendus Physique* **2016**, *17*, 242-263.

(120) Schure, M. R.; Maier, R. S.; Kroll, D. M.; Ted Davis, H. *Journal of Chromatography A* **2004**, *1031*, 79-86.

(121) Malkin, D. S. *An Invesitgation of a Novel Monolithic Chromatography Column, Silica Colloidal Crystal Packed Columns*. 2010.

(122) Fee, C.; Nawada, S.; Dimartino, S. *Journal of Chromatography A* **2014**, *1333*, 18-24.

(123) Yin, H.; Brennen, R. A.; Lyster, E.; Slocum, R. **2016 (US Patent 20160231293)**.

(124) De Malsche, W.; Eghbali, H.; Clicq, D.; Vangelooven, J.; Gardeniers, H.; Desmet, G. *Analytical Chemistry* **2007**, *79*, 5915-5926.

(125) Robson, M. M.; Roulin, S.; Shariff, S. M.; Raynor, M. W.; Bartle, K. D.; Clifford, A. A.; Myers, P.; Euerby, M. R.; Johnson, C. M. *Chromatographia* **1996**, *43*, 313-321.

(126) Tong, D.; Bartle, K. D.; Clifford, A. A. *Journal of Microcolumn Separations* **1994**, *6*, 249-255.

(127) Inagaki, M.; Kitagawa, S.; Tsuda, T. *Kuromatogurafi* **1993**, *14*, 55R-60R.

(128) Fermier, A. M.; Colón, L. A. *Journal of Microcolumn Separations* **1998**, *10*, 439-447.

(129) Fermier, A. M., Colón, L. A. In *HPLC 1996 in High Performance Liquid Phase Separations and Related Techniques*: San Francisco, CA, 1996.

(130) McCall, J. P. *A Twist on Packing Analytical Columns for Reversed Phase Liquid Chromatography*. Florida State University, Florida, 2004.

(131) Camenzuli, M.; Ritchie, H. J.; Ladine, J. R.; Shalliker, R. A. *Analyst* **2011**, *136*, 5127-5130.

(132) Wang, C.; Jiang, C.; Armstrong, D. W. *Journal of Separation Science* **2008**, *31*, 1980-1990.

(133) Ikegami, T.; Tomomatsu, K.; Takubo, H.; Horie, K.; Tanaka, N. *Journal of chromatography A* **2008**, *1184*, 474-503.

(134) Guo, Y.; Gaiki, S. *Journal of Chromatography A* **2005**, *1074*, 71-80.

(135) McCalley, D. V. *Journal of Chromatography A* **2008**, *1193*, 85-91.

(136) Jandera, P. *Analytica Chimica Acta* **2011**, *692*, 1-25.

(137) Alpert, A. J. *Journal of Chromatography A* **1990**, *499*, 177-196.

(138) Ibrahim, M. E. A.; Liu, Y.; Lucy, C. A. *Journal of Chromatography A* **2012**, *1260*, 126-131.

(139) Ibrahim, M. E.; Wahab, M. F.; Lucy, C. A. *Analytica chimica acta* **2014**, *820*, 187-194.

(140) Pack, B. W.; Risley, D. S. *Journal of Chromatography A* **2005**, *1073*, 269-275.

(141) Oyler, A. R.; Armstrong, B. L.; Cha, J. Y.; Zhou, M. X.; Yang, Q.; Robinson, R. I.; Dunphy, R.; Burinsky, D. J. *Journal of Chromatography A* **1996**, *724*, 378-383.

(142) Yoshida, T. *Analytical Chemistry* **1997**, *69*, 3038-3043.

(143) Qiu, H.; Loukotková, L.; Sun, P.; Tesařová, E.; Bosáková, Z.; Armstrong, D. W. *Journal of Chromatography A* **2011**, *1218*, 270-279.

(144) Armstrong, D. W.; Jin, H. L. *Journal of Chromatography A* **1989**, *462*, 219-232.

(145) Liu, Y.; Urgaonkar, S.; Verkade, J. G.; Armstrong, D. W. *Journal of Chromatography A* **2005**, *1079*, 146-152.

(146) Spudeit, D. A.; Breitbach, Z. S.; Dolzan, M. D.; Micke, G. A.; Armstrong, D. W. **2015**.

(147) Perera, S.; Na, Y. C.; Doundoulakis, T.; Ngo, V. J.; Feng, Q.; Breitbach, Z. S.; Lovely, C. J.; Armstrong, D. W. *Chirality* **2013**, *25*, 133-140.

(148) DeStefano, J.; Langlois, T.; Kirkland, J. *Journal of chromatographic science* **2008**, *46*, 254-260.

(149) DeStefano, J. J.; Schuster, S. A.; Lawhorn, J. M.; Kirkland, J. J. *Journal of Chromatography A* **2012**, *1258*, 76-83.

(150) Bruns, S.; Stoeckel, D.; Smarsly, B. M.; Tallarek, U. *Journal of Chromatography A* **2012**, *1268*, 53-63.

(151) Sun, P.; Wang, C.; Breitbach, Z. S.; Zhang, Y.; Armstrong, D. W. *Analytical Chemistry* **2009**, *81*, 10215-10226.

(152) Uhlig, T.; Kyprianou, T.; Martinelli, F. G.; Oppici, C. A.; Heiligers, D.; Hills, D.; Calvo, X. R.; Verhaert, P. *EuPA Open Proteomics* **2014**, *4*, 58-69.

(153) López-Otín, C.; Matrisian, L. M. *Nature Reviews Cancer* **2007**, *7*, 800-808.

(154) Witt, K. A.; Gillespie, T. J.; Huber, J. D.; Egleton, R. D.; Davis, T. P. *Peptides* **2001**, *22*, 2329-2343.

(155) Roemer, D.; Pless, J. *Life sciences* **1979**, *24*, 621-624.

(156) Uchiyama, T.; Kotani, A.; Kishida, T.; Tatsumi, H.; Okamoto, A.; Fujita, T.; Murakami, M.; Muranishi, S.; Yamamoto, A. *Journal of pharmaceutical sciences* **1998**, *87*, 448-452.

(157) Su, Z.-D.; Sun, L.; Yu, D.-X.; Li, R.-X.; Li, H.-X.; Yu, Z.-J.; Sheng, Q.-H.; Lin, X.; Zeng, R.; Wu, J.-R. *Journal of molecular cell biology* **2011**, *3*, 309-315.

(158) Zhang, B.; Soukup, R.; Armstrong, D. W. *Journal of Chromatography A* **2004**, *1053*, 89-99.

(159) Tao, Y.; Quebbemann, N. R.; Julian, R. R. *Analytical chemistry* **2012**, *84*, 6814-6820.

(160) Erspamer, V.; Melchiorri, P.; Falconieri-Erspamer, G.; Negri, L.; Corsi, R.; Severini, C.; Barra, D.; Simmaco, M.; Kreil, G. *Proceedings of the National Academy of Sciences* **1989**, *86*, 5188-5192.

(161) Broccardo, M.; Erspamer, V.; Falconieri, G.; Improta, G.; Linari, G.; Melchiorri, P.; Montecucchi, P. *British journal of pharmacology* **1981**, *73*, 625-631.

(162) Chen, H.; Horváth, C. *Journal of Chromatography A* **1995**, *705*, 3-20.

(163) Underberg, W.; Hoitink, M.; Reubsaet, J.; Waterval, J. *Journal of Chromatography B: Biomedical Sciences and Applications* **2000**, *742*, 401-409.

(164) Péter, A.; Lázár, L.; Fülöp, F.; Armstrong, D. W. *Journal of Chromatography A* **2001**, *926*, 229-238.

(165) Takeuchi, Y. *Applications of NMR spectroscopy to problems in stereochemistry and conformational analysis*; Vch Pub, 1986; Vol. 6.

(166) Ewing, M. A.; Wang, J.; Sheeley, S. A.; Sweedler, J. V. *Analytical chemistry* **2008**, *80*, 2874-2880.

(167) Chankvetadze, B.; Lindner, W.; Scriba, G. K. *Analytical chemistry* **2004**, *76*, 4256-4260.

(168) Grossman, P. D.; Colburn, J. C.; Lauer, H. H.; Nielsen, R. G.; Riggin, R. M.; Sittampalam, G.; Rickard, E. C. *Analytical chemistry* **1989**, *61*, 1186-1194.

(169) Péter, A.; Tóth, G. *Analytica chimica acta* **1997**, *352*, 335-356.

(170) Péter, A.; Török, G.; Armstrong, D. W. *Journal of Chromatography A* **1998**, *793*, 283-296.

(171) Berthod, A.; Liu, Y.; Bagwill, C.; Armstrong, D. W. *Journal of Chromatography A* **1996**, *731*, 123-137.

(172) Soukup-Hein, R. J.; Schneiderheinze, J.; Mehelic, P.; Armstrong, D. W. *Chromatographia* **2007**, *66*, 461-468.

(173) Fekete, S.; Fekete, J.; Ganzler, K. *Journal of pharmaceutical and biomedical analysis* **2009**, *50*, 703-709.

(174) Inc., T. F. S., 2011, pp 1-8.

(175) John, H.; Walden, M.; Schäfer, S.; Genz, S.; Forssmann, W.-G. *Analytical and bioanalytical chemistry* **2004**, *378*, 883-897.

(176) Yates, J. R.; Speicher, S.; Griffin, P. R.; Hunkapiller, T. *Analytical biochemistry* **1993**, *214*, 397-408.

(177) Blanquet, R.; Bui, K.; Armstrong, D. *Journal of liquid chromatography* **1986**, *9*, 1933-1949.

(178) Armstrong, D. W.; Tang, Y. B.; Chen, S. S.; Zhou, Y. W.; Bagwill, C.; Chen, J. R. *Analytical Chemistry* **1994**, *66*, 1473-1484.

(179) Armstrong, D. W.; Boehm, R. E. *Journal of chromatographic science* **1984**, *22*, 378-385.

(180) Schuster, S.; Wagner, B.; Boyes, B.; Kirkland, J. *Journal of chromatographic science* **2010**, *48*, 566-571.

(181) Wahab, M. F.; Wimalasinghe, R. M.; Wang, Y.; Barhate, C. L.; Patel, D. C.; Armstrong, D. W. *Analytical Chemistry* **2016**, *88*, 8821-8826.

(182) Sahli, S.; Stump, B.; Welti, T.; Schweizer, W. B.; Diederich, F.; Blum-Kaelin, D.; Aebi, J. D.; Böhm, H. J. *Helvetica chimica acta* **2005**, *88*, 707-730.

(183) Golias, C.; Charalabopoulos, A.; Stagikas, D.; Charalabopoulos, K.; Batistatou, A. *Hippokratia* **2007**, *11*, 124-128.

(184) Grushka, E. *Analytical Chemistry* **1970**, *42*, 1142-1147.

(185) Neue, U. D. *Journal of Chromatography A* **2008**, *1184*, 107-130.

(186) Horvath, C. G.; Preiss, B. A.; Lipsky, S. R. *Analytical Chemistry* **1967**, *39*, 1422-1428.

(187) Hupe, K. P.; Jonker, R. J.; Rozing, G. *Journal of Chromatography* **1984**, *285*, 253-265.

(188) Ismail, O. H.; Ciogli, A.; Villani, C.; De Martino, M.; Pierini, M.; Cavazzini, A.; Bell, D. S.; Gasparrini, F. *Journal of Chromatography A* **2016**, *1427*, 55-68.

(189) Barhate, C. L.; Breitbach, Z. S.; Pinto, E. C.; Regalado, E. L.; Welch, C. J.; Armstrong, D. W. *Journal of Chromatography A* **2015**, *1426*, 241-247.

(190) Barhate, C. L.; Wahab, M. F.; Tognarelli, D. J.; Berger, T. A.; Armstrong, D. W. *Analytical Chemistry* **2016**, *88*, 8664-8672.

(191) Patel, D. C.; Wahab, M. F.; Armstrong, D. W.; Breitbach, Z. S. *Journal of Chromatography A*.

(192) Fekete, S.; Ganzler, K.; Fekete, J. *Journal of Pharmaceutical and Biomedical Analysis* **2011**, *54*, 482-490.

(193) Gritti, F.; Leonardis, I.; Abia, J.; Guiochon, G. *Journal of Chromatography A* **2010**, *1217*, 3819-3843.

(194) Jeong, E. S.; Kim, S.-H.; Cha, E.-J.; Lee, K. M.; Kim, H. J.; Lee, S.-W.; Kwon, O.-S.; Lee, J. *Rapid Communications in Mass Spectrometry* **2015**, *29*, 367-384.

(195) D'Attoma, A.; Heinisch, S. *Journal of Chromatography A* **2013**, *1306*, 27-36.

(196) Gargano, A. F. G.; Duffin, M.; Navarro, P.; Schoenmakers, P. J. *Analytical Chemistry* **2016**, *88*, 1785-1793.

(197) Le Masle, A.; Angot, D.; Gouin, C.; D'Attoma, A.; Ponthus, J.; Quignard, A.; Heinisch, S. *Journal of Chromatography A* **2014**, *1340*, 90-98.

(198) Uliyanchenko, E.; Cools, P. J. C. H.; van der Wal, S.; Schoenmakers, P. J. *Analytical Chemistry* **2012**, *84*, 7802-7809.

(199) Vankrunkelsven, S.; Clicq, D.; Cabooter, D.; De Malsche, W.; Gardeniers, J. G. E.; Desmet, G. *Journal of Chromatography A* **2006**, *1102*, 96-103.

(200) Giddings, J. C.; Keller, R. A. *Extracolumn Contributions to Chromatographic Band Broadening*; Marcel Dekker: New York 1966.

(201) Mandl, A.; Nicoletti, L.; Lämmerhofer, M.; Lindner, W. *Journal of Chromatography A* **1999**, *858*, 1-11.

(202) Atwood, J. G.; Golay, M. J. E. *Journal of Chromatography A* **1981**, *218*, 97-122.

(203) Gritti, F.; McDonald, T.; Gilar, M. *Journal of Chromatography A* **2015**, *1410*, 118-128.

(204) Shock, D.; Dennis, G. R.; Guiochon, G.; Dasgupta, P. K.; Shalliker, R. A. *Analytica Chimica Acta* **2011**, *703*, 245-249.

(205) Dasgupta, P. K.; Chen, Y.; Serrano, C. A.; Guiochon, G.; Liu, H.; Fairchild, J. N.; Shalliker, R. A. *Analytical Chemistry* **2010**, *82*, 10143-10150.

(206) Granizo, M. L.; Alonso, S.; Blanco-Varela, M. T.; Palomo, A. *Journal of the American Ceramic Society* **2002**, *85*, 225-231.

(207) Barbosa, V. F.; MacKenzie, K. J.; Thaumaturgo, C. *International Journal of Inorganic Materials* **2000**, *2*, 309-317.

(208) Alonso, S.; Palomo, A. *Cement and Concrete Research* **2001**, *31*, 25-30.

(209) Duxson, P.; Provis, J. L.; Lukey, G. C.; Mallicoat, S. W.; Kriven, W. M.; Van Deventer, J. S. *Colloids and Surfaces A: Physicochemical and Engineering Aspects* **2005**, *269*, 47-58.

(210) Kriven, W. M.; Bell, J. L.; Gordon, M. *Ceramic Transactions* **2003**, *153*.

(211) Qian, K.; Peng, Y.; Zhang, F.; Yang, B.; Liang, X. *Talanta* **2018**.

(212) Wang, Y.; Wahab, M. F.; Breitbach, Z. S.; Armstrong, D. W. *Analytical Methods* **2016**, *8*, 6038-6045.

(213) Ibrahim, M. E. A.; Wahab, M. F.; Lucy, C. A. *Analytica Chimica Acta* **2014**, *820*, 187-194.

(214) Buszewski, B.; Noga, S. *Analytical and bioanalytical chemistry* **2012**, *402*, 231-247.

(215) Guo, Y. *Analyst* **2015**, *140*, 6452-6466.

(216) Wimalasinghe, R. M.; Weatherly, C. A.; Breitbach, Z. S.; Armstrong, D. W. *Journal of Liquid Chromatography & Related Technologies* **2016**, *39*, 459-464.

(217) Muñiz-Villarreal, M.; Manzano-Ramírez, A.; Sampieri-Bulbarela, S.; Gasca-Tirado, J. R.; Reyes-Araiza, J.; Rubio-Ávalos, J.; Pérez-Bueno, J.; Apatiga, L.; Zaldivar-Cadena, A.; Amigó-Borrás, V. *Mater. Lett.* **2011**, *65*, 995-998.

(218) Kong, D. L.; Sanjayan, J. G.; Sagoe-Crentsil, K. *Cement and Concrete Research* **2007**, *37*, 1583-1589.

(219) Duxson, P.; Lukey, G. C.; van Deventer, J. S. *Journal of Non-Crystalline Solids* **2006**, *352*, 5541-5555.

(220) He, P.; Jia, D.; Wang, M.; Zhou, Y. *Ceramics International* **2011**, *37*, 59-63.

(221) Gritti, F.; Bell, D. S.; Guiochon, G. *Journal of Chromatography A* **2014**, *1355*, 179-192.

(222) Gritti, F.; Guiochon, G. *Journal of Chromatography A* **2014**, *1355*, 164-178.

(223) Zhang, Z.; Wang, H.; Provis, J. L.; Bullen, F.; Reid, A.; Zhu, Y. *Thermochimica acta* **2012**, *539*, 23-33.

(224) Wang, H.; Li, H.; Yan, F. *Colloids Surf Physicochem Eng Aspects* **2005**, *268*, 1-6.

(225) Laurent, C.; Billiet, H.; De Galan, L. *Chromatographia* **1983**, *17*, 253-258.

(226) Pesek, J. J.; Sandoval, J. E.; Su, M. *Journal of Chromatography A* **1993**, *630*, 95-103.

(227) Jaroniec, C.; Jaroniec, M.; Kruk, M. *Journal of Chromatography A* **1998**, *797*, 93-102.

(228) Warson, H.; Finch, C. A. *Applications of Synthetic Resin Latices, Latices in Diverse Applications*; John Wiley & Sons, 2001; Vol. 3.

(229) O'Gara, J. E.; Alden, B. A.; Gendreau, C. A.; Iraneta, P. C.; Walter, T. H. *Journal of Chromatography A* **2000**, *893*, 245-251.

(230) Claessens, H. A.; van Straten, M. A.; Kirkland, J. J. *Journal of Chromatography A* **1996**, *728*, 259-270.

(231) Kirkland, J. J.; Van Straten, M.; Claessens, H. *Journal of Chromatography A* **1995**, *691*, 3-19.

(232) Claessens, H.; Van Straten, M.; Cramers, C.; Jezierska, M.; Buszewski, B. *Journal of chromatography A* **1998**, *826*, 135-156.

(233) Davidovits, J. In *IUPAC International Symposium on Macromolecules, Stockholm*, 1976.

(234) Ejaz, T.; Jones, A. G.; Graham, P. *J. Chem. Eng. Data* **1999**, *44*, 574-576.

(235) Gasteiger, H. A.; Frederick, W. J.; Streisel, R. C. *Ind. Eng. Chem. Res.* **1992**, *31*, 1183-1190.

(236) Dinh, N. P.; Jonsson, T.; Irgum, K. *Journal of Chromatography A* **2011**, *1218*, 5880-5891.

(237) Mahmood, T.; Saddique, M. T.; Naeem, A.; Westerhoff, P.; Mustafa, S.; Alum, A. *Industrial & Engineering Chemistry Research* **2011**, *50*, 10017-10023.

(238) Nawrocki, J.; Rigney, M.; McCormick, A.; Carr, P. *Journal of Chromatography A* **1993**, *657*, 229-282.

(239) Unob, F.; Wongsiri, B.; Phaeon, N.; Puanngam, M.; Shiowatana, J. *Journal of hazardous materials* **2007**, *142*, 455-462.

(240) Zhou, T.; Lucy, C. A. *Journal of Chromatography A* **2010**, *1217*, 82-88.

(241) Anne Mack, A. B.; Agilent Technologies, I., 2017.

(242) Bergstroem, P. A.; Lindgren, J.; Kristiansson, O. *J. Phys. Chem.* **1991**, *95*, 8575-8580.

(243) Lucy, C. A.; Wahab, M. F. *LC GC North America* **2013**, *31*, 38-42.

(244) Pohl, C. *LC GC North America* **2013**, *31*, 16-22.

(245) Schmitt, G. L.; Pietrzyk, D. J. *Analytical chemistry* **1985**, *57*, 2247-2253.

(246) Shinabarger, D. L.; Marotti, K. R.; Murray, R. W.; Lin, A. H.; Melchior, E. P.; Swaney, S. M.; Dunyak, D. S.; Demyan, W. F.; Buysse, J. M. *Antimicrobial agents and chemotherapy* **1997**, *41*, 2132-2136.

(247) Zhang, T.; Creek, D. J.; Barrett, M. P.; Blackburn, G.; Watson, D. G. *Analytical chemistry* **2012**, *84*, 1994-2001.

BIOGRAPHICAL INFORMATION

Rasangi M. Wimalasinghe earned her Bachelor of Science (Hons) degree from the University of Peradeniya in 2013. She joined Dr. Armstrong research group in 2015 at the University of Texas at Arlington and obtained her Doctor of Philosophy degree in analytical chemistry in 2018. Her research focus is based on fundamental studies on ultrafast separations and development of ultrastable stationary phase material. She has significantly contributed to sub-second chromatography separations, world fastest liquid chromatographic separations. Also, she is one of the primary contributors of the invention of geopolymer particle based stationary phase media, the first amorphous ceramic type base stable chromatographic media. She has published her work in top-tier peer-reviewed journals and presented her work in several international conferences.